A study of echinoderm immune agents with a special focus on the sea cucumber *Cucumaria frondosa* and constructing a comprehensive understanding of its health and well-being

by

© Sara Miller Jobson

A thesis submitted to the School of Graduate Studies

in partial fulfillment of the requirements for the degree of

Master of Science in Marine Biology

Department of Ocean Sciences

Memorial University

August 2021

St. John's, Newfoundland and Labrador

Abstract

Immune responses are among the most well recognized markers of health and well-being in animals; however, they remain far less studied in invertebrate than vertebrate models. Nevertheless, research on invertebrate taxa can provide valuable information on the evolution of innate immunity and subsequently lead to groundbreaking work in vertebrates, including mammals. As deuterostomes possessing remarkable regenerative abilities, echinoderms have held interdisciplinary research interest for decades, particularly in the fields of immunology and developmental biology. Echinoderms are also keystone representatives of marine ecosystems around the globe, and many are the target of exploitation, highlighting the importance of understanding their resilience to environmental and anthropogenic stress. To explore this, I first examined the cellular immune agents of 23 echinoderm species from all five extant classes of this phylum (holothuroids, echinoids, asteroids, ophiuroids, crinoids). I determined that the formation, morphology, and dynamics of coelomocyte aggregates in response to foreign material are fairly conserved across taxa, with some characteristics distinct to each class, including the nature of initial catalysts, pigmentation and the expulsion pathways. Secondly, I examined several bioindicators of stress (cellular, hormonal, and behavioural responses) within the commercial holothuroid *Cucumaria frondosa* after exposure to stressors common within the fisheries industry (e.g., lower salinities and air exposure at various temperatures). *Cucumaria. frondosa* displayed measurables responses in all bioindicators that were proportional to the severity of the stress encountered. This research serves both an academic and industry purpose as it further characterizes echinoderm immunity and demonstrates how this information is valuable for stakeholders aiming to sustainably exploit or protect valuable marine resources.

Acknowledgments

Most importantly, I would like to thank my supervisor, Annie Mercier for her support and mentorship throughout this degree. I am immensely grateful to have worked with a supervisor who guided with wisdom and nurtured my curiosity at every step. I would also like to acknowledge the invaluable contributions of Jean-Francois Hamel, who shared my excitement about this project and supported me professionally and personally through each learning curve.

This project received continuous support from other members of the Mercier lab, including Janet Ferguson-Roberts, Jiamin Sun, Brittney Stuckless, Kaitlin Casey and Rachel Morrison, who helped to care for my study organisms, offered collaborative inspiration and encouragement, thank you. Special thanks to Heather Penney, Taylor Hughes, and Andrew Tucker who provided substantial support through technical assistance and personal encouragement.

I am sincerely grateful to my committee, Javier Santander and Emaline Montgomery for offering consistent and sound counsel for the duration of this project and for being available if I needed extra help.

This project was funded by the Government of Canada and the Canada First Research Excellence Fund from the Ocean Frontier Institute to Annie Mercier. I appreciate the opportunities afforded to me as a result, even during a global pandemic.

Finally, I would like to thank, Catlen Huseby, for his unrelenting support and willingness to move across the country to pursue my dreams, and my parents, Darrell and Katie Jobson for listening to every excruciating detail and sharing genuine joy and excitement as I worked towards this milestone.

Table of Contents

List of Tables

Supplementary Table S2-1: Echinoderm species from the five extant classes, their size (length or diameter in cm) and amount of carbon particles injected (based on their size). 73

Supplementary Table S2-2: Free coelomocytes identified across various species of echinoderms. The name used is the currently accepted/most consistently used name within the literature 74

List of Figures

Figure 2-5 (previous page): A-J) Large aggregates from various asteroid species. A) *Asterias rubens* (scale bar = 94 µm). B) *Ceramaster granularis* (scale bar = 110 µm). C) *Crossaster papposus* (scale bar = 240 µm). D) *Henricia lisa* (scale bar = 67 µm). E) *Henricia perforata* (scale bar = µm). F) *Hippasteria phrygiana* (scale bar = 120 µm). G) *Leptasterias polaris* (scale bar = 150 µm). H) *Poraniomorpha hispida* (scale bar = 63 µm). I) *Stephanasterias albula* (scale bar = 120 µm). J) *Solaster endeca* (scale bar = 16 µm). Arrows in A-J indicate carbon particles. K-T) Small aggregates from various asteroid species, arrows indicate specific coelomocytes: a = amoebocyte, pr = progenitor cell, m = morula cell. K) *A. rubens* (scale bar = 15 µm). L) *C. granularis* (scale bar = 20 µm). M) *C. papposus* (scale bar = 18 µm). N) *H. lisa* (scale bar = 15 µm). O) *H. perforata* (scale bar = 15 µm). P) *H. phrygiana* (scale bar = 15 µm). Q) *L. polaris* (scale bar = 15 µm). R) *P. hispida* (scale bar = 10 µm). S) *S. albula* (scale bar = 15 µm). T) *S. endeca* (scale bar = 15 µm). U-Z) Free coelomocytes from various asteroid species. U) bladder (inactive) amoebocyte from *H. phrygiana* (scale bar = 9 µm). V) petaloid amoebocyte from *L. polaris* (scale bar = 15 µm). W) filopodial amoebocyte from *C. papposus* (scale bar = 20 µm). X) two colourless spherule cells *C. granularis* (scale bar = 6 µm). Y) fusiform cell from *S. endeca* (scale bar = 20 µm). Z) progenitor cell from *H. phrygiana* (scale bar = 50 µm). 65

Figure 2-6 (previous page): A-B) Large aggregates from various ophiuroid species (arrows indicate carbon particles). A) *Gorgonocephalus arcticus* (scale bar = 97 µm). B) *Ophiopholis aculeata* (scale bar = 70 µm). C-D) Small aggregates from various ophiuroid species, arrows indicate specific coelomocytes: p = phagocyte, dd = dedifferentiated cell, g = granulocyte. C) *G. arcticus* (scale bar = 20 µm). D) *O. aculeata* (scale bar = 10 µm). E-I) Free coelomocytes from two ophiuroid species. E) filopodial phagocyte from *G. arcticus* (scale bar = 15 µm) F)

Co-Authorship Statement

The research outlined in this thesis, including experimental design and data collection and analysis, was conducted by Sara Jobson under the supervision and guidance of Annie Mercier and Jean-Francois Hamel. Taylor Hughes participated in data collection as part of her Honours project. All manuscripts were written by Sara Jobson with intellectual and editorial input offered by co-authors as follows:

Authorship for **Chapter 2**: Jobson, S; Hamel, J.-F.; Mercier, A.

Authorship for **Chapter 3**: Jobson, S; Hamel, J.-F.; Hughes, T; Mercier, A.

Chapter 1 - General Introduction

1.1 Innate immunity

A universal component of animal health and wellness is reliance on innate immunity. Innate immunity is comprised of two integral components, cellular (i.e., the ability to detect an immune threat) and humoral (i.e., the ability to eliminate an immune threat) responses (Beutler, 2004). To further complement the capacity of the innate immune system, adaptive immunity later evolved in vertebrates, boasting the ability to remember specific pathogens and respond with targeted immune attacks (Boraschi, 2014). While vertebrate members of phylum Chordata have both innate and adaptive immunity, invertebrates that form the rest of metazoan diversity (over 25 phyla) rely only on the former, which has perpetuated the idea of vertebrates possessing a "sophisticated" immune system as compared to the so-called "primitive" system of invertebrates (i.e., different species present similar cell types and relative quantities in different compartments; Boraschi, 2014). As research in the field of innate immunology within invertebrates has long been overshadowed by work being done on the innate and adaptive systems in humans (Turvey and Broide, 2010), our understanding of immunity in basal animals remains superficial and incomplete (Beutler, 2004, Chiaramonte and Russo, 2015, Little *et al.*, 2005). Issues caused by knowledge gaps in this field are compounded by the fact that most of the framework (e.g., terminology, methodology) is based on what has been learned from vertebrates (Boraschi and Italiani, 2018, Gourbal *et al.*, 2018, Little *et al.*, 2005). This perspective limits the scope and creativity of research on innate immunity and also tends to obscure similitudes and distinctions across more than 30 invertebrate phyla. For example, innate immune systems have traditionally (and universally) been considered non-anticipatory, non-specific and non-clonal, mobilizing quickly upon exposure rather than being enhanced by memory from past exposure (Canesi and Procházková, 2014). Interestingly, recent work on sea cucumbers (Holothuroidea:

Echinodermata) has demonstrated their ability to appraise impending threats (e.g., scent of a predator or injured conspecific) and react immunologically before they materialize, i.e., multiplication of immune cells in anticipation of physical injury (Appendix 2; Hamel *et al.*, 2021). In addition to support for echinoderms having anticipatory immune abilities, there is evidence to suggest that several factors (including genetic diversity and protein interactions) are able to provide a similar level of specific response to parasite challenge in invertebrates when compared to the adaptive immune system (Schulenburg *et al.*, 2007). Finally, several studies have also demonstrated how innate immune systems may have the capacity for immune memory through their improved success rate when dealing with previously encountered pathogens (Kurtz and Franz, 2003). Regardless of this mounting evidence, innate immunity is still considered less sophisticated than adaptive immunity.

Although historically considered simple, in reality, the immune system of invertebrates operates with two closely linked systems: 1) physicochemical barriers and 2) innate immunity (cellular and humoral; Boraschi, 2014). As expected, physicochemical barriers use pre-existing physiology (i.e., cuticle, mucus, exoskeletons, etc.; Ray *et al.*, 2015) as well as freely circulating chemicals in body fluids. Infections that are able to break through both the physical and chemical barriers are then met by the cellular and humoral components of innate immunity. The humoral component of innate immunity includes a variety of soluble factors such as lectins, agglutinins, complement proteins, and antimicrobial peptides (Melillo *et al.*, 2018, Turvey and Broide, 2010). Humoral factors work in conjunction with cell-mediated responses to detect and respond to the invasion of foreign particles (Beutler 2004). For example, lectins are responsible for non-self-recognition and intracellular signaling (Rathinam *et al.*, 2020, Rinkevich and Müller, 1996) and are believed to be secreted by a specific type of immune cell in invertebrates, sometimes referred

to as granulocytes (Melillo *et al.*, 2018). Often, immune cells are portrayed as the primary defenders of innate immunity and are labeled as either "phagocytes" (not to be confused with their ability to phagocytose, which can apply to more than one type of cell) or more generally as "coelomocytes", which are reportedly responsible for and restricted to neutralizing and removing harmful material (Boraschi, 2014, Gourbal *et al.*, 2018, Murphy and Weaver, 2009). However, the diversity and functions of invertebrate immune cells, including but not limited to phagocytes, have only been superficially documented since the early 20th century (Kindred, 1924).

In most invertebrate phyla, the immune agents conventionally and collectively known as coelomocytes (analogous to vertebrate leukocytes) are considered equivalent to hematopoietic stem cells because of their role and the proposed versatility of differentiation based on the needs of the immune system (Homa, 2018, Rinkevich and Müller, 1996). While there are many invertebrate groups that have produced useful insight into the working of innate immunity (e.g., molluscs, crustaceans, tunicates; Rinkevich and Müller, 1996), insects and earthworms are among the most prominent. Insect model systems (primarily *Drosophila* sp.) have served as one of the most well studied within the field of invertebrate immunology and provided excellent insights into both the cellular (coelomocytes, synonymously known as hemocytes in insects) and humoral responses involved (Tzou *et al.*, 2002). One of the most profound breakthroughs pioneered by work on *Drosophila* was the discovery of Toll pathway/receptors, subsequently allowing researchers to characterize how insects detect infection and communicate that to other defense cells (Kurata, 2010, Satyavathi *et al.*, 2014). Apart from being an upstream component of invertebrate immunity, Toll pathways also play an important role in development by helping to establish boundaries between developmental planes (Ganguly *et al.*, 2005). This work on insects has not only helped us understand how these different systems are integrated but also led

to the discovery of Toll-like receptors (TLRs) in mammals (Satyavathi *et al.*, 2014). Earthworms are another sentinel invertebrate for immunological studies as they possess immune agents comparable to those in both invertebrate and vertebrate systems and are sensitive to slight environmental changes (Cooper and Roch, 2003). Research on earthworms (primarily conducted on species within the genera *Lumbrica* or *Eisenia*) has explored the role of cellular and humoral elements in phagocytosis, graft rejection, wound healing, and cellular encapsulation or aggregation (Bilej *et al.*, 2010), making it foundational in supporting other interdisciplinary work.

Echinoderms belong to the deuterostome clade and, as such, sit closer to vertebrates than the previously mentioned models like flies and worms, which are protostomes. Thus, research within this phylum offers potential clarity to the evolutionary link between invertebrate and vertebrate immunity (Smith *et al.*, 2018). An example of where this link has been helpful is the study of vertebrate regeneration. In most cases, vertebrates are only able to regenerate limbs that have been lost to autotomy (Delorme *et al.*, 2012) and while this also occurs in different species of asteroids (Diaz-Guisado *et al.*, 2006) and ophiuroids (Wilkie, 1978), echinoderms as a whole demonstrate a much higher capacity for regeneration (Carnevali, 2006). For example, some sea stars of the *Linkia* genus have the ability to not only regrow a lost limb but a whole new individual from a limb that has been autotomized (Carnevali, 2006). The missing or inactive processes that keep higher vertebrates from regenerating pieces of their central nervous system, organs, or limbs lost for reasons other than autotomy has sparked research interest in echinoderms and provided information on the evolution of vertebrate systems (Byrne, 2020). The importance of understanding regeneration capacity extends beyond major limb and organ regrowth to include more universal processes like the loss of tissue homeostasis (i.e., tissue

maintenance) as organisms age. Echinoderms have provided valuable information regarding the regeneration of tissues as they display the ability to maintain tissue homeostasis throughout their life, regardless of lifespan (Bodnar and Coffman, 2016).

Echinoderm coelomocytes have been primarily studied in holothuroids (briefly described in Caulier *et al.*, 2020) and echinoids (Brothers *et al.*, 2016, Smith *et al.*, 2006, Smith *et al.*, 2019), with limited work relating to sea stars (Oweson *et al.*, 2008), and minimal knowledge existing for ophiuroids (Ben Khadra *et al.*, 2018) and crinoids (Di Benedetto *et al.*, 2014, Smith *et al.*, 2018). Coelomocytes are conventionally divided into six main cell types: phagocytes, morula cells, progenitor cells, hemocytes, crystal cells, and vibratile cells (Smith *et al.*, 2018; Table 1-1). They are involved in many immune responses including the recognition and removal of foreign matter, cytotoxic response, fluid circulation and clotting (Branco *et al.*, 2014, Smith *et al.*, 2006, Smith *et al.*, 2018). Coelomocyte research in echinoderms, and other invertebrate taxa, suggests that they communicate via secretion of humoral factors like lectins and glycoproteins for cell-cell signaling (Ben Khadra *et al.*, 2018, Tetreau *et al.*, 2017) or eicosanoids (Satyavathi *et al.*, 2014) to perform cohesive tasks. A primary task involving cell communication is the gathering of coelomocytes around large particles of foreign matter to create an aggregate that is able to neutralize and/or expel harmful particles (Caulier *et al.*, 2020, Melillo *et al.*, 2018). The versatility of these cells offers researchers the ability to begin understanding how invertebrates thrive even under the most adverse conditions.

1.2 Echinoderms as a focal phylum

Beyond occupying a critical place in the evolutionary hierarchy (Smith *et al.*, 2018), echinoderms are an important and ubiquitous phylum of marine invertebrates, foundational in ecosystems across the world, from the Arctic to tropical waters and from the shore to the abyss,

with many considered keystone species (Gizzi *et al.*, 2020, Hermosillo-Núñez, 2020). Most echinoderms share a sedentary lifestyle in the benthos, primarily acting as suspension or detritus/scavenging feeders with some active hunters, making echinoderms invaluable to the maintenance of ecosystems.

In an effort to provide a comprehensive look at echinoderm immunology, I selected species from each class (holothuroids, echinoids, asteroids, ophiuroids, crinoids) of this phylum, with a special focus on the holothuroid *Cucumaria frondosa* due to its commercial value. Sea cucumbers are among the most lucrative seafood in the world, fetching upwards of USD 2500 kg^{-1} depending on the species (Purcell, 2014). As the value of sea cucumbers has increased, populations have noticeably decreased (Anderson *et al.*, 2011). With an interest in curating sustainable marine industries, sea cucumbers have been identified as a potential candidate for integrated, multitrophic aquaculture (Gianasi *et al.*, 2020). The economic, environmental, and research value of echinoderms, specifically sea cucumbers, have motivated a recent push to develop a better understanding of echinoderm physiology and the recent mapping and assemblage of the sea cucumber genome (Zhang *et al.*, 2017).

1.3 Research gaps in invertebrate immunology with a focus on echinoderms

Coelomocytes have been studied for decades with interest steadily gaining since the 1960s (Hetzel, 1963). Unfortunately, the various methodologies used, and the complex nature of this discipline have resulted in incohesive and convoluted descriptions (Table 1-1; Ben Khadra *et al.*, 2018, Brothers *et al.*, 2016, Di Benedetto *et al.*, 2014, Oweson *et al.*, 2008). These inconsistencies have made it difficult to characterize coelomocytes, their morphology, function, and interactions, resulting in very few comparative studies within the phylum Echinodermata and even fewer attempts to compare between phyla regardless of acknowledged similarities (Cooper

and Roch, 2003, Smith *et al.*, 2018, Tzou *et al.*, 2002). Until some level of analogy across model organisms can be achieved, it will remain difficult to make meaningful comparisons or draw any evolutionarily relevant conclusions.

As coelomocytes are a well-documented (although not well understood in all classes of echinoderms) immune marker (Smith *et al.*, 2018), it is important to partner them with other indicators of organism health and well-being to flesh out our understanding of stress. Cortisol is a widely studied glucocorticoid stress hormone in humans that is commonly accepted across vertebrate research as a marker of well-being (Uren Webster *et al.*, 2020) but its use in invertebrate research as a metric of stress is limited (Hou *et al.*, 2019, Pei *et al.*, 2012). Similarly, behaviour has been broadly accepted as a vertebrate indicator of stress but is not often effectively transferred to use within echinoderms. Bose *et al.* (2019) were able to use the behaviour of sea urchins in captivity to determine the varying levels of stress induced by handling versus the holding in captivity of individual organisms. Studies like this reinforce the value of using various indices of stress measurement to create a more wholistic understanding of organism well-being.

Several studies have outlined a preliminary baseline for how stress alters cortisol levels and manifests as behaviour (Gianasi *et al.*, 2016, Hamel *et al.*, 2019, Hou *et al.*, 2019); however, these indicators have not been used in conjunction with each other and coelomocytes to elucidate how an echinoderm responds to adverse situations.

A second and equally important knowledge gap within invertebrate immunology is the relationship between the cellular immune response and overall health and well-being of an individual. The inexistent or minimal research ethics protecting most invertebrate phyla create bias suggesting that since echinoderms and most other invertebrate animals do not feel pain, they also do not experience stress relatable to humans. As living organisms across our planet begin to

feel cumulatively more stress through anthropogenic events like harvesting, accelerated climate change, and pollution, it is essential that we can appropriately evaluate how their overall health and well-being are affected. Without creating precise methods to determine the baseline of animal health and healthy ecosystems, we will never be able to accurately monitor changes and negative impacts.

1.4 Methodological considerations of the proposed study

When using coelomocytes to assess the immune response of an individual, it is conventional to use a hemocytometer to estimate cell density from a subsample of body fluid (Hou *et al.*, 2019, Kaneshiro and Karp, 1980, Li *et al.*, 2018, Mather and Roberts, 1998). The body fluid in which coelomocytes are usually measured is taken from the perivisceral coelom of echinoderms either using a hypodermic needle or other dissecting instruments to puncture the body wall (Fontaine and Lambert, 1977, Hou *et al.*, 2019, Li *et al.*, 2013, Vazzana *et al.*, 2015). Unfortunately, this method harbors a certain level of uncertainty as the internal anatomy of sea cucumbers, and other echinoderms, is more complex than expected. When using a needle or draining the body cavity, it is impossible to verify that the fluid was collected from the intended perivisceral coelom and not from a different system/organ. To circumvent this, I used dissection to take fluid samples from several different body cavities (perivisceral coelom, Polian vesicle, and ampullae of the tentacles or podia). This approach provided clean and discreet fluid measurements allowing for confident cellular comparison within and between individuals (Figure 1-1).

Monitoring cortisol within sea cucumbers is still quite novel and uses methodology reliant on radioimmunoassay (Chen *et al.*, 2018b, Hou *et al.*, 2019), which is costly, not easily accessible to all scientists, and produces hazardous radioactive waste (Cerda-Kipper *et al.*, 2019). Since this

technique is falling out of popularity, hormonal analysis using enzyme-linked immunosorbent assays (ELISA) has become a widely used replacement in laboratories and commercial workplaces (Aydin, 2015). While these kits are extensively used on vertebrates, a methodology compatible with hormone analysis in holothuroid echinoderms had not been designed at the outset of the present study. An objective of this research was to design a new methodology, corrected for the unique aspects of sea cucumber coelomic fluid (e.g., sensitive pH, viscosity, high cellular count, etc.) so as to obtain a cortisol reading using an ELISA kit (Cayman Chemical) originally designed for vertebrates.

1.5 Research questions and thesis structure

The main objectives of my thesis can be split into two research questions, corresponding to the two data chapters:

Objective 1: Are coelomocytes conserved across Echinodermata in terms of presence, formation, morphology, and interactions?

Objective 2: Are coelomocytes reliable indicators of health and well-being in sea cucumbers and can we use this knowledge to develop bioindicators that can complement organism behavioural monitoring in echinoderms?

In Chapter 2, I studied how freely circulating coelomocytes form cellular aggregates. I stimulated immune responses and monitored the free coelomocyte and aggregate morphologies in different body cavities within and across representatives from all five extant classes of echinoderms (Figure 1-2: Steps 1, 2 & 4). In Chapter 3, I conducted an experimental study of coelomocyte dynamics in response to specific environmental stressors that can find parallels in harvesting and handling protocols. These cellular reactions were then compared to organism behavioural and hormonal (cortisol levels) responses to the same stress exposure (Figure 1-2:

Steps 1-5). Chapter 3 was presented at the International Marine Conservation Congress in August 2020 and is in press in a special issue of *Frontiers in Marine Science*.

During the data collection for Chapter 2, a fortuitous discovery of mine led to the publication of a short special interest piece on the separate but related topic of fission and regeneration in the sea cucumber *Chiridota laevis*. This paper was published in *Frontiers in Ecology and the Environment* and is included in Appendix 1 (Jobson *et al.*, 2020). I also had an opportunity to collaborate to an experimental study looking at the immune capacity of sea cucumbers and how it can inform on their ability to anticipate stressful experiences (like predatory cues). This paper was published in *Scientific Reports* and is included in Appendix 2 (Hamel *et al.*, 2021).

1.6 Literature Cited

Anderson, S. C., J. M. Flemming, R. Watson, and H. K. Lotze. 2011. Serial exploitation of global sea cucumber fisheries. *Fish Fish* **12**:317-339.

Aydin, S. 2015. A short history, principles, and types of ELISA, and our laboratory experience with peptide/protein analyses using ELISA. *Peptides* **72**:4-15.

Ben Khadra, Y., M. Sugni, C. Ferrario, F. Bonasoro, P. Oliveri, P. Martinez, and M. D. Candia Carnevali. 2018. Regeneration in stellate echinoderms: Crinoidea, Asteroidea and Ophiuroidea. Pp. 285-320 in *Marine Organisms as Model Systems in Biology and Medicine*, M. Kloc and J. Z. Kubiak, eds. Springer International Publishing, Cham.

Beutler, B. 2004. Innate immunity: An overview. *Mol Immunol* **40**:845-859.

Bilej, M., P. Procházková, M. Šilerová, and R. Josková. 2010. Earthworm immunity. Pp. 66-79 in *Invertebrate Immunity*, K. Söderhäll, ed. Springer US, Boston, MA.

Bodnar, A. G., and J. A. Coffman. 2016. Maintenance of somatic tissue regeneration with age in short- and long-lived species of sea urchins. *Aging Cell* **15**:778-787.

Boraschi, D. 2014. How innate and adaptive immunity work. Pp. 1-7 in *Nanoparticles and the Immune System* D. Boraschi, ed. Academic Press, Oxford, UK and Waltham, USA.

Boraschi, D., and P. Italiani. 2018. Innate immune memory: Time for adopting a correct terminology. *Front Immunol* **9**.

Bose, A. P. H., D. Zayonc, N. Avrantinis, N. Ficzycz, J. Fischer-Rush, F. T. Francis, S. Gray, F. Manning, H. Robb, C. Schmidt, C. Spice, A. Umedaly, J. Warden, and I. M. Côté. 2019. Effects of handling and short-term captivity: a multi-behaviour approach using red sea urchins, Mesocentrotus franciscanus. *PeerJ* **7**:e6556.

Branco, P. C., D. A. L. Figueiredo, and J. da Silva. 2014. New insights into innate immune system of sea urchin: Coelomocytes as biosensors for environmental stress. *OA Biol* **18**:1-7.

Brothers, C. J., J. Harianto, J. B. McClintock, and M. Byrne. 2016. Sea urchins in a high CO_2 world: The influence of acclimation on the immune response to ocean warming and acidification. *Proc R Soc B: Biol Sci* **283**:20161501.

Byrne, M. 2020. The link between autotomy and CNS regeneration: Echinoderms as non-model species for regenerative biology. *Bioessays* **42**:1900219.

Canesi, L., and P. Procházková. 2014. The invertebrate immune system as a model for investigating the environmental impact of nanoparticles. Pp. 91-112 in *Nanoparticles and the Immune System* Elsevier.

Carnevali, C. 2006. Regeneration in echinoderms: Repair, regrowth, cloning. *Invert Surv J* **3**:64-76.

Caulier, G., J.-F. Hamel, and A. Mercier. 2020. From coelomocytes to colored aggregates: Cellular components and processes involved in the immune response of the holothuroid *Cucumaria frondosa*. *Biol Bull* **239**:95-114.

Cerda-Kipper, A. S., B. E. Montiel, and S. Hosseini. 2019. Immunoassays | radioimmunoassays and enzyme-linked immunosorbent assay. Pp. 55-75 in *Encyclopedia of Analytical Science* P. Worsfold, C. Poole, A. Townshend and M. Miró, eds. Academic Press, Oxford.

Chen, J., Y. Ren, G. Wang, B. Xia, and Y. Li. 2018b. Dietary supplementation of biofloc influences growth performance, physiological stress, antioxidant status and immune response of juvenile sea cucumber *Apostichopus japonicus* (Selenka). *Fish Shellfish Immunol.* **72**:143-152.

Chiaramonte, M., and R. Russo. 2015. The echinoderm innate humoral immune response. *Ital J Zool* **82**:300-308.

Cooper, E. L., and P. Roch. 2003. Earthworm immunity: A model of immune competence. *Pedobiologia* **47**:676-688.

Delorme, S. L., I. M. Lungu, and M. K. Vickaryous. 2012. Scar-free wound healing and regeneration following tail loss in the leopard gecko, *Eublepharis macularius*. *Anat Rec* **295**:1575-1595.

Di Benedetto, C., L. Parma, A. Barbaglio, M. Sugni, F. Bonasoro, and M. D. Candia Carnevali. 2014. Echinoderm regeneration: An in vitro approach using the crinoid *Antedon mediterranea*. *Cell Tissue Res.* **358**:189-201.

Diaz-Guisado, D., C. F. Gaymer, K. B. Brokordt, and J. M. Lawrence. 2006. Autotomy reduces feeding, energy storage and growth of the sea star *Stichaster striatus*. *J Exp Mar Biol Ecol* **338**:73-80.

Fontaine, A. R., and P. Lambert. 1977. The fine structure of the leucocytes of the holothurian, *Cucumaria miniata*. *Can J Zool* **55**:1530-1544.

Ganguly, A., J. Jiang, and Y. T. Ip. 2005. Drosophila WntD is a target and an inhibitor of the Dorsal/Twist/Snail network in the gastrulating embryo. *Development* **132**:3419-3429.

Gianasi, B. L., J.-F. Hamel, and A. Mercier. 2016. Experimental test of optimal holding conditions for live transport of temperate sea cucumbers. *Fish Res* **174**:298-308.

Gianasi, B. L., J.-F. Hamel, E. M. Montgomery, J. Sun, and A. Mercier. 2020. Current knowledge on the biology, ecology, and commercial exploitation of the sea cucumber *Cucumaria frondosa*. *Rev Fish Sci Aquac*.

Gizzi, F., J. Jiménez, S. Schäfer, N. Castro, S. Costa, S. Lourenço, R. José, J. Canning-Clode, and J. Monteiro. 2020. Before and after a disease outbreak: Tracking a keystone species recovery from a mass mortality event. *Mar Environ Res* **156**:104905.

Gourbal, B., S. Pinaud, G. J. M. Beckers, J. W. M. Van Der Meer, U. Conrath, and M. G. Netea. 2018. Innate immune memory: An evolutionary perspective. *Immunol Rev* **283**:21-40.

Hamel, J.-F., S. Jobson, G. Caulier, and A. Mercier. 2021. Evidence of anticipatory immune and hormonal responses to predation risk in an echinoderm. *Sci Rep* **11**.

Hamel, J.-F., J. Sun, B. L. Gianasi, E. M. Montgomery, E. L. Kenchington, B. Burel, S. Rowe, P. D. Winger, and A. Mercier. 2019. Active buoyancy adjustment increases dispersal potential in benthic marine animals. *J Anim Ecol* **88**:820-832.

Hermosillo-Núñez, B. B. 2020. Contribution of echinoderms to keystone species complexes and macroscopic properties in kelp forest ecosystems (northern Chile). *Hydrobiologia* **847**:739-756.

Hetzel, H. R. 1963. Studies on holothurian coelomocytes. i. A survey of coelomocyte types. *Biol Bull* **125**:289-301.

Homa, J. 2018. Earthworm coelomocyte extracellular traps: structural and functional similarities with neutrophil NETs. *Cell Tissue Res.* **371**:407-414.

Hou, S., Z. Jin, W. Jiang, L. Chi, B. Xia, and J. Chen. 2019. Physiological and immunological responses of sea cucumber *Apostichopus japonicus* during desiccation and subsequent resubmersion. *PeerJ* **7**:e7427.

Jobson, S., H. D. Penney, J.-F. Hamel, and A. Mercier. 2020. Split personality. *Front Ecol Environ* **18**:557-557.

Kaneshiro, E. S., and R. D. Karp. 1980. The ultrastructure of coelomocytes of the sea star *Dermasterias imbricata*. *Biol Bull* **159**:295-310.

Kindred, J. E. 1924. The cellular elements in the perivisceral fluid of echinoderms. *Biol Bull* **46**:228-251.

Kurata, S. 2010. Fly immunity: Recognition of pathogens and induction of I immune responses. Pp. 205-217 in *Invertebrate Immunity*, K. Söderhäll, ed. Springer US, Boston, MA.

Kurtz, J., and K. Franz. 2003. Evidence for memory in invertebrate immunity. *Nature* **425**:37-38.

Li, Q., R.-R. Qi, Y.-N. Wang, S.-G. Ye, G. Qiao, and H. Li. 2013. Comparison of cells free in coelomic and water-vascular system of sea cucumber, *Apostichopus japonicus*. *Fish Shellfish Immunol.* **35**:1654-1657.

Li, Q., Y. Ren, C. Liang, G. Qiao, Y. Wang, S. Ye, and R. Li. 2018. Regeneration of coelomocytes after evisceration in the sea cucumber, Apostichopus japonicus. *Fish Shellfish Immunol.* **76**:266-271.

Little, T. J., D. Hultmark, and A. F. Read. 2005. Invertebrate immunity and the limits of mechanistic immunology. *Nat Immunol* **6**:651-654.

Mather, J. P., and P. E. Roberts. 1998. *Introduction to Cell and Tissue Culture: Theory and Technique*. Springer Science & Business Media.

Melillo, D., R. Marino, P. Italiani, and D. Boraschi. 2018. Innate immune memory in invertebrate metazoans: A critical appraisal. *Front Immunol* **9**:1915.

Murphy, K. M., and C. Weaver. 2009. *Janeway's immunobiology*. Garland Science, New York and London

Oweson, C., H. Skold, A. Pinsino, V. Matranga, and B. Hernroth. 2008. Manganese effects on haematopoietic cells and circulating coelomocytes of *Asterias rubens* (Linnaeus). *Aquat. Toxicol.* **89**:75-81.

Pei, S., S. Dong, F. Wang, X. Tian, and Q. Gao. 2012. Effects of density on variation in individual growth and differentiation in endocrine response of Japanese sea cucumber *Apostichopus japonicus* (Selenka). *Aquaculture* **356**:398-403.

Purcell, S. W. 2014. Value, market preferences and trade of Beche-de-mer from Pacific island sea cucumbers. *PLoS One* **9**:e95075.

Rathinam, R. B., S. A. Iburahim, and G. Tripathi. 2020. The immune system of sea cucumbers: An evidential approach. *Food Sci Rep* **1**:6.

Ray, S., S. Mukherjee, N. S. Bhunia, A. S. Bhunia, and M. Ray. 2015. Immunotoxicological threats of pollutants in aquatic invertebrates. InTech.

Rinkevich, B., and W. E. G. Müller. 1996. *Invertebrate immunology*. Springer Berlin Heidelberg, Berlin, Heidelberg.

Satyavathi, V. V., A. Minz, and J. Nagaraju. 2014. Nodulation: An unexplored cellular defense mechanism in insects. *Cell Signal* **26**:1753-1763.

Schulenburg, H., C. Boehnisch, and N. K. Michiels. 2007. How do invertebrates generate a highly specific innate immune response? *Mol Immunol* **44**:3338-3344.

Smith, L., R. Jp, B. V, T. Dp, S. Nair, K. Buckley, and A. Majeske. 2006. The sea urchin immune system. *Invert Surv J* **3**.

Smith, L. C., V. Arizza, M. A. Barela Hudgell, G. Barone, A. G. Bodnar, K. M. Buckley, V. Cunsolo, N. M. Dheilly, N. Franchi, S. D. Fugmann, R. Furukawa, J. Garcia-Arraras, J. H. Henson, T. Hibino, Z. H. Irons, C. Li, C. M. Lun, A. J. Majeske, M. Oren, P. Pagliara, A.

Pinsino, D. A. Raftos, J. P. Rast, B. Samasa, D. Schillaci, C. S. Schrankel, L. Stabili, K. Stensväg, and E. Sutton. 2018. Echinodermata: The complex immune system in echinoderms. Pp. 409-501 in *Advances in Comparative Immunology*, E. L. Cooper, ed. Springer, Cham.

Smith, L. C., T. S. Hawley, J. H. Henson, A. J. Majeske, M. Oren, and B. Rosental. 2019. Methods for collection, handling, and analysis of sea urchin coelomocytes. *Methods Cell Biol* **150**:357-389.

Tetreau, G., S. Pinaud, A. Portet, R. Galinier, B. Gourbal, and D. Duval. 2017. Specific pathogen recognition by multiple innate immune sensors in an invertebrate. *Front Immunol* **8**:1249.

Turvey, S. E., and D. H. Broide. 2010. Innate immunity. *J. Allergy Clin. Immunol.* **125**:24-32.

Tzou, P., E. De Gregorio, and B. Lemaitre. 2002. How *Drosophila* combats microbial infection: A model to study innate immunity and host–pathogen interactions. *Curr Opin Microbiol* **5**:102-110.

Uren Webster, T. M., D. Rodriguez-Barreto, S. Consuegra, and C. Garcia de Leaniz. 2020. Cortisol-related signatures of stress in the fish microbiome. *Front Microbiol* **11**:1621.

Vazzana, M., T. Siragusa, V. Arizza, G. Buscaino, and M. Celi. 2015. Cellular responses and HSP70 expression during wound healing in Holothuria tubulosa (Gmelin, 1788). *Fish Shellfish Immunol.* **42**:306-315.

Wilkie, I. C. 1978. Functional morphology of the autotomy plane of the brittle star *Ophiocomina nigra* (Abildgaard) (Ophiuroidea, Echinodermata). *Zoomorphologie* **91**:289-305.

Zhang, X., L. Sun, J. Yuan, Y. Sun, Y. Gao, L. Zhang, S. Li, H. Dai, J.-F. Hamel, C. Liu, Y. Yu, S. Liu, W. Lin, K. Guo, S. Jin, P. Xu, K. B. Storey, P. Huan, T. Zhang, Y. Zhou, J. Zhang, C. Lin, X. Li, L. Xing, D. Huo, M. Sun, L. Wang, A. Mercier, F. Li, H. Yang, and J.

Xiang. 2017. The sea cucumber genome provides insights into morphological evolution and visceral regeneration. *PLoS Biol* **15**:e2003790.

1.7 Tables

Table 1-1: Summary of the main coelomocyte types reported in echinoderms. The most commonly proposed name is presented alongside synonyms (alternate names) and morphological characteristics. The proposed names were extracted from the works of Smith et al. 2018 and Caulier et al. 2020.

Proposed name Alternate names	**Fundamental characteristics** Based on previous literature and experimental observation	**Class where documented**	**Literature** Primary Sources: Smith et. al. (2018) and Caulier et al. 2020
Phagocytes (bladder, petaloid & filapodial phases) - Petaloid - Leukocytes - Amebocyte - Bladder amebocytes - Filiform amebocytes	- Nucleus surrounded by a microtubule/filament fan (Fontaine and Lambert 1975) - Displays a resting (bladder) and active (petaloid and filopodial) phases - bladder– filamentous fan is wrapped around the nucleus in a tight sphere - Petaloid – fan is extended around the nucleus. - Filopodial – the cytoplasm fan retracts leaving branching microtubules extended. - 20-50 µm	- Asteroids - Echinoids - Holothuroids - Ophiuroids	Fontaine and Lambert (1975) Chia and Xing (1996)
Red spherule cells - Amebocyte - Spherulocyte - Morula	- Red pigmentation from echinochrome A molecules (Branco et al. 2014) - Cytoplasm is filled with red granules - Demonstrates ameboid locomotion - 8-20 µm	- Echinoids	De Faria and da Silva (2007) Branco et. at. (2014) Matranga et. al. (2000) Gross et. al. (1999)
Colorless spherule cells - Morula - Amebocyte - Spherulocyte - White Spherule cell	- Un-pigmentated - Cytoplasm is filled with granules of different sizes that are randomly distributed - Demonstrates ameboid locomotion - Commonly confused with morula cells - 8-20 µm	- Asteroids - Echinoids - Holothuroids - Ophiuroids	Matranga et. al. (2000) Queiroz and Custodio (2015) Gross et. al. 1999
Progenitor cells - Lymphocytes - Hyaline cells	- Spherical - Large nuclei with minimal cytoplasm - Hypothesized to be precursor coelomocytes - 2-8 µm	- Asteroids - Echinoids - Holothuroids - Ophiuroids	Ramirez-Gomez et. al. (2010) Eliseikina and Magarlamov (2002) Taguchi et. al. (2016)
Vibratile cells ---	- One flagellum attached to distinct head. Nucleus is only occasionally visible depending on echinoderm species and angle of viewing - Head contains large granules - 5-10 µm	- Asteroids - Echinoids - Holothuroids - Ophiuroids	Pinsino et. al. (2007) Ramirez-Gomez and GarciaArraras (2010) Matranga (2005)

Fusiform cells ---	- Two flagella attached to center nodule at 180 degrees from each other - 15-20 µm length and 6-12 µm diameter	- Asteroids - Echinoids - Holothuroids - Ophiuroids	Boolootian and Giese (1958) Xing et. al. (2008) Li et. al. (2018)
Hemocytes ---	- Round/oval and biconcave in appearance - Red colour from hemoglobin content (can appear yellow when free or aggregated in small numbers) - Has nucleus but it is only visible under specific magnification - 10-23 µm	- Holothuroids	Ramirez-Gomez and Garcia Arraras (2010) Eliseikina and Magarlamov (2002)
Crystal Cells ---	- Commonly assumed to be the rarest coelomocyte - Variety of geometric shapes: rectangular, rhomboid, hexagonal, star shaped - 2-24 µm	- Holothuroids	Li et. al. (2013) Elisekina & Magarlamov (2001) Boolootian & Giese (1958) Hetzel (1963) Ramirez-Gomez & Garcia-Arraras (2010)
Minute corpuscles - Undifferentiated cells - Progenitor cells	- Working description	- Asteroids - Echinoids - Holothuroids - Ophiuroids	Hetzel 1963 Not included in Smith et. al. 2018 or Caulier et al. 2020

1.8 Figures

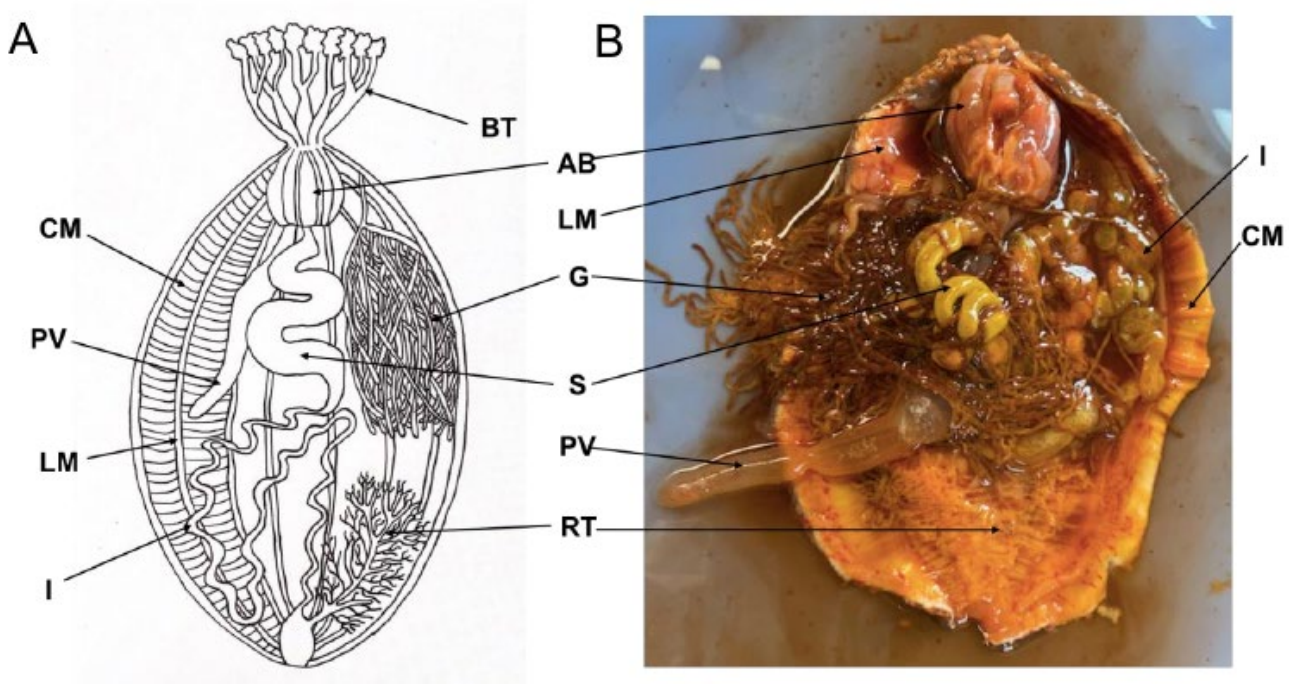

Figure 1-1: Internal anatomy of the sea cucumber *Cucumaria frondosa*. BT = branching tentacles, AB = aquapharyngeal bulb, LM = longitudinal muscles, CM = circular muscles, G = gonads, I = intestine, PV = Polian vesicle, RT = respiratory tree, S = stomach. Photo and diagram courtesy of Kate Tobin.

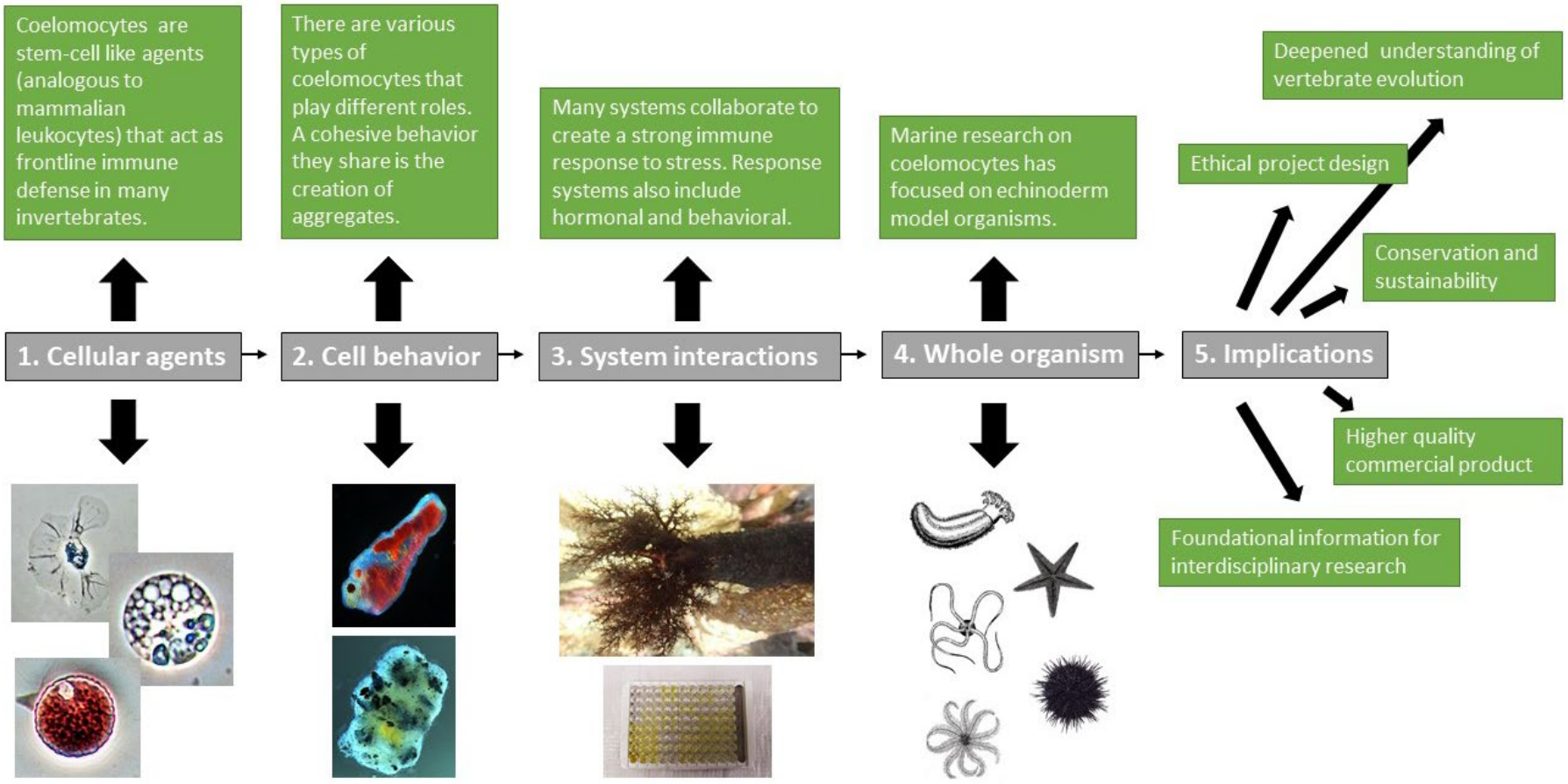

Figure 1-2: Schematic outline showing how this thesis integrates various levels of cellular (1-2), hormonal (3), and behavioural (3) biomarkers to characterize echinoderm immunity as a whole (4) and the implications of this research within and beyond academia (5).

Chapter 2 - Rainbow bodies: revisiting the diversity of coelomocyte aggregates and their synthesis in echinoderms

2.1 Abstract

The innate immunity of echinoderms has been a research focus since the early twentieth century, consistently providing ever deeper knowledge of its complexity and evolutionary aspects. At its core are coelomocytes, which are diverse cells collectively known to respond in a variety of ways, including via movement, phagocytosis, and aggregation. However, features of cellular immunity have never been compared in echinoderms from phylogenetic and distributional perspectives, to provide insight into ecological and evolutionary patterns. The present study catalyzed and characterized the formation of coelomocyte aggregates in members of all five extant classes of echinoderms. The morphological characteristics of these aggregates (including their colour, shape, texture, size) were assessed, as well as the major cells composing them. Coelomocyte diversity (both as free and aggregated forms) was determined to be maximum in class Holothuroidea, followed by Echinoidea, with the other classes showing similar levels of diversity. The colours of coelomocyte aggregates appeared to be more closely linked to phylogeny (classes, orders) rather than geographic range, or external colour of the species themselves. Asteroids and ophiuroids displayed primarily light-coloured aggregates, from transparent to green; while holothuroids, echinoids and crinoids demonstrated more vivid variants, from red to deep purple. The kinetics of aggregate formation and expulsion were monitored in selected species, showing immediate cellular response to foreign particulate matter in the form of encapsulation and various methods of expulsion, including through the dermal papillae of asteroids and the anus of holothuroids. The findings support that coelomocyte aggregate formation is a conserved immune response across all five extant classes of echinoderms with variations in their cell catalysts, complexity, shape, colour, and size.

Keywords: Immunity, Brown bodies, Phagocytes, Morula cells, Hemocytes, Crystal cells

2.2 Introduction

Innate immunity is the basal form of the immune system that has evolved within all eukaryotes (Boraschi, 2014). While vertebrates eventually evolved a complementary system referred to as adaptive immunity, other metazoans still rely solely on innate immune responses (Canesi and Procházková, 2014); hence, this "primitive" immunity has allowed the bulk of animal diversity to thrive in a plethora of ecosystems across the globe, demonstrating a robust capacity for immune protection (Boraschi, 2014, Kudryavtsev and Polevschikov, 2004, Murphy and Weaver, 2009).

The presence of pigmented aggregates described as the agglutination of individual cells (Kindred, 1924) has been noted, mainly within the perivisceral coelom (i.e., general body cavity), in several animal taxa, including annelids (Poinar and Hess, 1977), sipunculids (Lunetta *et al.*, 2004), insects (Satyavathi *et al.*, 2014) and echinoderms (Smith *et al.*, 2018). Within echinoderms, the colloquial name "brown bodies" was coined at least half a century ago (Hetzel, 1965, Hyman, 1955) to refer to these aggregates. This term is still largely used today, even though the appearance of these aggregates has now been found to vary from colourless to deep red to brown (Bilej *et al.*, 2010, Boolootian and Giese, 1958, Caulier *et al.*, 2020, Jans *et al.*, 1995, Pagliara *et al.*, 2003). Thus, in order to capture the different synonyms and polymorphic appearance of these entities (e.g., brown and red bodies, corpuscles, granules), they will be herein defined as aggregates, as per Caulier *et al.* (2020).

Within Echinodermata, cellular aggregates have been primarily studied in holothuroids (sea cucumbers), both in the perivisceral coelomic fluid (Jans *et al.*, 1995) and the hydrovascular system (Caulier *et al.*, 2020). Aggregates have also been documented in echinoids (sea urchins) in response to foreign particles and serving coagulation purposes (Branco *et al.*, 2014, Coffaro

and Hinegardner, 1977, Matranga, 2005, Pinsino *et al.*, 2007). Despite not having been described as independent aggregates in asteroids, some studies showed the clotting of numerous cells at wound sites (Furukawa *et al.*, 2009, Furukawa *et al.*, 2016, Gorshkov *et al.*, 2009, Reinisch and Bang, 1971). A similar involvement in wound healing was reported in ophiuroids (brittle stars) and crinoids (feather stars; Ben Khadra *et al.*, 2018, Biressi *et al.*, 2010), with no description of the presence of aggregates. Overall, the forms and functions of aggregates are still poorly understood in echinoderms, although they are generally believed to be associated with cellular drivers of the immune system and, by association, of the innate immune response (Canicatti and Quaglia, 1991, Majeske *et al.*, 2013, Söderhäll, 2010). For the purpose of this research, aggregation is defined as the active process through which freely circulating coelomocytes come together in the coelomic (perivisceral or hydrovascular) fluid, whereas clotting is defined as the general clumping of coelomocytes, at a wound site. A study has recently provided details regarding the kinetics of aggregate development in response to foreign particles and other stressors in sea cucumbers, showing that particles or damaged tissues need to be packaged as aggregates in order to be removed from the body (Caulier *et al.*, 2020).

The independent cells that constitute the building blocks of aggregates are known as coelomocytes and have been the topic of echinoderm immunology since the early 20th century (Hetzel, 1963, Kindred, 1924, Stein *et al.*, 1977). They are the basal cellular agents of echinoderm physiology, yet they are still incompletely understood in terms of their origin, function, and intercellular relationships (Caulier *et al.*, 2020, Chia and Xing, 1996, Edds, 1993, Hamel *et al.*, 2021). Collectively, coelomocytes have been associated with allograft rejection, cytotoxic responses, neutralization/removal of bacteria and foreign particles, wound healing, and various other functions within holothuroids, echinoids, and asteroids (Smith *et al.*, 2018). .

However, similar to the pattern seen in cell aggregate research, little information exists on coelomocytes in ophiuroids and crinoids (Branco *et al.*, 2014, Chia and Xing, 1996, Smith *et al.*, 2018). The coelomocytes described in the literature can be divided into six major groups: phagocytes, spherule cells (colourless and red), hemocytes, progenitor cells, crystal cells and fusiform cells (Canicattì *et al.*, 1989, Caulier *et al.*, 2020, Smith *et al.*, 2018), although not all six types have been documented in each echinoderm class. Holothuroids are described as having a more diverse range of coelomocyte types than echinoids and asteroids (Smith *et al.*, 2018). The poorly known coelomic agents of crinoids are seemingly the most primitive in this phylum (Di Benedetto *et al.*, 2014). Coelomocytes in crinoids are described as progenitor cells, phagocytes, granulocytes and amoebocytes (Di Benedetto *et al.*, 2014, Kondo and Akasaka, 2010, Mozzi *et al.*, 2006); however, these cells are sometimes categorized as corpuscles instead of as coelomocytes (Carnevali *et al.*, 2001). A probable reason for the vague descriptions of immune agents in crinoids thus far is that research in this class focuses largely on the regeneration process rather than the immune system as a whole (Di Benedetto *et al.*, 2014, Kondo and Akasaka, 2010, Mozzi *et al.*, 2006). Comprehensively understanding echinoderm immune systems requires an integrated study of aggregates and coelomocytes. While the literature on free coelomocytes is richer than the work that has been done on aggregates, there are still many gaps and terminology discrepancies in the descriptions of these cells (Chia and Xing, 1996, Hetzel, 1965, Noble, 1970, Smith, 1980). These inconsistencies make it difficult to fully understand the functions of coelomocytes, including the processes leading to their aggregation and the roles aggregates serve during and after their creation.

The present study is a first attempt at directly assessing the presence and nature of aggregates in 23 species belonging to the five extant classes of echinoderms, including their

major attributes (i.e., colour, size) and cellular make-up, to provide a uniform framework for future studies. The first segment of this study sought to confirm our assumption that all classes in this phylum display coelomocyte aggregates and to compare aggregate features (i.e., colour, size, composition) among them, and a second segment aimed to determine the main coelomocyte groups present and identify those involved in the formation of aggregates. The colour, size, shape, and composition of small (early synthesis) and large (mature or late stage of synthesis) aggregates were characterized. Members of Holothuroidea, Echinoidea, Asteroidea, Ophiuroidea, and Crinoidea were predicted to develop coelomocyte aggregates in response to the presence of foreign particles and it was anticipated that these aggregates would display different compositions, morphologies, and colours across different classes and possibly different species. It was further predicted that aggregates encasing foreign materials would ultimately be expelled from the body cavity through class-specific (morphology related) pathways. Because echinoderms sit next to chordates in the deuterostome clade, exploring the diversity and dynamics of their cellular immune responses may improve our understanding of the evolution of immunity in chordates (Edds, 1993, Gross *et al.*, 1999, Smith and Davidson, 1994). To assess these hypotheses, a standard catalyst was used to stimulate, trace and confirm the presence of coelomocytes and subsequent aggregates across all classes of extant echinoderms.

2.3 Materials and Methods

2.3.1 Collection and holding

Species of echinoderms belonging to the five extant classes (Holothuroidea, Echinoidea, Asteroidea, Ophiuroidea, and Crinoidea) were obtained from a variety of locations (Supplementary Table S2-1). Species from temperate and polar habitats were collected: (i) with

the CCGS *Amundsen* in the Northwestern Atlantic and Arctic Oceans in July 2019 between 500 and 3000 m depths; (ii) with the CCGS *Teleost* in northeastern Newfoundland and Labrador between November 2017 and November/December 2019 at 200-1500 m depths; and (iii) by scuba divers along the coast of the Avalon Peninsula (Newfoundland) between fall 2018 and fall 2019 at 4-20 m depths. Most cold-water species were held alive at the Ocean Sciences Centre of Memorial University (Newfoundland, eastern Canada; see Supplementary Table S2-1, Primary taxa). A few individuals collected in 2017 on the CCGS *Amundsen* were preserved in ethanol and analyzed (see Supplementary Table S2-1, Supplementary taxa).

Live individuals were kept in 20-500 L tanks supplied with running ambient seawater at a rate of 75-250 L h^{-1}. The water temperature in the holding tanks fluctuated over the annual cycle between 0-8°C and the photoperiod mirrored the natural environment. All filter/suspension feeding species (e.g., *Cucumaria frondosa*) were fed on natural seston found in the ambient seawater (Gianasi *et al.*, 2019). The carnivorous echinoderms were fed bi-weekly using known elements of their diet: whole sea cucumbers (*C. frondosa*), cracked mussels (*Mytilus edulis*) or whole sea urchins (*Strongylocentrotus droebachiensis*; Gaymer *et al.*, 2001). Only feeding individuals attached to substrate, with no sign of injuries, were used for the experiment. Three species of tropical Crinoidea were also collected off the coast of Sri Lanka (5.98957N: 80.2216E) at 15 m depth; they were briefly held in a seawater tank at 25°C and processed within a week of reception (see Supplementary Table S2-1, Primary taxa).

2.3.2 Standard processing protocol

Activated carbon particles (Fluval®) were chosen for this study based on their traceability and previous documentation of successfully triggering the aggregation of free coelomocytes within various echinoderm classes (Bertheussen, 1981, Caulier *et al.*, 2020,

Hetzel, 1965, Smith *et al.*, 2018). The amount of carbon particles injected into each organism varied between 3600.00 and 6200.00 µg depending on the size of the individual (Supplementary Table S2-1). The average granular size of the carbon particles was assessed by measuring samples using microscopy (Leica stereoscope using LASX software and a Leica DFC 7000T camera) and determined to be 25.39 ± 25.28 µm in diameter. Samples of carbon particles were diluted with filtered seawater at a ratio of 1:5 (carbon: seawater) for injection (Bertheussen, 1981, Hetzel, 1965, Smith *et al.*, 2018). Each individual was injected at taxon-specific locations using an 18 G needle. In Holothuroidea the injection was done at the base of two extended tentacles, just right of the genital papilla, as per Caulier *et al.* (2020). Echinoidea were injected ventrally through the peristomal membrane. Asteroidea were injected in two arms just right of the madreporite and two thirds of the way down the arm, closer to the tip and away from the hepatopancreas and gonad. Ophiuroidea were injected directly into the central disk between two arms. The injection was along the side of the central disk, parallel and closer to the ventral surface to avoid puncturing organs like the stomach and gonads. Crinoidea were injected into the calyx. All injected individuals were held for a minimum of 96 h before being processed, as per Caulier *et al.* (2020), and no longer than one week (Dales, 1992) under the holding conditions described above.

Before processing (n = 4 individuals per species, including 3 injected with carbon and 1 not injected) the entire individual was photographed and its total wet weight measured after 3min blotting on paper towel, using a digital scale (Scout^{TM} Pro scale). In holothuroids, the contracted length (mouth to anus) and the contracted girth (circumference) at mid-body length was measured. Echinoids were measured for the maximum test diameter. Asteroids were measured for radius, using the mean distance measured from the centre of the disk to the arm tip of three

arms. In ophiuroids, the diameter of the central disk was measured and in crinoids the length of the calyx was used.

Following weight and size measurements, individuals were sacrificed. They were opened as superficially as possible to avoid damaging internal organs that could contaminate the results (e.g., gonads, intestine or stomach, hepatopancreas). Areas with radial canals, podia or pedicellaria were also avoided. The dissection technique used, varied between classes to ensure the collection of free coelomocytes and aggregates from the perivisceral coelom and/or the hydrovascular system. The coelomic fluid from the perivisceral coelom was collected from each species studied. In addition, fluid from the ampullae of the podia was collected in asteroids and echinoids (except for *Echinarachnius parma*); in holothuroids, fluid from the Polian vesicle and the ampullae of the tentacles was also collected (except for the sea cucumber *Chiridota laevis*). Processing the coelomic fluid allowed for the characterization of colour, and size of aggregates as well as the general presence of coelomocyte types. The sex of each individual was determined by taking a gonad smear and identifying either spermatozoa or oocytes under the microscope (Nikon Eclipse 80i).

The fluid of each target cavity (either the perivisceral coelom or hydrovascular system) was drained into a falcon tube and the total volume was recorded. To document the free coelomocytes within individuals of each species, coelomocytes were photographed under the microscope (described above) at 400X using an Olympus DP73 camera. Photos were taken of live coelomocytes within five minutes after extraction before preservation of subsamples in 95% ethanol and 4% formalin in sea water.

To support accurate photo analysis of aggregates, they were split into two different categories: small/early (< 200 μm) and large/mature (≥ 200 μm), although the focus, in terms of

size, remained on the mature aggregates. Due to aggregates appearing in a wide variety of sizes, dividing them into subgroups allowed for more precise measurement and analysis (Caulier *et al.*, 2020). Small aggregates were measured and counted on a hemacytometer (LW Scientific) under the microscope at 40X. Large aggregates were measured and counted by taking a 2 ml sample of perivisceral coelomic fluid or hydrovascular fluid, diluted with filtered seawater at a 1:5 (fluid: seawater) and poured evenly into gridded Petri dishes (36 grids, 13 X 13 mm). Five of the numbered grids in the dish were randomly identified for analysis using CalculatorSoup© (random number generator). Aggregates were examined under an automated Leica stereoscope (using LASX software and a Leica DFC 7000T camera) for size.

2.3.3 Aggregate formation and phylogenetics

Aggregates were examined to better understand the cell types involved in their formation. In all species across the five extant classes of echinoderms (n=23) all coelomocytes were examined and when possible, identified in both the early and late aggregate forms. Recognizable individual cells were identified based on the observed free coelomocytes from each species.

From the various large colour aggregates (fully formed and ready to be expelled) observed in the various species tested, phylogenetic correlations were examined at the class and order levels. Correlation with depth of collection and body colour of the species itself was also considered.

2.3.4 Complementary observations

The expulsion of aggregates out of the body was monitored daily. Their size, colour and the time of their expulsion was determined and compared to the latest form of aggregates found inside the coeloms. Both the bottom of the tanks and the external surfaces of organisms were visually examined during the three-day incubation period (described above) using a Nikon SMZ

1500 boom microscope (with Olympus SC50 camera). Characteristics of aggregates were confirmed under automated Leica stereoscope (described above), as appropriate. The texture and colour of expelled aggregates were compared with the counterparts found inside the coeloms, as per Caulier *et al.* (2020) where aggregates in a holothuroid changed from red to brown after their expulsion.

Differences in mean size of large and small aggregates (both pre- and post-expulsion) (always followed in the text by the standard deviation, SD) were assessed separately using one-way ANOVAs and, where applicable, a Holm-Sidak post-hoc test. This was done using SigmaPlot software. Significant differences were considered where the p-value fell below the conventional alpha of 0.05.

2.4 Results

2.4.1 Colour, morphology and size of large aggregates

Aggregates of free coelomocytes catalyzed by the presence of carbon particles were detected across all five classes of echinoderms. Diversity in colour, shape and size of these aggregates was noted among the various classes (Figure 2-1). Each aggregate was composed of one or more coelomocyte types, with the diversity of these cells demonstrating varying levels of conservation within and across the phylum.

2.4.1.1 Holothuroids

All three species of holothuroids examined, produced large aggregates with different intensities of red pigmentation (Figure 2-1, 2-2A-D). Those found in the apodid *Chiridota laevis* were deep red with undertones of purple; whereas among the two dendrochirotid species, aggregates of *Cucumaria frondosa* were bright scarlet red and those of *Psolus fabricii* had

orange hues. However, the core of the aggregates in all species was translucent white; the red pigmentation appearing mainly in the outer layer. Their shapes varied from oblong in *C. laevis* (Figure 2-2A), angular or oblong in *C. frondosa* (Figure 2-2B, C), to round in *P. fabricii* (Figure 2-2D). The superficial appearance of aggregates also varied. In *C. laevis,* a loosely packed external layer created a bumpy and uneven surface, lacking structural definition (Figure 2-2A); in *C. frondosa*, the external layer was smooth and tight, forming a packed bundle with a well-defined and glossy surface (Figure 2-2B); in *P. fabricii* aggregates appeared matte and feathery (Figure 2-2D) and did not have the glossy "coating" seen in *C. frondosa.* Aggregates in the three holothuroid species also differed in the way they encapsulated carbon particles and in the size they reached. In *C. laevis*, particles were distributed randomly throughout the aggregate (Figure 2-2A); whereas in *C. frondosa*, they were grouped together as a distinct core (Figure 2-2C). Aggregates in *P. fabricii* were too opaque to assess this feature. Finally, the aggregates of the two dendrochirotids, *C. frondosa* and *P. fabricii*, were similar in size (284.69 ± 134.33 μm and 280.15 ± 107.88 μm, respectively) and clearly smaller ($p < 0.001$) than those of the apodid *C. laevis* (791.43 ± 430.40 μm; Figure 2-3).

2.4.1.2 Echinoids

Within echinoids, the species examined presented large aggregates of varying colour (Figure 2-4). In *Echinarachnius parma* they were light green (Figure 2-1, 2-4A) sometimes with a faint red overcoat (Figure 2-4B); in *Strongylocentrotus droebachiensis* they were a purple colour over a whitish core (Figure 2-4C); in *Brisaster fragilis* they were brown (Figure 2-4D). Due to preservation, the aggregates in *Phormosoma placenta* were more degraded and not as brilliant in hue; however, they still showed traces of purple pigmentation (Figure 2-4E). In *E. parma*, *S. droebachiensis* and *B. fragilis*, the aggregates seemed tightly packed with a defined

shape and shiny, bumpy external texture (Figure 2-4A-D); however, in *P. placenta* the aggregates were more fragmented, possibly due to preservation. In aggregates where carbon particles were visible, they were scattered randomly throughout (e.g., *E. parma*, Figure 2-4A). Average aggregate sizes in the neognathostome *E. parma,* the echinacean *S. droebachiensis*, the atelostome *B. fragilis*, and the echinothuroid *P. placenta*, were 284.67 ± 137.60 µm, 458.18 ± 621.35 µm, 506.11 ± 220.98 and 260.00 ± 87.18 µm (Figure 2-3), respectively, with no clear differences in mean aggregate sizes emerging among those orders (Figure 2-3; $p = 0.089$).

2.4.1.3 Asteroids

Large aggregates in all ten asteroid species examined showed uniform colouration from the outer surface to the centre, displaying a range of pale or pastel tints including: translucent white (*Asterias rubens*, Figure 2-5A), pale yellow (*Ceramaster granularis* and *Henricia lisa*, Figure 2-5B, D), pale orange (*Crossaster papposus*, Figure 2-5C), pale green (*Henricia perforata*, Figure 2-5E), brown (*Hippasteria phrygiana*, *Leptasterias polaris*, *Stephanasterias albula*, Figure 2-5F, G, I) and beige (*Poraniomorpha hispida, Solaster endeca,* Figure 2-5H, J). Aggregates were generally ovoid in shape, smooth and tightly packed (Figure 2-5A, D, F, J), occasionally with protrusions (Figure 2-5C, G), or appearing unstructured in the case of *P. hispida* (Figure 2-5H). It was possible to see carbon particles encapsulated within, although the density and partitioning of particles varied among species. Some were distributed evenly (e.g., *A. rubens* and *S. endeca*, Figure 2-5A, J) and others packaged in smaller units (i.e., "polka dots" with clear space between particle bundles seen in *H. perforata*, Figure 2-5E). Carbon particles formed a core in the middle of the aggregates in some species (*C. papposus* and *H. phrygiana*; Figure 2-5C, F). Within the order Valvatida, aggregate sizes were as follows: *C. granularis* (284.76 ± 114.74 µm), *C. papposus* (254.17 ± 61.92 µm), *H. phrygiana* (256.98 ± 80.97 µm), *P.*

hispida (240.00 ± 14.14 µm) and *S. endeca* (271.51 ± 71.96 µm), with an overall mean of 265.43 ± 77.69 µm. In order Forcipulatida, the size of aggregates was: *A. rubens* (259.26 ± 110.38 µm), *L. polaris* (333.91 ± 148.86 µm), and *S. albula* (269.33 ± 57.53 µm), with an overall average of 307.06 ± 131.92 µm. In Spinulosida, they were: *H. lisa* (340 ± 10.0 µm), and *H. perforata* (250 ± 62.0 µm), with an overall average of 300.21 ± 163.63 µm (Figure 2-3). The mean aggregate size of species within Valvatida were thus different from those within both Forcipulatida ($p = 0.016$) and Spinulosida ($p = 0.049$), however there was no difference between the mean aggregate sizes of Forcipulatida and Spinulosida ($p = 0.832$).

2.4.1.4 Ophiuroids

Large aggregates appeared uniformly coloured in both species of ophiuroids examined. In the basket star *Gorgonocephalus arcticus*, they were a translucent light beige (Figure 2-6A); whereas in the brittle star *Ophiopholis aculeata* they were a light green (Figure 2-6B). Large aggregates in both species displayed a bumpy external texture and irregular shapes (i.e., some were oblong, others spherical, with random protrusions on their surface). The aggregate bundles were not tightly compacted and appeared fragmented, especially the larger ones found in *G. arcticus* (Figure 2-6A). Encapsulated carbon particles were located in a distinct area of the aggregate, leaving most of the outer mass clear and barren. The euryalid *G. arcticus* showed aggregates with an average size of 260.00 ± 54.92 µm while those in the amphilepidid *O. aculeata* were 280.00 ± 62.45 µm (Figure 2-3), with no difference between the two ($p = 0.64$).

2.4.1.5 Crinoids

Large aggregates were found within all crinoids examined, with the possible exception of *Rhizocrinus lofotensis* where preservation had caused many of the aggregates to disintegrate. Pigmentation was always spread uniformly in aggregates; their colour was either yellow or red

brown within *Oxymetra* sp. (Figure 2-7A, B), or dark brown (*Dichrometra palmata* Figure 2-7C, D). Pigmentation was not seen in the preserved samples of *Heliometra glacialis* and *R. lofotensis*. All aggregates presented a bumpy external texture and the largest appeared to have a glossy surface (Figure 2-7A, B). Some aggregates (Figure 2-7A, C) demonstrated loosely packed cells, causing the overall shape to be less defined and more fragmented. However, the red aggregates from *Oxymetra* sp. were ovoid in shape, with greater structural integrity (Figure 2-7B). In aggregates where carbon particles were visible, they were randomly distributed throughout the mass. All crinoids studied belong to the order Comatulida. Aggregates from *D. palmata* averaged 311.82 ± 83.52 µm in diameter, in *H. glacialis* they were 387.50 ± 205.49 µm and in *Oxymetra* sp. they were 425.00 ± 318.20 µm (Figure 2-3), with no clear difference among them ($p = 0.49$).

2.4.1.6 Potential drivers of large aggregate characters

Overall, among all five classes of echinoderms, the colour of the large aggregates varied from whitish to purple, including yellow, beige, green, red and brown (Figure 2-1). Red was found in members of Dendrochirotida and Apodida in holothuroids. Differently, various aggregate colours were observed among orders in Echinoidea, from light brown in Atelostomata, green to red in Neognathostomata, and purple in Echinacea and Echinothuroida. In ophiuroids, light beige aggregates were seen in Euryalida and light green in Amphilepidida. In asteroids, Spinulosida species showed light to dark green hues, whereas the three Forcipulatida species showed aggregate colours varying from blue to green-brown and the five Valvatida species exhibited aggregate colours from light beige to light orange or brown. Among crinoids, colours varied from yellow to reddish-brown or brown.

The depth distribution of the various species studied (subtidal or bathyal) did not influence the shape and colour of aggregates inside the various orders. For example, the purple colour characteristic of the aggregates in the shallow echinoids *S. droebachiensis* (Figure 2-4C) was also found in the deep-sea *P. placenta* (Figure 2-4E). Likewise, *C. granularis* (a deep-sea asteroid) and *L. polaris* (a subtidal asteroid) demonstrated similar shades of beige pigmentation in their aggregates (Figure 2-5B, G). Moreover, the colour of the adult themselves did not reflect in the colour of the aggregates observed. For example, in the transparent sea cucumber *C. laevis* and the brown sea cucumber *C. frondosa*, the aggregates were consistently red (Figure 2-2A-B). The echinoids examined had body colourations varying from brown (*E. parma* and *B. fragilis*), to light purple with a white test (*P. placenta*) to green (*S. droebachiensis*), which did not consistently match the red or purple colour of their cellular aggregates. However, *B. fragilis* and *P. placenta* exhibited aggregates with colours similar to their external pigmentation (brown and purple, respectively). Asteroids demonstrated a wide variety of body colouration from light purple (*A. rubens*) to beige (*C. granularis*) to red (*C. papposus*). Only the beige or yellow asteroids (i.e., *C. granularis* and *H. lisa*) had external pigment that somewhat matched the colour of their aggregates. In *C. papposus* and *S. endeca*, the body colour was red and purple, respectively, yet the aggregates still presented pastel orange and beige colours respectively. The brittle star *O. aculeata* exhibited brown and beige external colour but its aggregates were green, where the basket star *G. arcticus* was a light beige and had matching aggregates (Figure 2-6A-B). In crinoids, both *D. palmata* and *Oxymetra* sp. exhibited a red body colour; the latter presented aggregates of a similar pigmentation (red brown) while those of the former were brown (Figure 2-7A-B).

2.4.2 Synthesis and composition of aggregates

The initial formation of aggregates was consistent across species; free coelomocytes gathered around carbon particles, consolidating them into ever larger bundles until they fully encapsulated them. It should be noted that, while carbon encapsulated by coelomocytes was consistently observed in the early stages of aggregate formation, photos of early aggregates where carbon is not visible are included in Figures 2-2, 2-4 - 2-7 for clarity of illustration. The first stage (i.e., the core) was generally composed of a single coelomocyte type, but this catalyst was not the same among echinoderm classes, as detailed below. The next stage was the addition of more coelomocytes, of either the same or different types (i.e., whichever coelomocyte type began the aggregation process, formed a center core of three or more individual coelomocytes before cells of other types joined the aggregate). The number of coelomocyte types involved in this process also differed across classes of echinoderms.

2.4.2.1 Holothuroids

There was little difference in the fine cellular composition of aggregates among holothuroids (*C. laevis, C. frondosa* and *P. fabricii*); phagocytes were always the catalysts in early aggregates. The distinct pseudopodia of phagocytes were easily identifiable as those in the earlier stage of maturation (i.e., the petaloid phase) demonstrated primarily lamellipodia (Figure 2-2E-G) where those at a later stage of maturation (i.e., the filopodial phase) demonstrated filopodial pseudopodia (Figure 2-2K). After the initial aggregation of three or more phagocytes, other coelomocytes (i.e., progenitor cells, hemocytes; Figure 2-2F, G) joined to embed the carbon and/or phagocyte core (Figure 2-2G). The hemocyte layer accumulating at the surface of the large aggregates imparted their red pigmentation in all three species (Figure 2-2A-D). Phagocytes, morula cells, hemocytes, progenitor cells, fusiform cells and crystal cells occurred

freely in the coelomic fluid, although not all these cell types were identified within the aggregates (Figure 2-2H-M).

2.4.2.2 Echinoids

The aggregates of *B. fragilis* were nominally comprised of phagocytes and progenitor cells (Figure 2-4F) and those of *E. parma* appeared solely as a cluster of active phagocyte cells with distinctly webbed lamellipodia as well as the finer filopodial extensions (Figure 2-4G). In *S. droebachiensis*, the catalysts of aggregates were more variable, including phagocytes, colourless and red spherule cells and progenitor cells (Figure 2-4H).). As the aggregates matured, red spherule cells accumulated on the outer surface to give it its red and purple colouration (Figure 2-4B-C). Within echinoids, free coelomocytes that were identified included phagocytes (Figure 2-4I), colourless and red spherule cells (Figure 2-4J, K), progenitor cells (Figure 2-4L), as well as fusiform cells (Figure 2-4M) which have not been documented in this class previously. All coelomocytes, with the exception of fusiform cells, were present in the early aggregates. Along with demonstrating a striking colour contrast to other coelomocytes, red spherule cells also exhibited a unique ameboid locomotion which is seemingly shared only by specific morphologies of colourless spherule cells.

2.4.2.3 Asteroids

The core coelomocyte composition of early aggregates in asteroids generally differed between species. In *C. granularis*, *C. papossus, H. phrygiana, L. polaris, S. albula* and *S. endeca* the catalysts were phagocytes; their lamellipodial and filopodial extensions appeared to act as scaffolding to catch other coelomocytes and bundle them into the aggregate (Figure 2-5L- M, P-Q, S-T). These pseudopodial extensions created a more oblong structure. Comparatively, aggregates in *A. rubens*, *H. lisa*, and *P. hispida* (Figure 2-5K, N, R, respectively) were initially

formed by progenitor cells. These round coelomocytes grouped more compactly from the beginning to create rounder aggregates. As aggregates grew, the primary coelomocytes appeared to merge, forming a cohesive core. The variety of coelomocyte sizes and types involved generated a wide diversity of aggregate phenotypes (Figure 2-5). Amoebocytes (Figure 2-5U-W), colourless spherule cells (Figure 2-5X), and fusiform cells (Figure 2-5Y) occurred freely in the coelomic fluid of asteroids, as well as progenitor cells (Figure 2-5Z). Not all the coelomocytes present in the coelomic fluid were present in aggregates. While each type of coelomocyte consistently presented key morphological features (i.e., spherule cells were always comprised of granules encased by a hyaline structure), there were morphological variations between, and sometimes within, species.

2.4.2.4 Ophiuroids

The formation of aggregates in ophiuroids seemed to be catalyzed primarily by what looks like granulocytes and didifferentiated cells (synonymous with morula and progenitor cells, respectively) depending on the species, with dominance of the former in *G. arcticus* and the latter in *O. aculeata* (Figure 2-6C-D). Regardless of catalyst, the coelomocytes in the center typically lost their shape and appeared to merge with surrounding cells (Figure 2-6C-D), which gave an overall rounder shape in these aggregates than in those catalyzed by phagocytes in other classes. Free coelomocytes in the two species examined included phagocytes (Figure 2-6E), granulocytes (Figure 2-6F), didifferentiated cells (Figure 2-6G), and fusiform cells (Figure 2-6H). The latter two have not been reported in ophiuroids previously.

2.4.2.5 Crinoids

The aggregates of crinoids were formed through the bundling of phagocytes and red corpuscles (Figure 2-7E-F; see below for details). In some instances, phagocytes catalyzed

aggregate formation (extended pseudopodia visible in Figure 2-7E) and were covered by a layer of small spherical corpuscles. However, some aggregates were formed only of small spherical corpuscles. The aggregating coelomocytes did not lose their shape or create a core, leading to an irregular shape with many protrusions. The free coelomocytes of this class were documented as: phagocytes (Figure 2-5G), red corpuscles (Figure 2-5H), granulocytes (Figure 2-5I), progenitor cells (Figure 2-5J), and small spherical corpuscles (Figure 2-5K).

2.4.3 Corollary observations on encapsulation and expulsion of particles

About 24 h after the injection of carbon particles, dark spots appeared on the external surface of all asteroid species, which were easiest to detect along the arms of light-coloured soft-bodied species with clear dermal papillae (e.g., *A. rubens* and *L. polaris*; Figure 2-8). Evidence of encapsulation inside the hydrovascular system was found earlier in *H. perforata*, where individuals used coelomic fluid to flush the puncture site within 30 s and carbon particles released through this process were already surrounded by coelomocytes. Encapsulated carbon particles ultimately clustered at the arm tips of asteroids (Figure 2-9A) and were expelled out of the hydrovascular system via excretion through the dermal papillae (Figure 2-9A-D). In contrast, aggregates in holothuroids were expelled through the cloaca and anus (Figure 2-10A). While the active process of aggregate expulsion was not observed in echinoids and ophiuroids, carbon-filled aggregates were discovered around the individuals within 96 h post-injection. No evidence of aggregate expulsion was found in crinoids. Note that, since not all species released aggregates during the post-injection period, this comparison was restricted to 15 species from 4 classes.

While expelled aggregates were not documented in all echinoderm species, those that were found post-release usually exhibited different appearances than the internal aggregates. For example, the red aggregates found inside the hydrovascular system of the holothuroids *C.*

frondosa and *P. fabricii* were consistently brown when expelled (Figure 2-10A). In the echinoid *E. parma*, the aggregate colour changed from green-red to light red (Figure 2-10B), while, in the asteroid *L. polaris* the aggregate colour remained brown, both inside and outside of the coelom (Figure 2-10C). However, in the ophiuroid *O. aculeata* it went from light green to light brown (Figure 2-10D). Generally, the aggregates were more densely packed when found outside of the body (Figure 2-10A, B and C) of holothuroids, echinoids, and asteroids, while they remained loose in the case of ophiuroids (Figure 2-10D).

2.5 Discussion

This study documents and compares for the first time the appearance and composition of coelomocyte aggregates in all five classes of extant echinoderms. The presence of pigmented aggregates associated with internal organs or occurring freely in the coelomic fluid or hydrovascular system was previously only described in holothuroids and echinoids (Caulier *et al.*, 2020, Majeske *et al.*, 2013, Smith *et al.*, 2018, 2019). Here, similar occurrences are additionally characterized in several species of asteroids, ophiuroids, and crinoids. Findings confirm that encapsulation of foreign particles, and possibly pathogens, is a shared feature of innate immunity in all echinoderms, and insightful similarities and contrasts are brought to light.

Cell aggregates of various sizes and shapes described from the internal cavities of echinoids (Ridder and Jangoux, 1984) and holothuroids (Hetzel, 1965, Jans *et al.*, 1995) have commonly been dubbed brown bodies (Canicatti and Quaglia, 1991, Canicatti and Seymour, 1991, Hetzel, 1965, Jans *et al.*, 1995). However, the present study emphasized that aggregates can display a wide range of colours, from nearly transparent to purple, including yellow, green, brown, and red, along with various intensities, from bright to pastel. Interestingly, the largest aggregates documented here (mean diameter of 800 µm) were found in the smallest holothuroid

species examined (which is also among the smallest holothuroids ever studied), the apodid *C. laevis*. In the 22 other species of echinoderms under study, aggregates were smaller, with a mean around 400 µm in diameter, suggesting a maximum size that may be constrained by the adhesion properties of coelomocytes and by the aggregate size that can be expelled out of the body. As suggested by Jans *et al.* (1995), the expulsion of aggregates in holothuroids occurs as they pass through coelo-rectal canaliculi (Shinn *et al.*, 1990), described as openings located under the anal fold. *Chiridota laevis* has the capacity to undergo rapid transversal fission under stress (Jobson *et al.*, 2020), suggesting that a different method of expulsing larger-sized foreign material may exist in this species. Irrespective of their size, the majority of aggregates documented in the holothuroid species were circular/ovoid with minor protrusions, probably favoring their movement in the perivisceral fluid and hydrovascular system until expulsion. Caulier et al. (2020) suggested that the well-defined structure of aggregates in the holothuroid *C. frondosa*, with an outer layer of fusiform cells, favoured their expulsion through the cloaca-anus. However, the aggregates observed in *C. laevis* remained loosely packed, supporting that the entire mechanisms of encapsulation and expulsion may not be consistent across holothuroid orders.

There was no clear link between the colour of the aggregates and either the depth of collection or the external colour of the species itself. However, a phylogenetic trend was determined to be primarily driven by taxonomic classes and orders. Within holothuroids, red aggregates were observed herein all orders analyzed, i.e., the dendrochirotid *Psolus fabricii* and *C. frondosa*, and the apodid *Chiridota laevis*. They have also been previously reported in Molpadida (Baker and Terwilliger, 1993, Terwilliger and Terwilliger, 1988), suggesting that the red colour is consistent among holothuroid taxa. However, the aggregate colour homogeneity seen to date in Holothuroidea is absent in other classes. In two echinoid orders, i.e., Echinacea

(*Strongylocentrotus droebachiensis*) and Echinothuroida (*Phormosoma placenta*), the aggregates were purple. However, green and red aggregates were observed in the order Neognathostomata (*Echinarachnius parma*) and brown aggregates in the order Atelostomata (*Brisaster fragilis*), illustrating a greater variability of colours within this class. Among asteroids, species from the three orders showed relative uniformity in pastel colours, from translucent white to pale hues, departing from the more vivid colours seen in other classes. More precisely, pale green and light blue aggregates were only seen in Spinulosida while the two other orders showed a mix of pastel shades, from beige to brown. Within ophiuroids, the order Amphilepidida (*Ophiopholis aculeata)* showed aggregates of a light green colour and Euryalida (*Gorgonocephalus arcticus*) had beige aggregates. All crinoids belonged to one order (Comatulida), and their aggregates were shades of yellow, red brown and brown. Together, these results suggest that red aggregates are a main feature of holothuroids, purple is unique to echinoids, pastel colours characterize asteroids and green is more common in ophiuroids. Moreover, two species displayed dual colours of aggregates. The echinoid *E. parma* exhibited both green and red aggregates surrounding a white translucent core. It is likely that the green colour is transitory since three stages of green aggregates were observed. The first was wholly green aggregates, the second was green aggregates sprinkled with red coelomocytes, and the third was red aggregates with green undertones. Similarly, the crinoid *Oxymetra* sp. had yellow and red-brown aggregates; the former were assumed to be the original colour and the latter to characterize large forms where superficial cells were becoming darker. This phenomenon was also observed in the holothuroid *C. frondosa* where aggregates transitioned from red to brown during the maturation and expulsion process (Caulier et al. 2020).

Where does this variety in aggregate colours come from, and what purpose might it serve? As mentioned by Caulier *et al.* (2020), the red tint in the aggregates of the dendrochirotid *Cucumaria frondosa* is imparted by the external layer of hemocytes. Individually, hemocytes are a light orange but, when combined in large numbers, they take a deep red colour, as also observed here in Dendrochirotida (e.g., *P. fabricii*) and Apodida (e.g., *C. laevis*). The red pigment in the hemocytes of holothuroids results from the presence of hemoglobin, which explains the colour change to brown as the aggregates are expelled from the body and the hemoglobin is oxidized (Caulier *et al.*, 2020). It is also possible that the hemoglobin in holothuroid hemocytes (Fontaine and Lambert, 1973) creates oxidative stress, which is in turn used to neutralize harmful intruders during the aggregation process (Caulier *et al.*, 2020, Chaitanya *et al.*, 2016). The purple aggregates shown in the sea urchins *S. droebachiensis* and *P. placenta* come from the presence of red spherule cells on their outer surface. Despite being generally described as red in the nomenclature, these cells look purple when grouped on the surface of aggregates; they also stain the hands of investigators purple. The distinctive red to purple pigmentation in echinoids results from a naphthoquinone molecule known as echinochrome A, which has also been linked to bactericidal capabilities (Branco *et al.*, 2014, Coates *et al.*, 2018, Płytycz and Seljelid, 1993). It is possible that the colour discrepancy between red and purple comes from the oxidation of echinochrome A, subsequently altering the pigment type (Vasileva *et al.*, 2021), and possibly the visual perception. When characterizing the role of pigment within immune defense, it is also valuable to note that pigment cells are among the first immunocytes to appear at the larval phase and provide the first form of cellular immune defense. These cells are known to produce echinochrome A and other key genetic information also found in adult red spherule cells.

To our knowledge, no further work has been done to evaluate the source and purpose of other cellular pigmentation in echinoderm coelomocytes or in their aggregates; however, general work on melanin/melanization in invertebrates has contributed to the idea that pigments participate in cytotoxic defenses (Melillo *et al.*, 2018). In the present study, the green aggregates observed in the ophiuroid *Ophiopholis aculeata* could be explained by the presence of slightly tinted granulocytes and didifferentiated cells (morula and progenitor cells). Among crinoids, the red-brown aggregates seem to gain their colour from so called red corpuscles (red coelomocytes) similar to holothuroid hemocytes, with a characteristic light orange colour, spherule shape, and comparable size. Moreover, brown, and beige aggregates were observed in various species, including the echinoid *B. fragilis*, the asteroids *Solaster endeca, Hippasteria phrygiana, Leptasterias polaris, Stephanasterias albula* and the crinoid *D. palmata*. This colour of aggregates might be explained by the presence melanin (Calestani and Wessel, 2018). Melanisation is widely considered to be a conserved part of the encapsulation process across invertebrate taxa (Melillo *et al.*, 2018) and, in vertebrates, various types of melaninconsistently present earth-tone colours, including light yellows and browns (Sugumaran, 2002). In some species, including most asteroids, the exact colour of the aggregates could not be properly assessed due to their faint hues. It is possible that individual coelomocytes were not pigmented enough to generate vividly coloured aggregates.

The mechanism of coelomocyte aggregation around foreign material was relatively consistent in all five classes of echinoderms studied, although variations in the catalyst emerged. In holothuroids, the early aggregate core was composed of phagocytes across all three species. In echinoids, early aggregates were comprised primarily of phagocytes in *B. fragilis* whereas *S. droebachiensis* showed aggregate cores formed from almost all coelomocyte types available (i.e.,

phagocytes, progenitor cells, red and colourless spherule cells mixed together). Asteroids and ophiuroids formed primary aggregates from two types of coelomocytes. In asteroids, these were either amoebocytes (phagocytes) or progenitor cells and in ophiuroids they were either granulocytes (morula cells) or didifferentiated cells (progenitor cells). Crinoids initiated aggregates with either phagocytes or progenitor cells. The catalysts of coelomocyte aggregates in echinoderms show broad similarities with cells implicated in equivalent processes documented in other phyla. Among Arthropoda (Insecta), for example, *Drosophila* relies on hemocytes for nodulation to occur (Satyavathi *et al.*, 2014) whereas the tobacco hornworm *Manduca sexta* relies on granular hemocytes (most likely a morula-type cell) (Miller, 2005). Miller (2005) also noted that as these nodules matured, plasmocytes (i.e., phagocytes) gathered to form an "outer sheath" around the cellular aggregate, a process similar to what was seen as aggregates matured in the present study.

The data on aggregate synthesis from this study and the work done in other invertebrates remains broadly consistent with previous literature on echinoderms. Traditionally, the literature in this area has attributed the early synthesis of aggregate formation to various forms of amoebocytes (most likely referring to phagocytes) with pigmented cells joining later in the maturation process to create the 'brown body' (Canicatti and Quaglia, 1991, Canicatti and Seymour, 1991, Hetzel, 1965, Majeske *et al.*, 2013). Beyond this superficial look at aggregate formation, few studies have assessed the diversity and dynamics of coelomocytes involved in aggregate synthesis. Caulier *et al.* (2020) further determined that, following the initial gathering of phagocytes, a wide array of other coelomocytes (i.e., morula cells crystal cells and hemocytes) were added, before finally being coated in fusiform cells. This diversity of coelomocyte

involvement in aggregation supports the results gathered across all five extant classes in the present study.

The initial core of coelomocytes forming the early aggregates seemed to influence the overall shape. For instance, aggregates comprised mainly of phagocytes demonstrated uneven shapes with the fanned pseudopodia of these cells acting as scaffolding for other cells to latch onto and keep the aggregate growing in all directions. This can be contrasted to aggregates in which the primary coelomocytes were round (i.e., morula, progenitor or spherule cells in species like *P. hispida, G. arcticus* and *D. palmata*) where the structure seemed to grow more symmetrically, resulting in round/ovoid shapes. However, regardless of initial cell type and primary form, the shape of large aggregates was fairly consistent within and between echinoderm classes. The signaling method used to recruit massive amounts of coelomocytes into cooperative action has not been clearly described in echinoderms beyond being generally attributed to humoral factors (Boraschi, 2014, Melillo *et al.*, 2018). Some authors suggest that the lectins, most likely produced by morula-type coelomocytes, are responsible (Byrne, 1986, Caulier *et al.*, 2020). However, there are many theories regarding the mechanisms of intercellular communication in invertebrate immunology (Cherry and Silverman, 2006, Satyavathi *et al.*, 2014, Tzou *et al.*, 2002). Considering the unprecedented diversity of coelomocytes documented in the present study alone, it would be prudent to continue evaluating the mechanism more deeply before concluding.

The reaction time to the presence of foreign particles and the tempo of aggregate formation varied within the focal species, as aggregates at all stages of formation were observed at 96 h post-injection. Evidence of aggregate formation occurred as fast as a few seconds after the injection of carbon particles, especially in asteroids, suggesting that cells are standing by in

the coelomic and/or hydrovascular fluid to act rapidly on demand. However, many of those early aggregates, generally transparent, were lacking the typical colour of fully formed (large) aggregates in most of the echinoderm classes (especially in holothuroids and echinoids). Pigmentation could be largely explained by the successive layering of different coelomocyte types over time. As described in *C. frondosa*, the white early aggregates composed mainly of phagocytes and morula transform into a reddish mass when hemocytes are coating them (Caulier *et al.*, 2020, Hamel *et al.*, 2021). Moreover, Caulier *et al.* (2020) showed that depending on the coelom examined, the aggregates of the holothuroid *C. frondosa* were more or less packaged, with full maturity reached in the perivisceral cavity just before expulsion, at which time aggregates were darker in color. A similar pattern likely applies to the other echinoderms, working to explain the variable packaging results observed here among the focal species. Importantly, it cannot be excluded that inter-individual variability in aggregate features could also be due to the sex, age, or maturity of the organisms, and these aspects deserve further investigation.

The study of coelomocyte aggregates provided an indirect opportunity to assess free coelomocytes in the focal species and highlighted potentially new cell types in some of the classes, perhaps because more coeloms/cavities were explored. All free coelomocytes observed in the three holothuroids, including phagocytes, morula cells, hemocytes, fusiform cells, progenitor cells, and crystal cells had already been described previously (Caulier *et al.*, 2020). In echinoids, the phagocytes, colourless and red spherule cells, and progenitor cells had been documented (Branco *et al.*, 2014, Brothers *et al.*, 2016, de Faria and da Silva, 2008, Gross *et al.*, 1999, Smith *et al.*, 2019), but fusiform cells were seen for the first time here in *E. parma* and *S. droebachiensis*. In asteroids, amoebocytes (phagocytes), fusiform cells, progenitor cells and

hemocytes had been documented (Kanungo, 1982, Oweson *et al.*, 2008), but the present study adds colourless spherule cells to the diversity of types in this class. In ophiuroids, the presence of phagocytes, granulocytes (morula cells) and didifferentiated cells (progenitor cells) had been reported (Ben Khadra *et al.*, 2018, Biressi *et al.*, 2010), but not the fusiform cells seen here. Finally in crinoids, known coelomocytes included phagocytes, progenitor cells, and granulocytes (morula cells) (Di Benedetto *et al.*, 2014, Kondo and Akasaka, 2010, Mozzi *et al.*, 2006), to which small spherical corpuscles and red corpuscles (i.e., small spherical coelomocytes and red coelomocytes) can now be added, similar to hemocytes found in holothuroids (Boolootian and Giese, 1958).

The position of echinoderms in the deuterostome clade, partnered with their ability to thrive in a diversity of marine environments and regenerate most internal and external body parts (Zhang *et al.*, 2017) marks them as ideal interdisciplinary model organisms for fields like evolutionary developmental biology and immunology. Although coelomocyte aggregates are a conserved feature within echinoderms, differences highlighted here in their appearance and cellular composition raise questions as to their specific roles in innate immunity and how each major taxon evolved specific mechanisms to adapt to their environment. Building on the present study, a more unified characterization of the similarities and differences of cellular innate immunity among representatives of different phylogenies, living in various habitats across the globe, would provide a more solid framework for future research into the evolution of immune responses.

2.6 Acknowledgements

We would like to thank the members of the Mercier lab for their technical and intellectual support. We would also like to thank Emaline Montgomery and Javier Santander for their

contributions during the initial design and final editing of this paper. This research was partly funded by the Ocean Frontier Institute, through an award from the Canada First Research Excellence Fund to Annie Mercier.

2.7 Literature Cited

Baker, S. M., and N. B. Terwilliger. 1993. Hemoglobin structure and function in the rat-tailed sea cucumber, *Paracaudina chilensis*. *Biol Bull* **185**:115-122.

Ben Khadra, Y., M. Sugni, C. Ferrario, F. Bonasoro, P. Oliveri, P. Martinez, and M. D. Candia Carnevali. 2018. Regeneration in stellate echinoderms: Crinoidea, Asteroidea and Ophiuroidea. Pp. 285-320 in *Marine Organisms as Model Systems in Biology and Medicine*, M. Kloc and J. Z. Kubiak, eds. Springer International Publishing, Cham.

Bertheussen, K. 1981. Endocytosis by echinoid phagocytes in vitro I. Recognition of foreign matter. *Dev Comp Immunol* **5**:241-250.

Bilej, M., P. Procházková, M. Šilerová, and R. Josková. 2010. Earthworm immunity. Pp. 66-79 in *Invertebrate Immunity*, K. Söderhäll, ed. Springer US, Boston, MA.

Biressi, A. C. M., T. Zou, S. Dupont, C. Dahlberg, C. Di Benedetto, F. Bonasoro, M. Thorndyke, and M. D. Candia Carnevali. 2010. Wound healing and arm regeneration in *Ophioderma longicaudum* and *Amphiura filiformis* (Ophiuroidea, Echinodermata): Comparative morphogenesis and histogenesis. *Zoomorphology* **129**:1-19.

Boolootian, R. A., and A. C. Giese. 1958. Coelomic corpuscles of echinoderms. *Biol Bull* **115**:53-63.

Boraschi, D. 2014. How innate and adaptive immunity work. Pp. 1-7 in *Nanoparticles and the Immune System* D. Boraschi, ed. Academic Press, Oxford, UK and Waltham, USA.

Branco, P. C., D. A. L. Figueiredo, and J. da Silva. 2014. New insights into innate immune system of sea urchin: Coelomocytes as biosensors for environmental stress. *OA Biol* **18**:1-7.

Brothers, C. J., J. Harianto, J. B. McClintock, and M. Byrne. 2016. Sea urchins in a high CO_2 world: The influence of acclimation on the immune response to ocean warming and acidification. *Proc R Soc B: Biol Sci* **283**:20161501.

Byrne, M. 1986. The ultrastructure of the morula cells of *Eupentacta quinquesemita* (Echinodermata: Holothuroidea) and their role in the maintenance of the extracellular matrix. *J Morphol* **188**:179-189.

Calestani, C., and G. M. Wessel. 2018. These colors don't run: Regulation of pigment-biosynthesis in echinoderms. *Results and problems in cell differentiation* **65**:515-525.

Canesi, L., and P. Procházková. 2014. The invertebrate immune system as a model for investigating the environmental impact of nanoparticles. Pp. 91-112 in *Nanoparticles and the Immune System* Elsevier.

Canicattì, C., G. D'Ancona, and E. Farina-Lipari. 1989. The coelomocytes of *Holothuria polii* (Echinodermata). I. Light and electron microscopy. *Boll Zool* **56**:29-36.

Canicatti, C., and A. Quaglia. 1991. Ultrastructure of *Holothuria polii* encapsulating body. *J Zool* **224**:419-429.

Canicatti, C., and J. Seymour. 1991. Evidence for phenoloxidase activity in *Holothuria tubulosa* (Echinodermata) brown bodies and cells. *Parasitol Res* **77**:50-53.

Carnevali, C., M. Daniela, and F. Bonasoro. 2001. Microscopic overview of crinoid regeneration. *Microsc Res Tech* **55**:403-426.

Cary, G. A., and V. F. Hinman. 2017. Echinoderm development and evolution in the post-genomic era. *Developmental Biology* **427**:203-211.

Caulier, G., J.-F. Hamel, and A. Mercier. 2020. From coelomocytes to colored aggregates: Cellular components and processes involved in the immune response of the holothuroid *Cucumaria frondosa*. *Biol Bull* **239**:95-114.

Chaitanya, R. K., K. Shashank, and P. Sridevi. 2016. Oxidative stress in invertebrate systems. Pp. 51-68 in *Free Radicals and Diseases* InTech.

Cherry, S., and N. Silverman. 2006. Host-pathogen interactions in *Drosophila*: New tricks from an old friend. *Nat Immunol* **7**:911-917.

Chia, F. S., and J. Xing. 1996. Echinoderm coelomocytes. *Zool Stud* **35**:231-254.

Coates, C. J., C. McCulloch, J. Betts, and T. Whalley. 2018. Echinochrome A release by red spherule cells is an iron-withholding strategy of sea urchin innate immunity. *J Innate Immun* **10**:119-130.

Coffaro, K., and R. Hinegardner. 1977. Immune response in the sea urchin *Lytechinus pictus*. *Science* **197**:1389-1390.

Dales, R. P. 1992. Phagocyte interactions in echinoid and asteroid echinoderms. *J Mar Biol Assoc U K* **72**:473-482.

de Faria, M. T., and J. R. M. C. da Silva. 2008. Innate immune response in the sea urchin *Echinometra lucunter* (Echinodermata). *J Invertebr Pathol* **98**:58-62.

Di Benedetto, C., L. Parma, A. Barbaglio, M. Sugni, F. Bonasoro, and M. D. Candia Carnevali. 2014. Echinoderm regeneration: An in vitro approach using the crinoid *Antedon mediterranea*. *Cell Tissue Res.* **358**:189-201.

Edds, K. T. 1993. Cell biology of echinoid coelomocytes: I. Diversity and characterization of cell types. *Journal of Invertebrate Pathology* **61**:173-178.

Fontaine, A. R., and P. Lambert. 1973. The fine structure of the haemocyte of the holothurian, *Cucumaria miniata* (Brandt). *Can J Zool* **51**:323-332.

Furukawa, R., Y. Takahashi, Y. Nakajima, M. Dan-Sohkawa, and H. Kaneko. 2009. Defense system by mesenchyme cells in bipinnaria larvae of the starfish, *Asterina pectinifera*. *Dev Comp Immunol* **33**:205-215.

Furukawa, R., K. Tamaki, and H. Kaneko. 2016. Two macrophage migration inhibitory factors regulate starfish larval immune cell chemotaxis. *Immunol Cell Biol* **94**:315-321.

Gaymer, C. F., J. H. Himmelman, and L. E. Johnson. 2001. Distribution and feeding ecology of the seastars *Leptasterias polaris* and *Asterias vulgaris* in the northern Gulf of St Lawrence, Canada. *J Mar Biol Assoc U K* **81**:827-843.

Gianasi, B. L., J.-F. Hamel, and A. Mercier. 2019. Triggers of spawning and oocyte maturation in the commercial sea cucumber *Cucumaria frondosa*. *Aquaculture* **498**:50-60.

Gorshkov, A. N., M. I. Blinova, and G. P. Pinaev. 2009. Ultrastructure of coelomic epithelium and coelomocytes of the starfish *Asterias rubens* L. in norm and after wounding. *Cell Tissue Biol* **3**:477-490.

Gross, P. S., W. Z. Al-Sharif, L. A. Clow, and L. C. Smith. 1999. Echinoderm immunity and the evolution of the complement system. *Dev Comp Immunol* **23**:429-442.

Hamel, J.-F., S. Jobson, G. Caulier, and A. Mercier. 2021. Evidence of anticipatory immune and hormonal responses to predation risk in an echinoderm. *Sci Rep* **11**.

Hetzel, H. R. 1963. Studies on holothurian coelomocytes. i. A survey of coelomocyte types. *Biol Bull* **125**:289-301.

Hetzel, H. R. 1965. Studies on holothurian coelomocytes. ii. The origin of coelomocytes and the formation of brown bodies. *Biol Bull* **128**:102-111.

Hyman, L. H. 1955. The invertebrates: Echinodermata, the coelomate Bilateria. Pp. 763-763 in *The Quarterly Review of Biology*, A. Hudson, ed. McGraw-Hill.

Jans, D., P. Dubois, and M. Jangoux. 1995. Defensive mechanisms of holothuroids (Echinodermata): Formation, role, and fate of intracoelomic brown bodies in the sea cucumber *Holothuria tubulosa*. *Cell Tissue Res.* **283**:99-106.

Jobson, S., H. D. Penney, J.-F. Hamel, and A. Mercier. 2020. Split personality. *Front Ecol Environ* **18**:557-557.

Kanungo, K. 1982. *In vitro* studies on the effects of cell-free coelomic fluid, calcium and/or magnesium on clumping of coelomocytes of the sea star *Asterias rubens* (Echinodermata: Asteroidea). *Biol Bull* **163**:438-452.

Kindred, J. E. 1924. The cellular elements in the perivisceral fluid of echinoderms. *Biol Bull* **46**:228-251.

Kondo, M., and K. Akasaka. 2010. Regeneration in crinoids. *Dev Growth Differ* **52**:57-68.

Kudryavtsev, I. V., and A. V. Polevschikov. 2004. Comparative immunological analysis of echinoderm cellular and humoral defense factors. *Zhurnal obshcheĭ biologii* **65**:218-231.

Lunetta, G. D. a., E. Farina, and R. Manione. 2004. *Sipunculus nudus*: Particulate components of the coelomic fluid and its relationship with brown bodies. *Ital J Zool* **71**:191-199.

Majeske, A. J., C. J. Bayne, and L. C. Smith. 2013. Aggregation of sea urchin phagocytes is augmented in vitro by lipopolysaccharide. *PLoS One* **8**:e61419.

Matranga, V. 2005. *Echinodermata*. Springer, Berlin ; New York.

Melillo, D., R. Marino, P. Italiani, and D. Boraschi. 2018. Innate immune memory in invertebrate metazoans: A critical appraisal. *Front Immunol* **9**:1915.

Miller, J. S. 2005. Eicosanoids influence in vitro elongation of plasmatocytes from the tobacco hornworm, *Manduca sexta*. *Arch Insect Biochem Physiol* **59**:42-51.

Mozzi, D., I. Dolmatov, F. Bonasoro, and M. Carnevali. 2006. Visceral regeneration in the crinoid *Antedon mediterranea*: basic mechanisms, tissues and cells involved in gut regrowth. *Open Life Sci* **1**:609-635.

Murphy, K. M., and C. Weaver. 2009. *Janeway's immunobiology*. Garland Science, New York and London

Noble, P. B. 1970. Coelomocyte aggregation in *Cucumaria frondosa*: Effect of ethylenediaminetetratraacetate, adenosine and adenosine nucleotides. *Biol Bull* **139**:549-556.

Oweson, C., H. Skold, A. Pinsino, V. Matranga, and B. Hernroth. 2008. Manganese effects on haematopoietic cells and circulating coelomocytes of *Asterias rubens* (Linnaeus). *Aquat. Toxicol.* **89**:75-81.

Pagliara, P., C. Carnevali, P. Burighel, and L. Ballarin. 2003. The spherule cells of *Holothuria polii* Delle Chiaie, 1823 (Aspidochirota, Holothuroidea) during brown body formation: An ultrastructural study. *J Submicrosc Cytol Pathol* **35**:295-301.

Pinsino, A., M. C. Thorndyke, and V. Matranga. 2007. Coelomocytes and post-traumatic response in the common sea star *Asterias rubens*. *Cell Stress Chaperones* **12**:331.

Płytycz, B., and R. Seljelid. 1993. Bacterial clearance by the sea urchin, *Strongylocentrotus droebachiensis*. *Dev Comp Immunol* **17**:283-289.

Poinar, G. O., and R. T. Hess. 1977. Immune Responses in the Earthworm, *Aporrectodea trapezoides* (Annelida), Against *Rhabditis pellio* (Nematoda). Pp. 69-84 in *Comparative Pathobiology: Volume 3 Invertebrate Immune Responses*, L. A. Bulla and T. C. Cheng, eds. Springer US, Boston, MA.

Reinisch, C. L., and F. B. Bang. 1971. Cell recognition: Reactions of the sea star (*Asterias vulgaris*) to the injection of amebocytes of sea urchin (*Arbacia punctulata*). *Cell Immunol* **2**:496-503.

Ridder, C., and M. Jangoux. 1984. Intracoelomic parasitic: Sporozoa in the burrowing spatangoid echinoid *Echinocardium cordatum*: Coelomocyte reaction and formation of brown bodies. *Helgoländer Meeresuntersuchungen* **37**:225-231.

Satyavathi, V. V., A. Minz, and J. Nagaraju. 2014. Nodulation: An unexplored cellular defense mechanism in insects. *Cell Signal* **26**:1753-1763.

Shinn, G. L., S. A. Stricker, and M. J. Cavey. 1990. Ultrastructure of transrectal coelomoducts in the sea cucumber *Parastichopus californicus* (Echinodermata, Holothuroida). *Zoomorphology* **109**:189-199.

Smith, A. C. 1980. Immunopathology in an invertebrate, the sea cucumber, *Holothuria cinerascens*. *Dev Comp Immunol* **4**:417-431.

Smith, L. C., V. Arizza, M. A. Barela Hudgell, G. Barone, A. G. Bodnar, K. M. Buckley, V. Cunsolo, N. M. Dheilly, N. Franchi, S. D. Fugmann, R. Furukawa, J. Garcia-Arraras, J. H. Henson, T. Hibino, Z. H. Irons, C. Li, C. M. Lun, A. J. Majeske, M. Oren, P. Pagliara, A. Pinsino, D. A. Raftos, J. P. Rast, B. Samasa, D. Schillaci, C. S. Schrankel, L. Stabili, K. Stensväg, and E. Sutton. 2018. Echinodermata: The complex immune system in echinoderms. Pp. 409-501 in *Advances in Comparative Immunology*, E. L. Cooper, ed. Springer, Cham.

Smith, L. C., and E. H. Davidson. 1994. The echinoderm immune system: Characters shared with vertebrate immune systems and characters arising later in deuterostome phylogeny. *Ann N Y Acad Sci* **712**:213-226.

Smith, L. C., T. S. Hawley, J. H. Henson, A. J. Majeske, M. Oren, and B. Rosental. 2019. Methods for collection, handling, and analysis of sea urchin coelomocytes. *Methods Cell Biol* **150**:357-389.

Söderhäll, K. 2010. *Invertebrate Immunity*. Advances in Experimental Medicine and Biology.

Stein, E., R. R. Avtalion, and E. L. Cooper. 1977. The coelomocytes of the earthworm *Lumbricus terrestris*: Morphology and phagocytic properties. *J Morphol* **153**:467-477.

Sugumaran, M. 2002. Comparative biochemistry of eumelanogenesis and the protective roles of phenoloxidase and melanin in insects. *Pigm Cell Res* **15**:2-9.

Terwilliger, R., and N. B. Terwilliger. 1988. Structure and function of holothurian hemoglobins. P.^Pp. 589-595 in *Echinoderm Biology: Proceedings from the Sixth International Echinoderm Conference* Balkema, Rotterdam.

Tzou, P., E. De Gregorio, and B. Lemaitre. 2002. How *Drosophila* combats microbial infection: A model to study innate immunity and host–pathogen interactions. *Curr Opin Microbiol* **5**:102-110.

Vasileva, E. A., N. P. Mishchenko, V. T. T. Tran, H. M. N. Vo, and S. A. Fedoreyev. 2021. Spinochrome identification and quantification in pacific sea urchin shells, coelomic fluid and eggs using HPLC-DAD-MS. *Mar Drugs* **19**:21.

Zhang, X., L. Sun, J. Yuan, Y. Sun, Y. Gao, L. Zhang, S. Li, H. Dai, J.-F. Hamel, C. Liu, Y. Yu, S. Liu, W. Lin, K. Guo, S. Jin, P. Xu, K. B. Storey, P. Huan, T. Zhang, Y. Zhou, J. Zhang, C. Lin, X. Li, L. Xing, D. Huo, M. Sun, L. Wang, A. Mercier, F. Li, H. Yang, and J. Xiang. 2017. The sea cucumber genome provides insights into morphological evolution and visceral regeneration. *PLoS Biol* **15**:e2003790.

2.8 Figures

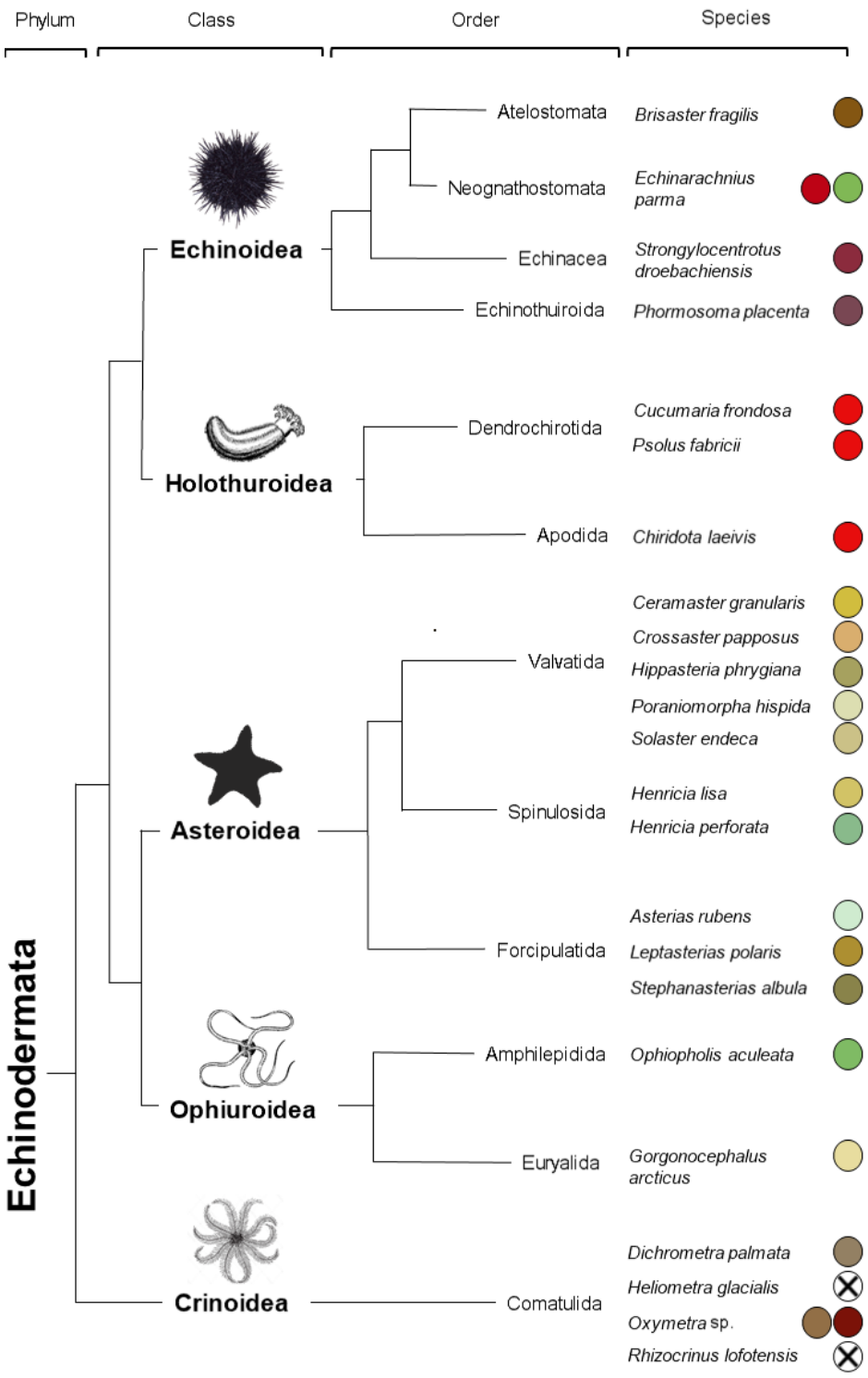
Phylum
Class
Order
Species
Echinodermata
Echinoidea
Holothuroidea
Asteroidea
Ophiuroidea
Crinoidea
Atelostomata
Neognathostomata
Echinacea
Echinothuroida
Dendrochirotida
Apodida
Valvatida
Spinulosida
Forcipulatida
Amphilepidida
Euryalida
Comatulida
Brisaster fragilis
Echinarachnius parma
Strongylocentrotus droebachiensis
Phormosoma placenta
Cucumaria frondosa
Psolus fabricii
Chiridota laeivis
Ceramaster granularis
Crossaster papposus
Hippasteria phrygiana
Poraniomorpha hispida
Solaster endeca
Henricia lisa
Henricia perforata
Asterias rubens
Leptasterias polaris
Stephanasterias albula
Ophiopholis aculeata
Gorgonocephalus arcticus
Dichrometra palmata
Heliometra glacialis
Oxymetra sp.
Rhizocrinus lofotensis

Figure 2-1 (previous page): Phylogenetic relationships within different classes of echinoderms, with colours of aggregates from each class represented by corresponding circles. White circles with an internal ‘X’ indicate species where no colour was obtained due to preservation in ethanol. Dendrogram adapted from Cary and Hinman (2017).

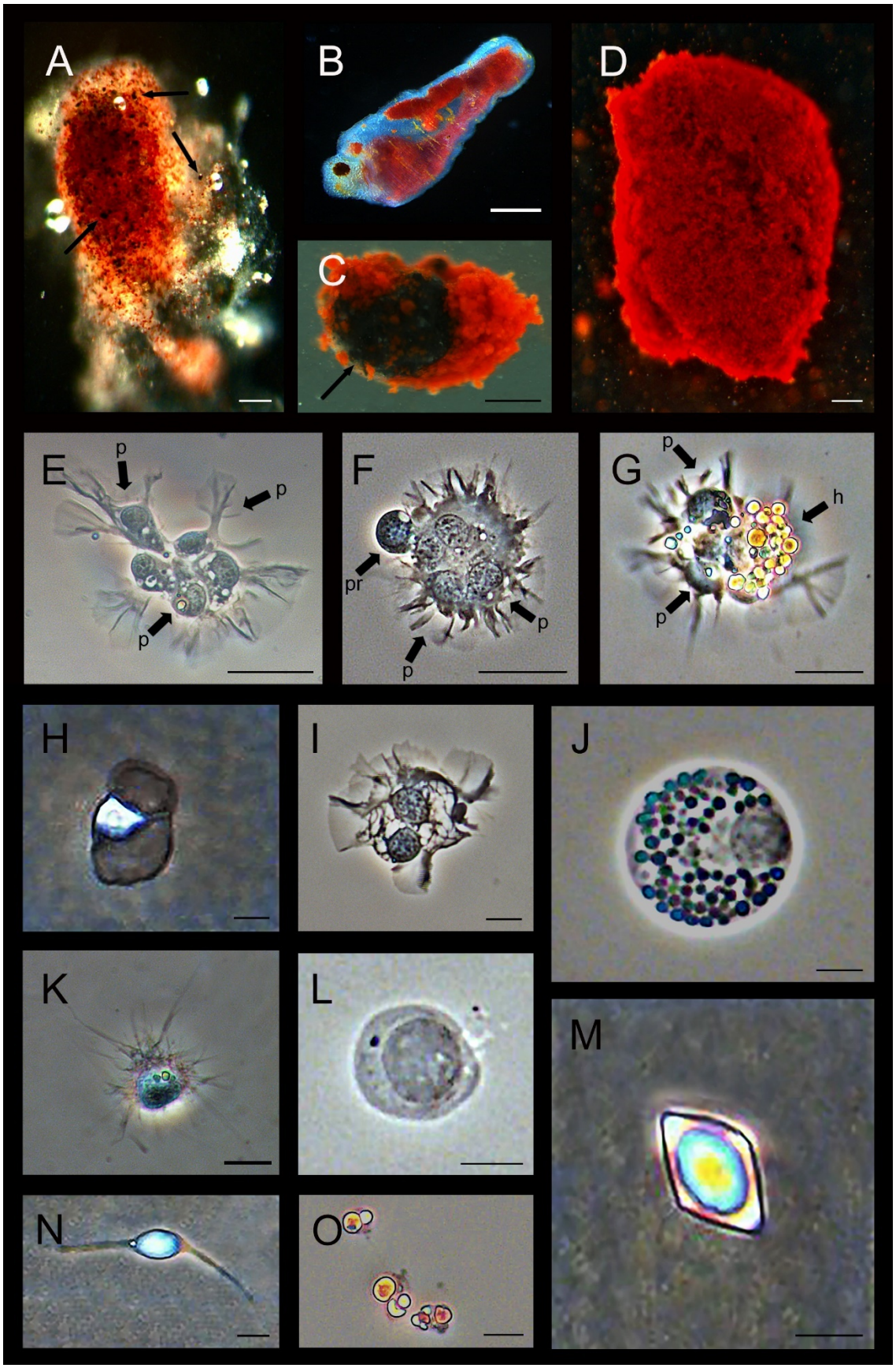
A
B
C
D
E
p
p
p
F
pr
p
p
G
p
h
p
H
I
J
K
L
M
N
O

Figure 2-2 (previous page): A-D) Large aggregates from various holothuroid species. A) large aggregate from *Chiridota laevis* (scale bar = 16 µm; arrows indicate carbon particles). B-C) large aggregates from *Cucumaria frondosa* (scale bar = 56 µm and 130 µm, respectively). B) demonstrates and small phase of large aggregation before the red colour changes to brown as seen in C) arrows indicate carbon particles. D) large aggregate from *Psolus fabricii* (scale bar = 28 µm). E-G) Small aggregates from two Holothuroid species, arrows indicate specific coelomocytes: p = phagocyte, pr = progenitor, h = hemocyte. E) small aggregate from *C. frondosa* (scale bar = 20 µm). F) Small aggregate from *P. fabricii* (scale bar = 15 µm). G) small aggregate from *P. fabricii* in transition to large aggregate form with hemocytes agglutinating on the outer surface (scale bar = 15 µm). H-O) Free coelomocytes from various Holothuroid species. H) bladder phagocyte from *P. fabricii* (scale bar = 10 µm). I) petaloid phagocyte from *C. frondosa* (scale bar = 10 µm). J) colourless spherule cell from *C. laevis* (scale bar = 7 µm). K) filapodial phagocyte from *C. frondosa* (scale bar = 22 µm). L) progenitor cell from *P. fabricii* (scale bar = 5 µm). M) crystal cell from *C. frondosa* (scale bar = 9 µm). N) fusiform from *C. frondosa* (scale bar = 4 µm). O) a cluster of hemocytes from *P. fabricii* (scale bar = 8 µm).

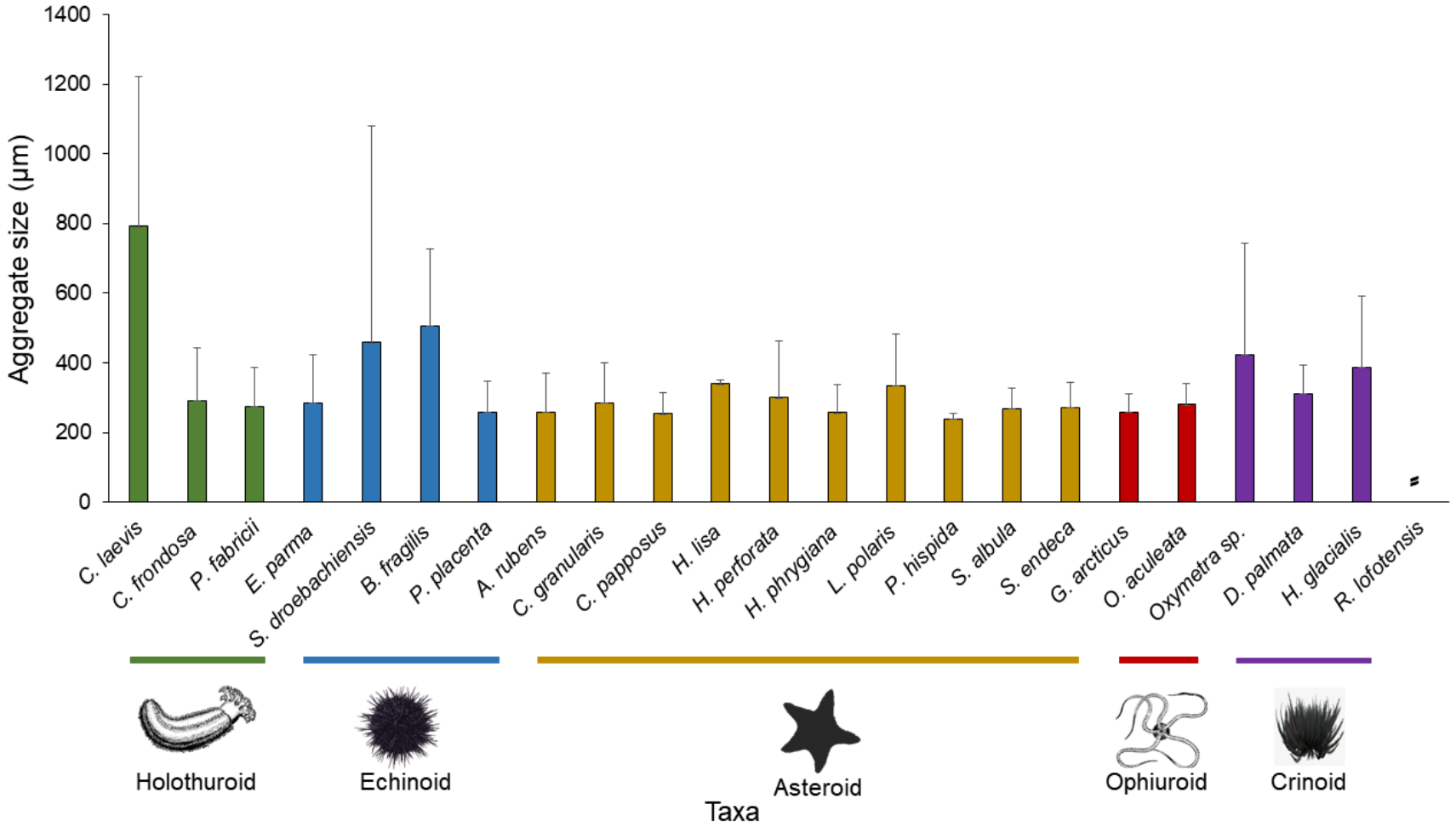

Figure 2-3: Mean diameter of large (≥ 200 µm) aggregates across all echinoderm species studied in each of the main echinoderm classes (colour-coded). Samples were taken from all coeloms. The symbol "≠" indicates that no aggregate data was present.

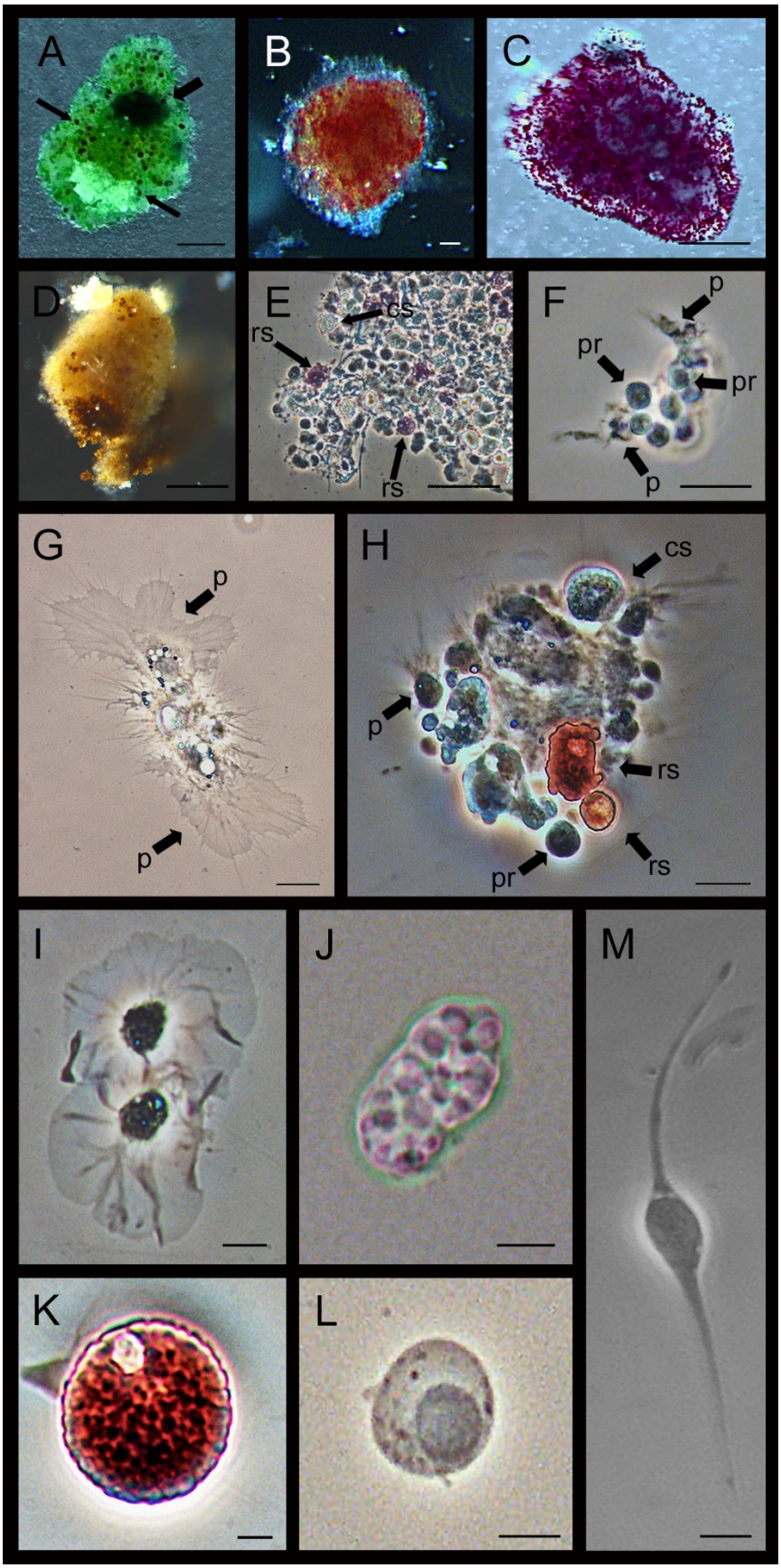
A
B
C
D
E
cs
rs
rs
F
p
pr
pr
p
G
p
p
H
cs
p
rs
pr
rs
I
J
M
K
L

Figure 2-4 (previous page): A-D) Large aggregates from various echinoid species. A-B) *Echinarachnius parma* (scale bars = 100 µm, arrows indicate carbon particles). C) *Strongylocentrotus droebachiensis* (scale bar = 200 µm). D) *Brisaster fragilis* (scale bar = 100 µm). E) Magnified view (X400) of a large aggregate in *Phormosoma placenta* (scale bar = 51 µm). F-H) Small aggregates from various echinoid species, arrows indicate specific coelomocytes: p = phagocyte, cs = colourless spherule cell, rs = red spherule cell, pr = progenitor cells. F) *B. fragilis* (scale bar = 18 µm). G) *E. parma* (scale bar = 20 µm). H) *S. droebachiensis* (scale bar = 15 µm). The two red spherule cells identified in this small aggregate are at different phases of amoeboid movement (confirmed through video observation). I-N) Free coelomocytes from various echinoid species. I) two petaloid phagocytes from *S. droebachiensis* (scale bar = 12 µm). J) colourless spherule cell from *E. parma* (scale bar = 5 µm). K) Red spherule cells from *S. droebachiensis* (scale bar = 10 µm). L) progenitor cell from *S. droebachiensis* (scale bar = 4 µm). M) fusiform cell from *E. parma* (scale bar = 6 µm).

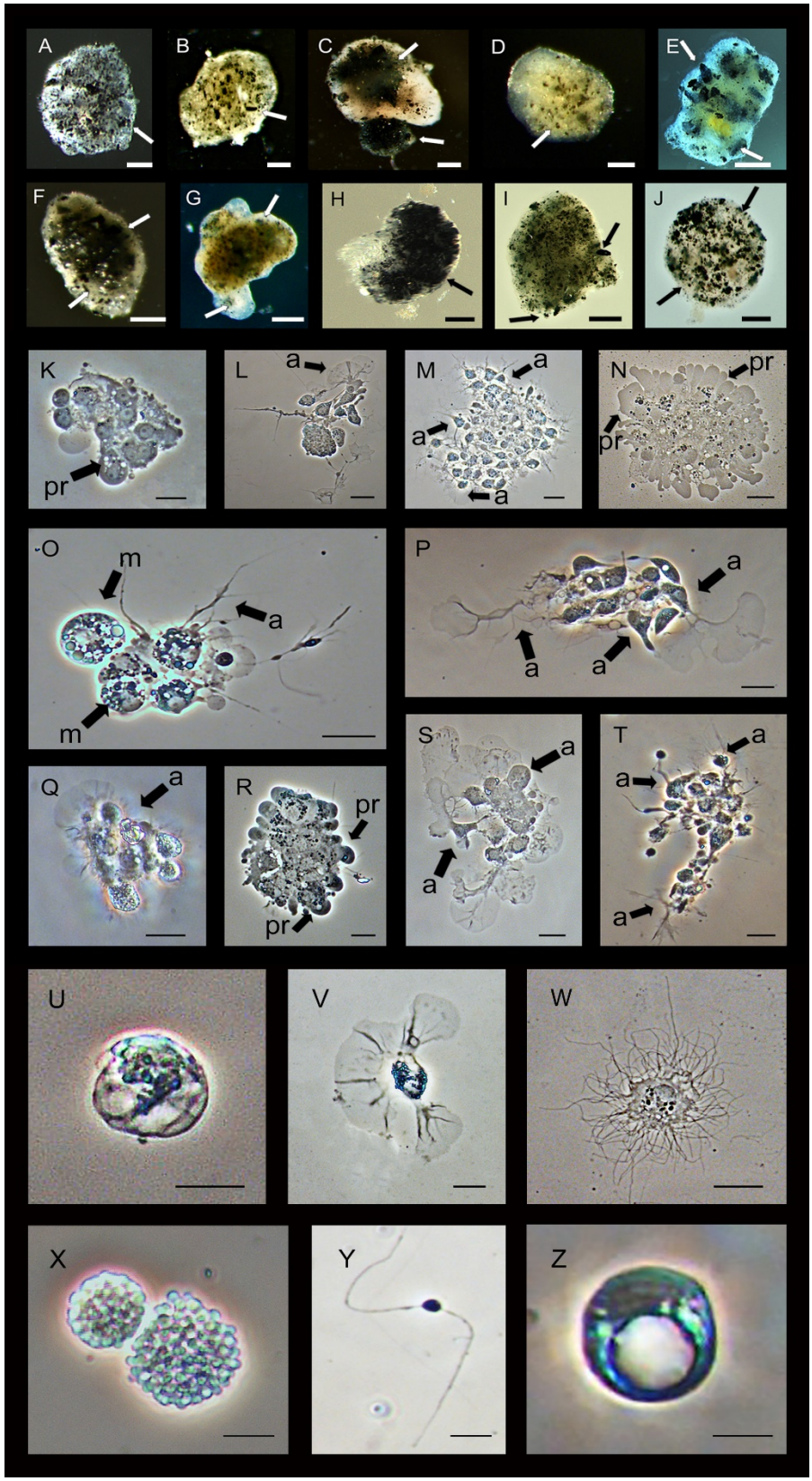
A
B
C
D
E
F
G
H
I
J
K
pr
L
a
M
a
a
a
N
pr
pr
O
m
a
m
P
a
a
a
Q
a
R
pr
pr
S
a
a
T
a
a
a
U
V
W
X
Y
Z

Figure 2-5 (previous page): A-J) Large aggregates from various asteroid species. A) *Asterias rubens* (scale bar = 94 µm). B) *Ceramaster granularis* (scale bar = 110 µm). C) *Crossaster papposus* (scale bar = 240 µm). D) *Henricia lisa* (scale bar = 67 µm). E) *Henricia perforata* (scale bar = µm). F) *Hippasteria phrygiana* (scale bar = 120 µm). G) *Leptasterias polaris* (scale bar = 150 µm). H) *Poraniomorpha hispida* (scale bar = 63 µm). I) *Stephanasterias albula* (scale bar = 120 µm). J) *Solaster endeca* (scale bar = 16 µm). Arrows in A-J indicate carbon particles. K-T) Small aggregates from various asteroid species, arrows indicate specific coelomocytes: a = amoebocyte, pr = progenitor cell, m = morula cell. K) *A. rubens* (scale bar = 15 µm). L) *C. granularis* (scale bar = 20 µm). M) *C. papposus* (scale bar = 18 µm). N) *H. lisa* (scale bar = 15 µm). O) *H. perforata* (scale bar = 15 µm). P) *H. phrygiana* (scale bar = 15 µm). Q) *L. polaris* (scale bar = 15 µm). R) *P. hispida* (scale bar = 10 µm). S) *S. albula* (scale bar = 15 µm). T) *S. endeca* (scale bar = 15 µm). U-Z) Free coelomocytes from various asteroid species. U) bladder (inactive) amoebocyte from *H. phrygiana* (scale bar = 9 µm). V) petaloid amoebocyte from *L. polaris* (scale bar = 15 µm). W) filopodial amoebocyte from *C. papposus* (scale bar = 20 µm). X) two colourless spherule cells *C. granularis* (scale bar = 6 µm). Y) fusiform cell from *S. endeca* (scale bar = 20 µm). Z) progenitor cell from *H. phrygiana* (scale bar = 50 µm).

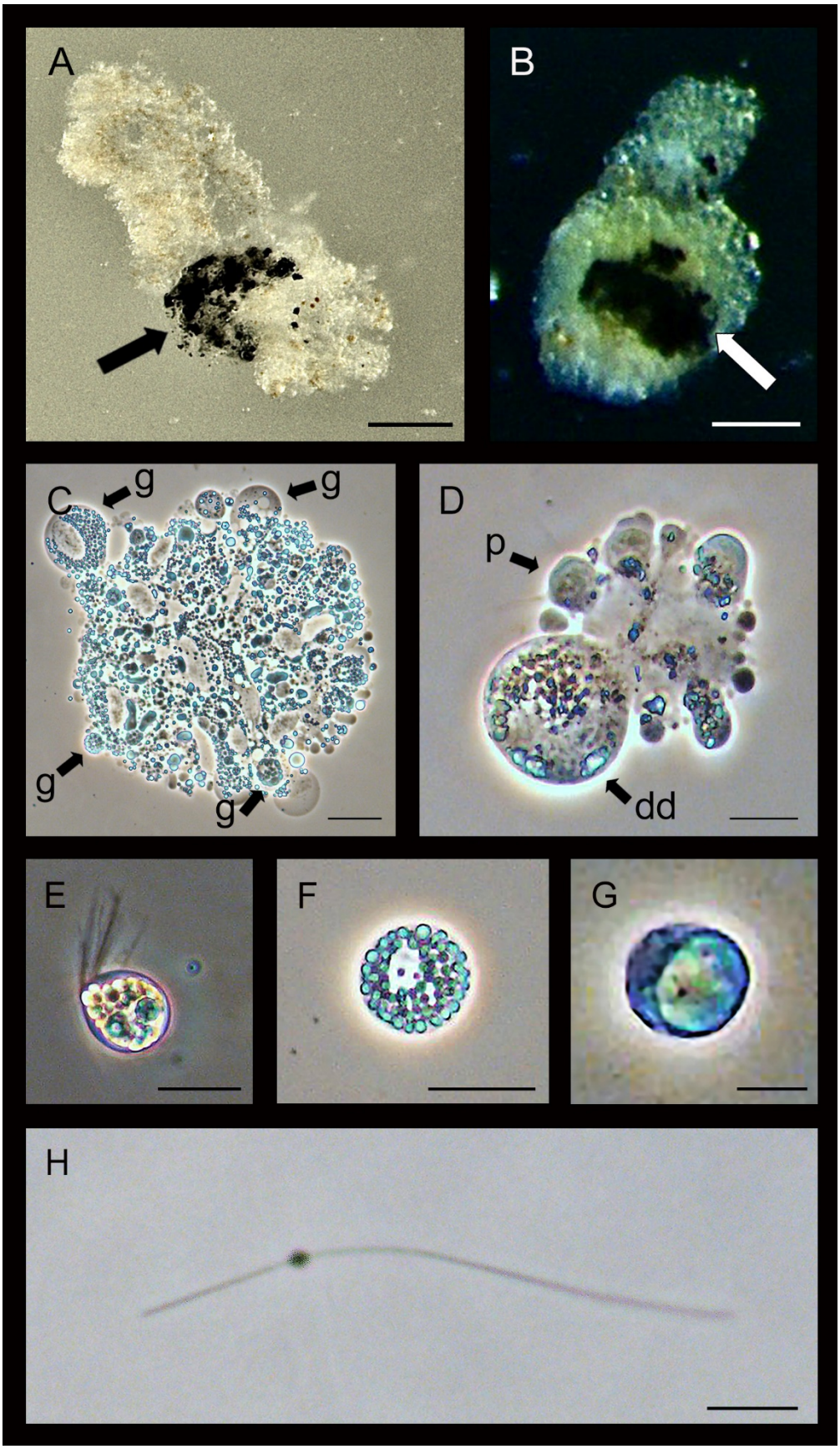
A
B
C
g
g
g
g
D
p
dd
E
F
G
H

Figure 2-6 (previous page): A-B) Large aggregates from various ophiuroid species (arrows indicate carbon particles). A) *Gorgonocephalus arcticus* (scale bar = 97 µm). B) *Ophiopholis aculeata* (scale bar = 70 µm). C-D) Small aggregates from various ophiuroid species, arrows indicate specific coelomocytes: p = phagocyte, dd = dedifferentiated cell, g = granulocyte. C) *G. arcticus* (scale bar = 20 µm). D) *O. aculeata* (scale bar = 10 µm). E-I) Free coelomocytes from two ophiuroid species. E) filopodial phagocyte from *G. arcticus* (scale bar = 15 µm) F) granulocyte from *G. arcticus* (scale bar = 11 m). G) dedifferentiated cell from *G. arcticus* (scale bar = 4 µm). H) fusiform from *O. aculeata* (scale bar = 5 µm).

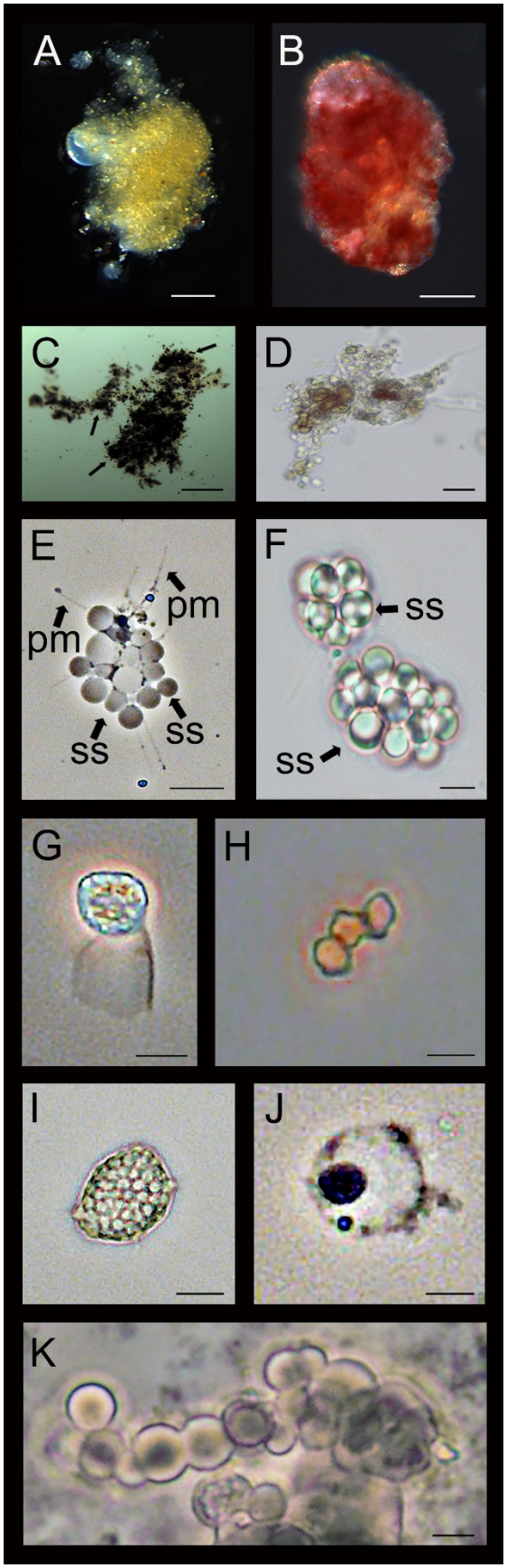
A
B
C
D
E
pm
pm
ss
ss
F
ss
ss
G
H
I
J
K

Figure 2-7 (previous page): A-D) Large aggregates from various crinoids. A-B) *Oxymetra* sp. (scale bars = 122 µm and 44 µm, respectively). C-D) *Dichrometra palmata* (scale bars = 160 µm and 64 µm, respectively). Arrows indicate carbon particles. E-F) Small aggregates from *D. palmata* (scale bars = 10 µm and 8 µm, respectively) arrows indicate specific coelomocytes, pm = phagocyte microtubule, ss = small spherical corpuscle. G-J) Live coelomocytes from various tropical crinoid species. G) phagocyte (petaloid) from *Oxymetra* sp. (scale bar = 5 µm). H) red corpuscle from *Oxymetra* sp. (scale bar = 5 µm). I) granulocyte from *Oxymetra* sp. (scale bar = 6.5 µm). J) progenitor cells (scale bar = 10 µm). K) small spherical corpuscle from *D. palmata* (scale bar = 8 µm).

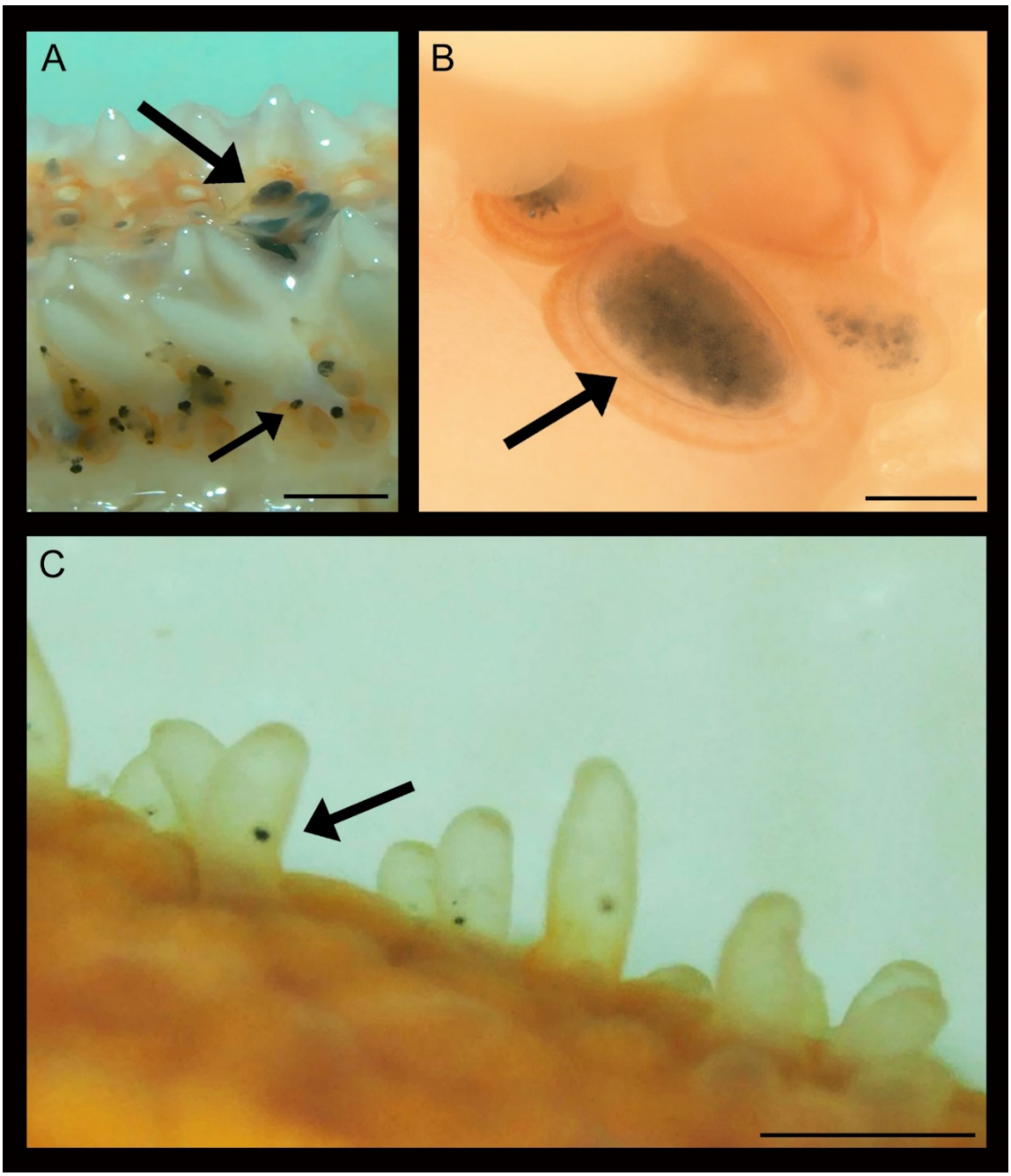

Figure 2-8 A-C) Dermal papillae of several sea star with carbon particles (arrows) visible through the tissue. A) *Asterias rubens* (scale bar = 800 µm). B) *Henricia perforata* (scale bar = 350 µm). C) *Leptasterias polaris* (scale bar = 1400 µm).

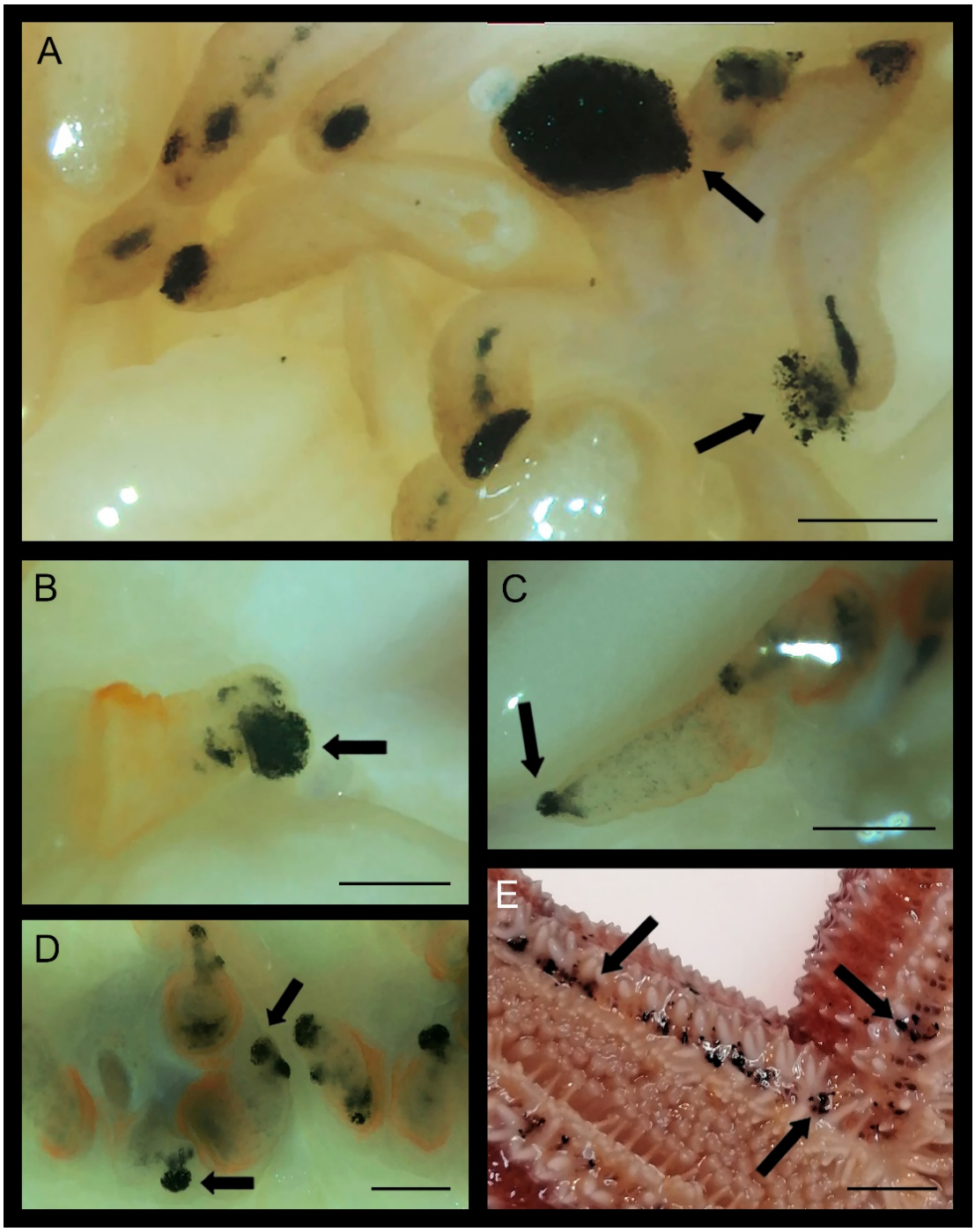

Figure 2-9: Aggregates being expelled from the dermal papillae of the asteroid *Asterias rubens*. Panels A-D) show microscopic magnification, and panel E) shows naked-eye view, of dermal papillae and carbon particles on the ventral surface. Scale bars = 800 µm in A, 370 µm in B, 420 µm in C, 400 µm in D and 4.5 mm in E.

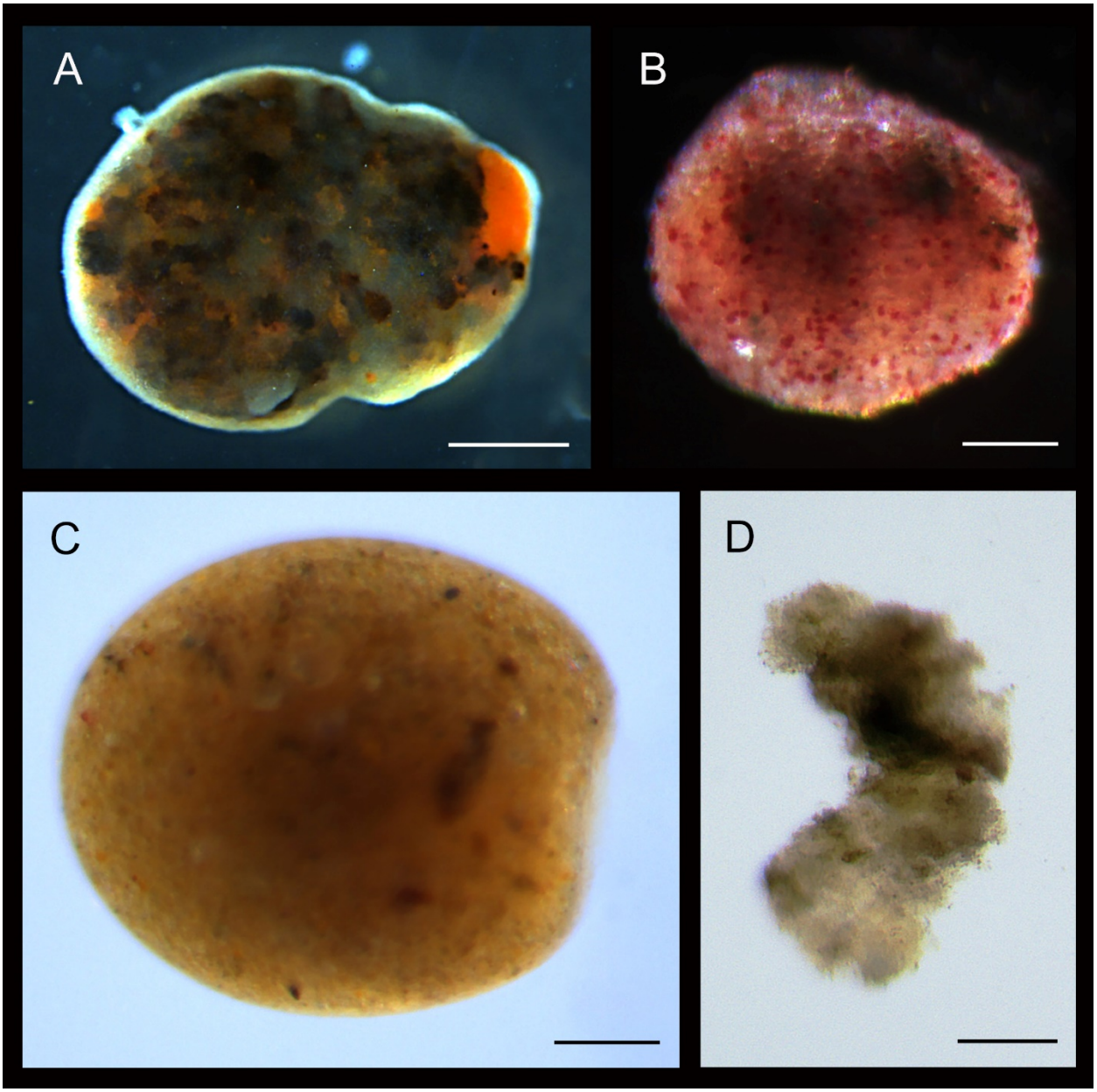

Figure 2-10: Aggregates from various echinoderms collected after expulsion from the body. A) *Cucumaria frondosa* (scale bar = 650 µm). B) *Echinarachnius parma* (scale bar = 120 µm). C) *Leptasterias polaris* (scale bar = 110 µm). D) *Ophiopholis aculeata* (scale bar = 110 µm).

2.9 Supplementary Material

2.9.1 Supplementary Tables

Supplementary Table S2-1: Echinoderm species from the five extant classes, their size (length or diameter in cm) and amount of carbon particles injected (based on their size).

Primary taxa			
Class	Species	Species Size range (cm)	Carbon Injected (µg)
Asteroidea	*Asterias rubens*	2-9	~ 4000 – 6200
	Ceramaster granularis	2-3.5	~4000
	Crossaster papposus	15-20	~ 6200
	Henricia lisa	3-9	~ 3600
	Henricia perforata	10-20	~ 6200
	Hippasteria phrygiana	5.5-7.5	~ 4000
	Leptasterias polaris	8-12	~ 6200
	Poraniomorpha hispida	1.5	~ 4000
	Solaster endeca	11-15	~ 6200
	Stephanasterias albula	5-7	~ 4000 – 5000
Crinoidea	*Dichrometra palmata*	1	<3000
	Oxymetra sp.	1	N/A
Echinoidea	*Echinarachnius parma*	5-7	~ 4500
	Strongylocentrotus droebachiensis	2-12	~ 5000
Holothuroidea	*Chiridota laevis*	5	~3600
	Cucumaria frondosa	6-11	~5000
	Psolus fabricii	8-12	~ 4000
Ophiuroidea	*Gorgonocephalus arcticus*	7.5-9	~4000
	Ophiopholis aculeata	0.25-2	~ 3600
Supplementary taxa			
Class	**Species**	**Species Size range (cm)**	**Carbon Injected (µg)**
Crinoidea	*Heliometra glacialis*	1	N/A
	Rhizocrinus lofotensis	2.5	N/A
Echinoidea	*Brisaster fragilis*	10	N/A
	Phormosoma placenta	3.5	N/A

Supplementary Table S2-2: Free coelomocytes identified across various species of echinoderms. The name used is the currently accepted/most consistently used name within the literature

Holothuroidea		**Phagocyte**	**Morula**	**Fusiform cells**	**Hemocytes**	**Progenitor cells**	**Crystal cells**	**Vibratile cells**
	Chiridota laevis	X	X	X	X	X		X
	Cucumaria frondosa	X	X	X	X	X	X	X
	Psolus fabricii	X	X	X	X	X		X
Echinoidea		**Phagocytes**	**Spherule Cells (Red/Colourless)**	**Progenitor Cells**	**Vibratile Cells**			
	Brisaster fragilis	**X**	X	X	X			
	Echinarachnius parma	X	X	X				
	Phormosoma placenta	X	X	X				
	Strongylocentrotus droebachiensis	X X	X X	X X	X X			
Asteroidea		**Amoebocytes**	**Haemocytes**	**Fusiform Cells**	**Vibratile Cells**			
	Asterias rubens	X		X	X			
	Ceramaster granularis	X		X	X			
	Crossaster papposus	X		X				
	Henricia lisa	X			X			
	Henricia perforata	X		X	X			
	Hippasteria phrygiana	X		X	X			
	Leptasterias polaris	X						
	Poraniomorpha hispida	X			X			
	Solaster endeca	X		X				
	Stephanasterias albula	X			X			
Ophiuroidea		**Phagocytes**	**Granulocytes**	**Dedifferentiated cells**				
	Gorgonocephalus arcticus	X	X	X				

	Ophiopholis aculeata	X	X	X
Crinoidea		**Phagocytes**	**Granulocytes**	**Progenitor cells**
	H. glacialis	X	X	X
	H. palmata	X		X
	D. palmata	X		X
	R. lofotensis	X		X
	Oxymetra sp.	X	X	X

Chapter 3- Cellular, hormonal, and behavioural responses of the holothuroid *Cucumaria frondosa* to environmental stressors[*]

[*] A version of this chapter is in press in the journal *Frontiers in Marine Science*.

3.1 Abstract

Holothuroids (sea cucumbers) are one of the most ubiquitous groups of benthic animals found across diverse marine ecosystems. As echinoderms, they also occupy an important place in the evolutionary hierarchy, sitting close to vertebrates in the deuterostome clade, making them valuable multidisciplinary model organisms. Apart from being ecologically and phylogenetically important, many species are commercially exploited for luxury seafood markets. With the global rise of aquaculture and fisheries, management and protection of these valuable species relies on a better understanding of how their immune systems respond to environmental and anthropogenic stressors. Here, the cellular, hormonal and behavioural indicators of stress in the North Atlantic sea cucumber *Cucumaria frondosa* were examined. The immediate and carry-over (post recovery) effects of a 1-h exposure to low salinities or to emersion (at two temperatures) highlighted that morphoplasticity in *C. frondosa* was accompanied by shifts in all monitored indicators. From their baseline levels measured in controls, densities of free coelomocytes increased, showing successions of specific cell types and subsequent coelomocyte aggregations, combined with a rise in cortisol levels. These responses mirrored increased fluctuations in cloacal opening rates, decreased force of attachment to the substrate, and enhanced movements and active buoyancy adjustment with increasingly severe stressors. The findings suggest that many systems of sea cucumbers are impacted by stresses that can be associated with harvesting and handling methods, with likely implications for the quality of the processed products. Gaining a deeper understanding of immune and hormonal responses of sea cucumbers is not only of broad ecological and evolutionary value, but also helpful for the development of sustainable fisheries and aquaculture practices, and conservation programs.

3.2 Introduction

Sea cucumbers (Echinodermata: Holothuroidea) are globally fished as a luxury seafood and many populations worldwide are fully or overfished (Purcell *et al.*, 2013). Their commercial value, which can reach over 2500 USD kg^{-1} (Purcell *et al.*, 2014), depends on the species and a suite of visual and organoleptic properties, such as size, shape, odor, and colour (Toral-Granda *et al.*, 2008). Harvesting, holding and processing conditions all have an impact on these characteristics as well as on the nutritional quality of the final products (Gianasi *et al.*, 2016, Qi *et al.*, 2016, Yang *et al.*, 2015). There is even a perceived difference in quality between wild-caught and farmed sea cucumbers, which determines their respective prices on the retail markets (Hossain *et al.*, 2020). In addition to being economically valuable, holothuroids are an important model organism (Zhang *et al.*, 2017). Their position as an echinoderm in the deuterostome clade also places them closer to vertebrates than the vast majority of other non-chordates in the evolutionary hierarchy (see Smith *et al.*, 2018, Figure 1).

While the anatomy of sea cucumbers appears quite simple, they have developed many unique adaptations that allow them to thrive in different marine environments across the globe. They can be suspension feeders, using branching oral tentacles to capture particulate matter from the water, or deposit feeders ingesting sedimented organic matter. They have traditionally been considered to live a fairly sedentary lifestyle apart from their free swimming larval phases (Grantham *et al.*, 2003, Hamel and Mercier, 1996, Young and Chia, 1982), yet the recent discovery of active buoyancy adjustment (ABA) has revealed that they can travel large distances through manipulation of their water-to-flesh ratio in response to stressful situations (Hamel *et al.*, 2019). The internal anatomy of sea cucumbers includes two main coeloms, the perivisceral cavity and the hydrovascular system. The former is the central body cavity holding most organs.

The latter is comprised of the ampullae of the tube feet, the vesicle of the tentacles and the Polian vesicle, as well as numerous canals and the madreporite (Figure 1-1), which aid in a variety of processes including locomotion, feeding, and immunity (Li *et al.*, 2013).

The two coeloms of sea cucumbers host populations of free coelomocytes (free floating in the fluid), which are considered among the most promising markers of stress (Bang, 1975, Caulier *et al.*, 2020, Coteur *et al.*, 2002, de Freitas Rebelo *et al.*, 2013, Franchi and Ballarin, 2017, Li *et al.*, 2013). Moreover, coelomocytes play pivotal roles in immune functions; they have been described across different classes of echinoderms as a line of defense against foreign particles/cells, including in Asteroidea (sea stars; Smith and Davidson, 1992, 1994); Echinoidea (sea urchins; Brothers *et al.*, 2016, Pinsino *et al.*, 2007) and Holothuroidea (sea cucumbers; Galimany *et al.*, 2018, Ramírez-Gómez *et al.*, 2010). Among sea cucumbers, coelomocytes have consistently been classified as phagocytes, morula cells, hemocytes, fusiform cells, and crystal cells (Caulier *et al.*, 2020). They are known to play roles in recognition of non-self-materials, cytotoxic defense, fluid circulation, clotting and encapsulation (Canicatti *et al.*, 1989, Chia and Xing, 1996, Smith *et al.*, 2018). Phagocytes are the most prominent coelomocytes, and they are documented to undergo transformation from petaloid to filopodial morphologies (Chia and Xing, 1996, Edds, 1980, Smith *et al.*, 2018). Coelomocytes that were monitored in sea cucumbers undergoing physical harm, intense disturbance/relocation and illness were shown to increase in abundance as both free and aggregated forms (Caulier *et al.*, 2020, Gross *et al.*, 1999, Hou *et al.*, 2019) a phenomenon also recorded in sea urchins (Branco *et al.*, 2014, Chiaramonte *et al.*, 2019, D'Andrea-Winslow *et al.*, 2012, Majeske *et al.*, 2013, Ridder and Jangoux, 1984).

The aggregation or clumping of free coelomocytes in echinoderms has been superficially mentioned in the literature but its drivers and roles have long remained poorly understood

(Canicatti and Seymour, 1991, Jans *et al.*, 1995, Ridder and Jangoux, 1984). In addition, aggregates are known under different terms in echinoderms, including encapsulates, bodies, aggregates or syncytia (Dan-Sohkawa *et al.*, 1995a, Dan-Sohkawa *et al.*, 1995b, Söderhäll, 2010) and as nodules in insects (Satyavathi *et al.*, 2014). In Holothuroidea, they were historically described as brown bodies (Canicatti and Quaglia, 1991, Hetzel, 1965, Ridder and Jangoux, 1984) despite the various colours that characterize them (see Chapter 2), making aggregates a more accurate designation. Caulier et. al., (2020) provided a detailed study of coelomocytes in the sea cucumber *Cucumaria frondosa* that included the formation of aggregates and their transition from un-pigmented to red and brown variants. The study also showed that their abundance rose with increasing severity of applied stressors, including exposure to a predator and injury.

Along with cellular markers, cortisol is a well-established hormonal marker of stress in vertebrate model systems (Sandner *et al.*, 2020, Uren Webster *et al.*, 2020, Xu *et al.*, 2019). Only recently have researchers begun testing cortisol levels in sea cucumbers (Chen *et al.*, 2018a, Hou *et al.*, 2019, Pei *et al.*, 2012) and other invertebrate taxa like mussels (Binder *et al.*, 2019, Chen *et al.*, 2018a). Cortisol levels in the sea cucumber *Apostichopus japonicus* rose from 4 mmol L^{-1} to above 6 mmol L^{-1} when individuals were placed in situations known to cause stress or agitation, e.g., high conspecific density, emersion or starvation (Hou *et al.*, 2019, Pei *et al.*, 2012, Xia *et al.*, 2017).

The sea cucumber *Cucumaria frondosa* is common and abundant in North Atlantic and Arctic waters (Gianasi *et al.*, 2020). It is also one of the most important emerging commercial species in the North Atlantic and is being considered a promising candidate for multitrophic aquaculture (Nelson *et al.*, 2012, Sun *et al.*, 2020). Over the years, behavioural responses of *C.*

frondosa have been studied and correlated with their well-being (Gianasi *et al.*, 2020). Among them, the rhythm of cloacal opening provides a metric to evaluate respiration rates, which were demonstrated to increase when individuals were exposed to various stressors (Gianasi *et al.*, 2015). The force of attachment of the ambulacral podia to the substrate was also used (Ammendolia *et al.*, 2018, Hamel *et al.*, 2019). Detachment from the substrate combined with increased motility through active buoyancy adjustments have been triggered by high conspecific densities, encounters with predators, sudden decreases in salinity, and increased turbidity (Hamel *et al.*, 2019, Sun *et al.*, 2018).

The present study took an integrative approach, seeking to explore the link between behavioural and internal biomarkers of health and stress in the sea cucumber *C. frondosa.* The objective was to tease out the relationship between free coelomocyte abundance and the specificity, type and abundance of their aggregates, cortisol levels in the fluid of hydrovascular system, and known behaviours. The various components of immune defense were examined in individuals exposed to stressors selected to mimic situations commonly experienced by sea cucumbers as they are harvested (e.g., emersion/exposure to air, temperature shocks and salinity changes) as stated in Gianasi *et al.* (2016). Exploring the link between cellular and hormonal responses could help devise more reliable means of monitoring, quantifying, and comparing the stress responses of sea cucumbers with a dual aim to help mitigate their impacts on commercial products and provide a framework for conservation and evolutionary studies. The main hypothesis was that an increase in free coelomocytes and aggregates would be proportional to the severity of the stressors and would follow a rise in cortisol levels in the hydrovascular system.

3.3 Materials and Methods

3.3.1 Collection and holding conditions

Individuals of *C. frondosa* were collected in the subtidal zone (10.5 -12 m depth) of Tors Cove, Newfoundland and Labrador (47.2172° N, 52.8515° W) during the fall of 2019. To minimize stress during transport and holding, all individuals were hand collected by divers and transported at low densities inside large coolers filled with seawater. Special measures were taken to ensure that individuals were handled gently and never exposed to air at any time throughout their relocation. Individuals were distributed in a 500 L tank supplied with unfiltered running ambient seawater at a rate of 250 L h^{-1}. The water temperature in the holding tank fluctuated naturally over the annual cycle between 0-8°C, at a salinity around 35 psu, and a natural photoperiod with peak light intensity of ≤200 lux (measured using Traceable ® Dual Display Light Meter) was provided through large windows. All individuals fed on natural seston present in the ambient unfiltered seawater. Only healthy individuals of medium size (13.53 ± 2.20 cm SD contracted length) that were firmly attached to the substrate, with tentacles periodically extended and showing no sign of injuries, were used in the experiments.

Experiments were conducted in clear bare tanks of 20 L (267 *394 * 216 mm), using a single sea cucumber per tank. Both control and exposure tanks were randomly distributed in shelves, and all were lined with white corrugated plastic along the bottom to enhance contrast between the background and the brown sea cucumbers for time-lapse photography. Illumination provided by fluorescent lights covered in a mesh shade was adjusted to 200 lux, as per Gianasi *et al.* (2015). Black tarps were used to isolate the tanks from other light sources. Where applicable, the flow rate in the tanks was set to 42 L h^{-1}. Sea cucumbers were always moved from holding to

experimental tanks inside 1-2 L beakers filled with seawater to keep them submerged at all times and surgical gloves were used as needed to avoid touching them directly.

To assess both the acute and carry-over effects of stressors, five control and five exposed individuals for each treatment group were processed at two points, the first was immediately after 1 h exposure to the stressor (described below) and the second was following 1 h of exposure to the stressor plus a recovery period of 23 h under control conditions (similar to holding conditions) totaling a 24 h treatment. After the exposure and recovery (after 1 h and 24 h, respectively), all individuals were first photographed and their whole-body wet weight (after draining for 3 min on paper towel), mid-length circumference and contracted length were recorded.

3.3.2 Treatments

3.3.2.1 Air exposure treatments

Two air temperatures were tested using bare tanks: 17°C and 5°C. The higher setting (16.75 ± 0.66ºC) is typically experienced by sea cucumbers at capture and during offloading in summer; it was achieved by keeping the tanks at room temperature. The lower setting (5.08 ± 0.90ºC) is experienced by sea cucumbers stored in ship hauls and refrigerated trucks during transport to the plants, as per Gianasi et al. (2016). It was achieved by placing the experimental tank into a larger 40 L vessel filled with crushed ice (Supplementary Figure S3-1). During both experiments, the temperature was recorded using a digital thermometer (Zacro®, Model FBA_ZDT1-AUX-1). To minimize desiccation of sea cucumber epithelia and reduce air movements, a lid was used to seal and keep the humidity inside the bare tanks at ~91%, measured with a Hygrometer/thermometer (Thomas scientific Traceable®). The controls for each of the two air-exposure treatments consisted of five individuals transferred to separate

seawater-filled tanks under environmental conditions similar to holding tanks (described above; mean of 7.3°C).

3.3.2.2 Salinity exposure treatments

Two salinities commonly experienced by sea cucumbers during transport post-harvesting were tested (15 and 22 psu) and compared to ambient salinity typical off the coast of Newfoundland (control, 35 psu). To reduce the salinity, natural seawater at 35 psu was mixed with filtered, demineralized freshwater until the desired level (measured with a Milwaukee MA871 Refractometer) was reached (Supplementary Figure S3-1). As salinity experiments were conducted under static conditions, dissolved oxygen (O_2) was measured periodically (Oakton™ DO Six+ Meter) to ensure its levels remained optimal and comparable to flow-through conditions for the duration of the exposure period. Under salinities of 35, 15 and 22 psu, the dissolved oxygen levels were 104.16 ± 8.58% (SD), 91.74 ± 8.52 %, and 98.29 ± 12.09% respectively, i.e., in the range of normoxia and well above hypoxia (Huo *et al.*, 2018, Huo *et al.*, 2019, Suh *et al.*, 2014).

3.3.3 Biomarker analyses

3.3.3.1 Cellular markers (free and aggregated coelomocytes)

The body wall of each sea cucumber was opened longitudinally from anus to mouth between two rows of tube feet using scissors or a scalpel, keeping the incision shallow to avoid puncturing the hydrovascular system and allow the removal of an intact Polian vesicle. The Polian vesicle is of special interest for the present study, as it is easy to isolate to collect its fluid filled with immune cells known as coelomocytes (Caulier *et al.*, 2020, Li *et al.*, 2019). While drawing fluid across the body wall using a syringe has commonly been used (e.g., Fontaine and Lambert, 1977, Galimany *et al.*, 2018, Hou *et al.*, 2019), this blind technique does not guarantee

the collection of coelomic fluid because the respiratory tree and hydrovascular system can be accidentally punctured. On the other hand, using the Polian vesicle had two advantages: (i) it allowed the collection of uncontaminated fluid known to contain coelomocytes (Li *et al.*, 2019), and (ii) it standardized the origin of the coelomocyte and aggregate samples across individuals. The whole Polian vesicle was emptied into a 25 mL Falcon tube to record fluid volume. To determine the number and type of coelomocytes, the fluid was resuspended using a mini vortexer (MV 1 from IKA®) for 3 s and 10 µl was loaded in a hemocytometer (Neubauer, LW Scientific). Contrary to conventional protocol, the coverslip was placed on the chamber after (rather than before) it was loaded to make sure naturally formed coelomocyte aggregates would enter the chamber. Because clotting is a main issue when working with coelomocytes (Caulier *et al.*, 2020, Smith *et al.*, 2018), the samples had to be analyzed immediately after sampling (within 5 min). Free coelomocytes (individual cells) and aggregates (groups of several coelomocytes) were measured (Feret diameter; i.e., the longest possible diameter) and photographed under a light microscope (Nikon Eclipse 80i) coupled to a digital camera (Olympus DP73). Identification of free coelomocyte types was based on Caulier *et al.* (2020) for *C. frondosa*, complemented by studies of other holothuroids (Chia and Xing, 1996, Smith *et al.*, 2018). Phagocytes were subdivided in two categories, i.e., inactive (pseudopodial fans still wrapped around the nucleus also known as the bladder form; Supplementary Figure S3-2), and active (pseudopodial fans extended as petaloid or filapodial forms; Supplementary Figure S3-2B-C) (Kindred, 1924). The presence of morula cells, fusiform cells, and crystal cells were also assessed (Supplementary Fig S3-1: D-H).

The coelomocyte aggregates were divided in two classes: small and large, which corresponded nearly perfectly with early and mature forms, respectively, based on the

classification proposed by Caulier *et al*. (2020). The small aggregates were characterized by a diameter <200 µm and mostly composed of translucent coelomocytes (with minimum size of ~5 µm in diameter). These small aggregates were counted using a hemocytometer (method described above). Large aggregates were composed of coelomocytes grouped in reddish clumps measuring ≥200 µm in diameter (maximum size of 6600.00 µm in Feret diameter). Because aggregates were too large to be analyzed with the hematocytometer, a 2 mL subsample of Polian vesicle fluid was diluted with 10 mL of filtered seawater and poured into a gridded Petri dish (square, 36 grids, 10,000 mm^2). Large aggregates were counted in five grid sections selected by a random number generator (CalculatorSoup©).

3.3.3.2 Hormonal marker (cortisol)

Two subsamples of fluid (1 mL) from the extracted Polian vesicle fluid were transferred into separate Eppendorf vials and stored at -80°C within 10 min of extraction, to be used for cortisol analysis. The frozen subsamples were thawed, and their pH lowered to 1.5 - 2.0 using 0.5 M HC1 before washing once with 4 mL of undiluted methylene chloride, following a standard procedure for a competitive cortisol ELISA assay (enzyme-linked immunosorbent assay; Cayman Chemical - Item 500360, Ann Arbor, USA). To wash, methylene chloride was added to the fluid sample and vortexed for 5 seconds. After being allowed several minutes to separate, the clear bottom layer of methylene chloride was removed with a pipette, and the remainder was evaporated under a nitrogen stream before adding 250 µL of ELISA buffer (1 M phosphate solution containing 1% BSA, 4 M sodium chloride, 10 mM EDTA and 0.1% sodium azide that was diluted by a factor of 10 using UltraPure water). Preparation of assay-specific reagents followed the ELISA kit protocol (Cayman, Item No. 500360). Before plating, each sample of extracted cortisol was centrifuged at 4000 rpm for 5 min. A 96-well plate was used to

run all reagents and samples in duplicate (e.g., experimental samples, the 9-point standard curve, blank, total activity, non-specific binding and maximum binding wells). Following standard protocol, the plate was left to incubate for 24 h, washed and then shaken on an orbital shaker for 90 min. The plate was then shaken mechanically for 3 s on the microplate reader (Molecular Devices SpectraMax® M5, San Jose, USA) and read using a wavelength of 420 nm and the SoftMax® Pro v7.1 software. Data were analyzed using an Excel program designed by Cayman Chemical for this ELISA kit and publicly available (ELISADouble; https://www.caymanchem.com/analysisTools/elisa). Any readings outside the standard curve were removed as per Binder *et al.* (2019).

3.3.3.3 Behavioural markers

3.3.3.3.1 Force of attachment and cloacal opening

The force of attachment of the sea cucumbers to the substrate was quantified by attaching a zip tie to the mid-circumference of the body and pulling perpendicularly with a spring balance (Ohaus®, Model 8008-MO) as per Hamel *et al.* (2019). The weight necessary to detach the individual was converted to force in Newtons (1 N = 101.97 g). To quantify cloacal opening rhythm in *C. frondosa*, based on the work of Gianasi *et al*. (2015), the frequency of opening/closing of the anus (inspiration/expiration) was visually assessed for seven min in triplicates.

3.3.3.3.2 Behavioural scores

All other behavioural activity levels measured over the recovery period (Supplementary Table S3-1) were monitored using time-lapse videography. Two cameras were used (Brinno TLC 200 Pro and Brinno MAC 200 DN) combined with infrared lighting (ICAMI IR Illuminators, 96 pcs), which allowed continuous recording (night and day). They were mounted

above the tanks to capture the entire experimental arena and set to take one picture every 10 s, which were automatically stitched into clips by the camera software. Each metric (i.e., movement and speed, degree of attachment to the substrate, body inflation) was assigned a cumulative score on a scale from 0-4, with 0 indicating baseline levels (normal shape, immobile, firmly attached to the substrate with tentacles either extended or retracted) and 4 indicating extreme behaviour (ABA or full inflation of the body cavity, tentacle retraction combined with complete detachment from the substrate, as per Hamel *et al.* (2019). Intermediate scores (0.5-3.5) reflected the extent to which one or more parameters were affected, including body contractions, locomotion or rolling, bloating of the body wall with or without ambulacral podia extended (details in Supplementary Table S3-1).

3.3.4 Data analysis

Two-way analysis of variance (ANOVA) was conducted for each treatment (17°C, 5°C, 15 psu, 22 psu) to compare the cellular and hormonal data over both the exposure (exposed vs. control) and time (1 h vs. 24 h). All assumptions for parametric tests were met and any metrics of significance were investigated using pairwise comparison (Holm-Sidak method). Any extreme outliers were removed within each category provided that their removal did not change any overarching trends. The results from control individuals in the cortisol treatment group were not significantly different and were pooled together. All tests were performed with SigmaPlot statistical software and evaluated using $\alpha = 0.05$ to indicate strong significance although p-values <0.1 were noted as potential indicators of moderate significance based on Fisher's sorting method (Fisher, 1934). This approach is based on calls from statisticians to move away from arbitrary measures of significance (Dushoff *et al.*, 2019, Wasserstein and Lazar, 2016, Wasserstein *et al.*, 2019, Yoccoz, 1991).

To calculate percent increase in cell densities relative to baseline, the difference between the initial and final density in each exposed individual was divided by the mean baseline (control) cellular density, multiplied by 100 and averaged (mean ± SD). For comparisons of cell densities across time points, the difference between the means of each group were compared as a percentage.

3.4 Results

3.4.1 Cellular markers

3.4.1.1 Free coelomocytes

Individuals exposed to stressors, globally displayed higher densities of free coelomocytes in the Polian vesicle fluid than their respective controls (Figure 3-1). Specifically, an increase in coelomocyte density occurred after 1 h in three of the four treatments (17°C air, 15 and 22 psu salinities, Figure 3-1A, C, D) while it occurred only after 24 h under the 5°C air treatment (Figure 3-1B; for statistics see Supplementary Table S3-2). All treatments except 22 psu generated a greater departure from baseline coelomocyte densities after the recovery period (24 h) than immediately after exposure (1 h) (Figure 3-1; Supplementary Table S3-3).

Analysis of coelomocyte types showed that the most abundant were the phagocytes in all control and treatment groups (Figure 3-2). They represented 81.33 ± 8.76% of free coelomocytes after 1 h and 92.02 ± 2.76% after 24 h representing the peak increase under 17°C air exposure ($F_{1,23}$ = 4.45, p=0.046; Figure 3-2A). Similar proportions were also seen under 5°C air, and both salinities (Figure 3-2B, C and D). In air at 5°C, phagocyte densities showed no departure from baseline after 1 h (Figure 3-2B) and were 88.56 ± 7.11% higher after 24 h; this increase was too variable to be supported statistically ($F_{1,25}$ = 1.15, p=0.30; Figure 3-2B). When sea cucumbers

were exposed to 15 or 22 psu salinity, phagocyte densities showed with no clear departure from baseline (Figure 3-2C, D)

Looking at other coelomocyte types, when sea cucumbers were exposed to 17°C air, the density of fusiform cells showed a variable increase of 140.00 ± 309.84% after 1 h and 114.28 ± 327.32% after 24 h ($F_{1,23}$ = 1.05, p=0.32; Figure 3-2A). Both morula and crystal cells, which were absent from the controls, appeared in low numbers after 1 h (Figure 3-2A). Despite that the density of morula cells remained higher than baseline after 24 h, the crystal cells disappeared (Figure 3-2A). After 1 h under 5°C air, the fusiform cell densities remained comparable to baseline, but densities of morula and crystal cells were higher by 50.00 ± 41.67% and 100.00 ± 122.22%, respectively ($F_{1,25}$ = 0.71, p=0.41; $F_{1,25}$ = 4.66, p=0.040; Figure 3-2B). When exposed to 15 psu salinity, the fusiform cells increased after 1 h, the morula cells (absent in the controls) became detectable (35,000 ± 19,512 cells; $F_{1,16}$ = 0.48, p=0.50; t = 2.67, p=0.0.016, respectively) and no crystal cells were recorded after 1 h. After 24 h, the fusiform and morula cells disappeared (Figure 3-2C). At 22 psu, the morula cells increased compared to controls after 1 h ($F_{1,20}$ = 2.96, p=0.10; Figure 3-2D). However, the fusiform cells decreased by 49.40 ± 133.88% relative to baseline and no crystal cells were noted (Figure 3-2D). After 24 h, the fusiform were slightly higher than baseline and morula cells showed an increase of 188.00 ± 245.60% ($F_{1,20}$ = 1.51, p=0.25), and the crystal cells appeared for the first time in low numbers (~2000 cells).

Phagocytes were further subdivided into inactive and active cells. After 1 h under 17°C air exposure, the inactive forms in control individuals were roughly half the number of inactive cells present in exposed individuals (32.60 ± 20.82%; $F_{1,23}$ = 3.86, p=0.061; Figure 3-3A). After 24 h, proportions were similar in controls and in exposed individuals (Figure 3-3A). An increase in inactive phagocytes was observed under 17°C and 5°C air after 1 h, at 15 psu salinity after

both 1 and 24 h and at 22 psu salinity after 24 h only (Figure 3-3B-C). Inverse trends were noticed under 5°C air exposure after 24 h and at 22 psu salinity after 1 h, whereby the percentage of inactive phagocytes in exposed individuals compared to controls decreased, although not significantly, from 53.23 ± 27.62% to 36.26 ± 26.10% and 57.06 ± 19.58 to 43.82 ± 37.67%, respectively ($t = 0.11$, $p=0.92$; $t = 1.64$, $p=0.12$; Figure 3-3B-D).

3.4.1.2 Small coelomocyte aggregates

In groups exposed to 17°C air, the density of small (early stage) aggregates increased by 38.28 ± 45.60% after 1 h ($t = 2.73$, $p = 0.012$) and returned to baseline values after 24 h (Figure 3-4A; Supplementary Table S3-2). Inversely, under 5°C air exposure, small aggregate densities were similar between control and treatment groups after 1 h but were 91.54 ± 81.92% higher in exposed individuals after 24 h ($F_{1,16} = 3.86$, $p = 0.061$; Figure 3-4B). In individuals exposed to 15 psu salinity, the small aggregates increased compared to controls after 1 h ($F_{1,16} = 0.070$, $p = 0.80$) and fell to control levels after 24 h. The trend was inversed at 22 psu, where densities of small aggregates in individuals hovered around baseline after 1 h, and the difference amplified to 196.40 ± 59.91% after 24 h ($t = 2.39$, $p = 0.028$; Supplementary Table S3-2; Figure 3-4D).

3.4.1.3 Large coelomocyte aggregates

Densities of large (mature stage) aggregates were overall quite variable. Under 17°C air exposure, the density fluctuated around baseline after both 1 h and 24 h (Figure 3-5A; Supplementary Table S3-2). Under 5°C air, no clear departure occurred after 1 h but densities were 159.63 ± 411.02% higher after 24 h (Figure 3-5B; $t = 1.7$, $p = 0.10$). In the salinity treatments, individuals exposed to 15 psu displayed an increase in large aggregates by 500.00 ± 300.00% after 24 h only ($F_{1,12} = 0.049$, $p=0.83$; Figure 3-5C), whereas individuals exposed to 22

psu showed elevated densities both after 1 h exposure and 24 h recovery, by 33.33 ± 103.28% and 100.00 ± 282.84 %, respectively ($F_{1,12}$ = 0.019, p=0.89; $F_{1,12}$ = 0.088, p=0.77; Figure 3-5D).

3.4.2 Hormonal marker

Overall, cortisol levels in the Polian vesicle was variable but increased in all treatments after 1 h, except exposure to air at 5°C (Figure 3-6; Supplementary Table S3-2). This increase was statistically significant when individuals were exposed to 17°C air, passing from a mean of 25.17 ± 12.54 pg mL^{-1} in controls to 111.96 ± 36.30 pg mL^{-1} under the stressor (an increase of ~345%; Figure 3-6A). Values returned to baseline after 24 h (Figure 3-6A). Under 5°C air, no cortisol increase was noted at any time point (Figure 3-6B). In individuals exposed to 15 psu, the mean cortisol level was 21.58 ± 5.74 pg mL^{-1} under control and 33.04 ± 30.58 pg mL^{-1} under the stressor (representing an increase of ~ 52.8%); values remained elevated until the end of the experiment (Figure 3-6C). In individuals exposed to 22 psu salinity, the mean cortisol level after 1 h showed an increased from 14.60 ± 1.11 pg mL^{-1} in the control to 54.89 ± 58.31 pg mL^{-1} under the stressor (~276%; Figure 3-6D). Values remained higher than in controls until the end of the experiment (Figure 3-6D).

3.4.3 Behavioural markers

3.4.3.1 Cloacal opening rhythms and force of attachment to the substrate

All sea cucumbers that were used for the experiments showed around 1.50 cloacal openings min^{-1} in holding conditions (Supplementary Figure S3-3). When they were exposed to air, regardless of temperature, an interruption of the cloacal movements was noted, with their anus closed most of the time (Supplementary Figure S3-3A). However, release of water from the respiratory tree was observed on a regular basis, with no air intake during the process in all air exposed individuals. When these individuals were resubmerged in seawater for the recovery

period, cloacal opening resumed and increased from 0 to 1.94 and 0 to 2.16 openings min^{-1} after 1.5 h for 17°C and 5°C treatments, respectively (Supplementary Figure S3-3A). At times 2 h and 3 h, individuals exposed to 17°C air exhibited cloacal opening rhythms that were 11.2% to 23.2% faster than controls ($t = 5.79$, $p<0.001$; $t = 5.46$, $p<0.001$). Values decreased to 2.10 openings min^{-1} after 23-24 h and were too erratic to clearly differ from control values ($t = 2.27$, $p = 0.29$; $t = 2.71$, $p = 0.11$; Supplementary Figure S3-3A). Under 5°C air, cloacal movements were faster than controls after 2 h at 2.60 openings min^{-1} but decreased back to control values after 2.5 and 3 h, remaining low at 1.59 opening min^{-1} until the end of the recovery period ($t = 1.90$, $p = 0.69$; $t = 0.99$, $p = 0.99$; $t = 0.85$, $p = 0.98$; $t = 0.58$, $p = 0.98$, respectively; Supplementary Figure S3-3A). Individuals exposed to salinities of either 15 or 22 psu demonstrated an immediate decrease in cloacal opening rates relative to the baseline, from 1.41 to 0.86 and 1.03 openings min^{-1} for 15 and 22 psu ($F_{1,77} = 1.95$, $p = 0.057$; $t = 5.16$, $p <0.001$, respectively). After 1 h, the rhythm remained low at 1.01 openings min^{-1} under 15 psu but were higher at 1.50 openings min^{-1} under 22 psu ($t = 3.94$ $p = 0.0060$; Supplementary Figure S3-3B). From 1.5 h, individuals exposed to 22 psu exhibited baseline values until the end of the experiment ($t = 1.28$ $p = 1.00$). Under 15 psu, the average rate of cloacal opening remained low for the duration of the exposure to lowered salinity (0.86 openings min^{-1}). After transfer to the recovery tank, cloacal openings started to increase, peaking at about 1.57 openings min^{-1} after 2 h. Cloacal opening rhythm returned to baseline levels by 2.5 h and remained stable until the end of the recovery (Supplementary Figure S3-3B).

Under both air treatments (17°C and 5°C) the sea cucumbers remained unattached to the substratum over the 1 h exposure, resulting in a null force of attachment (0 N). Under low salinity treatments, sea cucumbers showed a force of attachment of 0 N at 15 psu and 0.41 ± 1.00

N at 22 psu. After the recovery period, individuals in both air exposure treatments had returned to control values (17°C, 2.86 ± 2.53 N; 5°C 2.65 ± 1.93 N; control, 2.71 ± 1.90 N). However, individuals exposed to 15 and 22 psu salinities did not return to control levels, showing values of 1.23 ± 2.35 N and 2.53 ± 3.26 N, respectively, after 24 h, which were lower than controls (6.60 ± 8.08 N).

3.4.3.2 Behavioural scores

Immediately after transfer to the 5 or 17°C air treatment (time 0), individuals showed increased activity scores compared to control individuals (Figure 3-7A). Individuals had stronger behavioural responses after 0.5 h, with scores up to 2.29 at 17°C and 1.45 at 5°C. While the scores remained high after 2.5 h under 17°C air, individuals exposed to 5°C air returned to control values after 1.5 h and remained thus until the end of the experiment. Individuals exposed to 17°C returned to baseline values after 3 h. Individuals exposed to both 5 and 17°C air showed minimum scores values of 0.50 after 23.5-24 h, similar to controls (Figure 3-7A).

The behavioural scores of individuals exposed to 15 psu salinity showed an increase from time 0 to a maximum (2.25) after 2.5-3 h; subsequently the scores decreased slowly to values around 1.38 after 23.5-24 h, still higher than controls (Figure 3-7B). Individuals exposed to 22 psu salinity exhibited a sharper increase in scores over the first 1.5 h to reach 2.00. The scores stabilized after 2 h and slightly decreased to reach 1.66 after 3 h. At the end of the recovery period (23.5 and 24 h), a few individuals still demonstrated slow movement, keeping the average scores around 1.36 for 15 psu and 0.50 for 22 psu, which were higher than controls (Figure 3-7B).

3.5 Discussion

Unlike most other marine species of commercial value, e.g., fishes, crabs, lobsters, shrimps, scallops, mussels and sea urchins, sea cucumbers are not protected by any scales or hard exoskeleton that may buffer sudden environmental changes. Thus, exposure to air during natural events (e.g., washing ashore after storms) or fishing activities and exposure to salinity drops during spring thaw or live storage on ice (Gianasi *et al.*, 2016, Hamel *et al.*, 2019) represent acute challenges for soft-bodied sea cucumbers. In addition, sea cucumbers may undergo autolysis when they are stressed (Qi *et al.*, 2016, Sun *et al.*, 2011). Any deterioration of the body wall and underlying collagenous and muscle tissues, which together constitute the chief marketable products of sea cucumbers, will likely translate into commercial products of a lower grade (Purcell *et al.*, 2014). In the present study, the response of the sea cucumber *Cucumaria frondosa* to realistic environmental stressors showed cellular, hormonal, and behavioural activity levels that related proportionally to the severity of the stressor. The greater the departure from optimal salinity and temperature conditions determined for the species (Hamel and Mercier, 1996), the stronger the response recorded, showing possible physiological and biological strategies that would confer resilience.

The results presented here are comparable to those of Wang *et al.* (2008) where the sea cucumber *Apostichopus japonicus* experienced greater challenges to its immune capacity (including phagocytic abilities and respiration) when exposed to increased water temperature than when exposed to low water temperature and lowered salinity. Here, emersion at the highest temperature and immersion at the lowest salinity elicited the greatest increase in free coelomocytes after 1 h, and subsequent spike in small aggregates, cortisol level in the coelomic fluid and the most dramatic change in cloacal opening rhythm (irrigation of respiratory tree),

indicating they were most stressful for *C. frondosa*. These severe treatments could result in more energy expenditure to cope with tissular damages, as suspected by Gianasi *et al.* (2016) or other internal fluctuations though processes like the removal of dead cells. A flight reaction was shown to be elicited by the moderately low salinity (22 psu) in this species (Hamel *et al.*, 2019) but not by the lowest salinity (15 psu), likely because it is below the tolerance threshold. Accordingly, *C. frondosa* was described to occur in brackish zones of the St. Lawrence Estuary (Québec, eastern Canada) but never below 22-25 psu (J-F Hamel, personal observation in Port-au-Saumon and Grande-Bergeronne, QC, Canada).

Exposure to suboptimal conditions, even to the most severe treatments discussed above, did not generate visible damages but instead activated an arsenal of specific defences. Lack of visible lesions is possibly due to the short exposure time, i.e., not sustained enough to completely overwhelm defence mechanisms in *C. frondosa*. A closer look at the various cell types involved provides some interesting insight. For instance, both exposure to air and lower salinities triggered an increase in phagocytes similar to results presented by Caulier *et al.* (2020) after injection of foreign particles and following trawl collection. Phagocyte counts also aligned with the cellular reaction reported by Hamel *et al.* (2021) who exposed *C. frondosa* to the predatory sea star *Solaster endeca*. Phagocytes were previously described as immune cells involved in phagocytosis of pathogens and in the release of humoral agents (Beck and Habicht, 1996, Rinkevich and Müller, 1996, Xue *et al.*, 2015), suggesting that a form of internal damage occurred in sea cucumbers exposed to the most severe stressors in the present study. Fusiform cells in *C. frondosa* increased most markedly during emersion, as also shown in *A. japonicus* by Xing *et al.* (2008); however, the function of these cells in echinoderms is still unknown (Söderhäll, 2010). Studies of fusiform cells in bivalves suggest that they aid in wound healing

(Sparks, 1976), which may be occurring in the most directly exposed tissues of *C. frondosa* like the ambulacral podia and epithelium of the respiratory tree (both part of the hydrovascular system). Morula cells spiked during emersion under both air temperatures and immersion in low salinity, similar to a study by San Miguel-Ruiz and García-Arrarás (2007) on the sea cucumber *Holothuria glaberrima* who documented increasing densities of those cells in direct response to body-wall injuries. Moreover, Byrne (1986) indicated that morula cells multiplied in individuals of *Eupentacta quinquesemita* exposed to physical abrasion and hypothesized that these cells provide the foundation for tissue repair. Consequently, the proliferation of these cells may be triggered by many types of challenges, including in response to emersion and exposure to low salinity. Furthermore, these cells reportedly secrete humoral effectors responsible for pathogen detection (Byrne, 1986, Melillo *et al.*, 2018) suggesting that increasing density results directly from immune stress. Crystal cells in sea cucumbers were previously suggested to play a role in osmoregulation (Eliseikina and Magarlamov, 2002). Xing *et al.* (2008) mentioned that osmotic pressure changes triggered a reversible crystallization of the intravacuolar material in crystal cells, thereby normalizing the osmotic pressure. However, these cells did not display any detectable change or proliferation in *C. frondosa* during exposure to any of the low salinity treatments. In fact, the only condition where an increase in crystal cells was noticed is exposure to cold air, downplaying any role in osmoregulation, at least in *C. frondosa*. Importantly, holothuroids do not have integral osmoregulation mechanisms and are found strictly in marine environments (Russell, 2013). Despite this, some species like *Holothuria scabra* can colonize brackish areas and sustain freshwater runoff during rainy seasons, although they cope by burrowing into the sediment (Mercier *et al.*, 1999). On the other hand, *C. frondosa* is exclusively epibenthic and consequently cannot burrow to withstand salinity drops. Instead, they can use

active buoyancy behaviour to roll or float away with the current (Hamel *et al.*, 2019), likely to limit exposure time.

Despite the fact that phagocytes were the most common coelomocytes found in the coelomic fluid of the Polian vesicle in both control and exposed individuals of *C. frondosa*, these cells were not always found in their active form, which was presumed to correspond to the active form reported by Kindred (1924). Surprisingly, elevated numbers of active phagocytes were only present in individuals exposed to a salinity of 22 psu and not in the other treatments. Caulier *et al.* (2020) showed that the finite pool of available free phagocytes (demarginated) in the hydrovascular fluid of *C. frondosa* can decrease rapidly as they aggregate around foreign particles. In line with this principle, individuals exposed to the most severe stressors in the present study exhibited the lowest number of active phagocytes, suggesting that they were utilized to form aggregates, as supported by the higher number of small aggregates under those conditions. In contrast, at 22 psu, it is possible that a lower demand for tissue repair/healing was sustained by the pool of active and inactive phagocytes already available in the hydrovascular fluid.

Under most conditions tested, free coelomocytes had formed small and large aggregates immediately after the 1-h exposure. These aggregates were described as the precursor step in the expulsion of foreign particles, damaged cells and pathogenic materials, both from the hydrovascular system and the perivisceral coelom (Caulier *et al.*, 2020; Chapter 2). Jans *et al.* (1995) showed formation of "brown bodies" (i.e., aggregates in the present study) in the sea cucumber *Holothuria tubulosa* within 24 h of the initial immune challenge. Similarly, cell aggregates were noticed after 24 h in the sea urchin *Strongylocentrotus droebachiensis* (Majeske *et al.*, 2013) and after 5 h in the sea star *Asterias rubens* (Gorshkov et al., 2009). In *C. frondosa*,

their presence was noticed as early as within one hour of exposure, suggesting that aggregation occurred concurrently with the increase of free coelomocytes, i.e., almost immediately upon exposure to the stressor and faster than what was expected based on previously published works. It can be assumed that dead cells from tissue damage were being packaged for expulsion (Chapter 2). This occurred in all conditions except emersion in cold air, possibly indicating that the latter generates less immediate damage than the other acute conditions tested. Accordingly, Gianasi *et al.* (2016) suggested that keeping *C. frondosa* damp, outside water, at 4-5°C would yield the least severe tissue damage and highest survival rate during transport from the wharfs to the plants. Here, sea cucumbers emersed at cold temperature also showed the slowest cloacal openings rhythm (upon being immersed again), even below controls, suggesting they rapidly resumed a resting state. This trend is substantiated by the behavioural scores; i.e., individuals exposed to warm air temperature reached peak scores early during the experiment (indicative of stress), in contrast to individuals exposed to cold air, which maintained scores similar to baseline values.

As anticipated, the cellular immune responses in *C. frondosa* mirrored the increasing trend in cortisol levels recorded under most severe stressors tested. While previous studies have described a cortisol increase in sea cucumbers (*A. japonicus*) exposed to stressors (Hou *et al.*, 2019) or reported rises in coelomocytes and in cortisol under stress (Chen *et al.*, 2018a, Chen *et al.*, 2018b, Hou *et al.*, 2019), to our knowledge a link between the two factors has never been reported, although hormone research in vertebrates has shown that glucocorticoids (including cortisol) are regulators of immune responses (i.e., increase in leukocytes and granulocytes) (Ince *et al.*, 2019). While the correlation between the rises in cortisol and in coelomocyte densities remains fragmentary in the present study, it highlights the need to tease out the link between the

cellular and hormonal responses in Holothuroidea. Recently, Hou *et al.* (2019) determined that peak cortisol levels in *A. japonicus* were reached several hours into emersion and then slowly dropped towards baseline levels over the following 20 h. In *C. frondosa* the rise in cortisol could be necessary to generate a pool of free coelomocytes from their marginated forms (i.e., attached to the membranes), as seen in Caulier *et al.* (2020). In line with this, cortisol increases were noticed in three of the four conditions tested, but emersion in warm air generated the most defined trend, which in combination with the other biomarkers (behavioural and cellular), points to this being the most detrimental treatment tested. In support, (So *et al.*, 2010) demonstrated that water temperatures above 18°C were deleterious for juveniles and adults of *C. frondosa*. Inversely, emersion in cold air coincided with a minimal cellular response, no measurable cortisol increase, and mild behaviour scores, reinforcing that it is not an immediately threatening condition, at least for a short time, as suggested by Gianasi *et al.* (2016) in the study of transport methods.

Based on most markers measured after 23 h of recovery post-exposure, it emerges that stressors may have long-lasting effects (i.e., beyond 24 h) on the wellbeing of sea cucumbers. Small aggregates showed an increase during recovery from cold air emersion and low salinity, and large aggregates multiplied during recovery from all conditions. There was no mortality in any of the treatments, but the presence of cell aggregates underlies the expulsion of materials resulting from infections or damaged tissues. Strangely, the stressors that elicited the mildest acute responses after 1 h (cold air and 22 psu salinity) yielded the highest counts of small and large aggregates during recovery, either due to a delayed response to the stress or to secondary infections. Inversely, the most severe acute responses (warm air and 15 psu) corresponded to the lowest aggregate counts during recovery, possibly because the immune response peaked earlier

and had already begun to wane. It must be emphasized that while the stressors tested here reflected common harvesting and handling practices, the temporal scale is a conservative estimate of what sea cucumbers could endure over the preprocessing period, which may last 48 h – 1 week (Gianasi *et al.*, 2016; S. Jobson personal communication). Prolonged exposures to stress may lead to more severe damage and possibly more drastic immune responses, which may in turn translate into mortality and into economic loss (Qi *et al.*, 2016, Wu *et al.*, 2013).

Globally, the present study showed the potential of using multiple biometrics to characterize the immediate and long-term effects of stress on economically and ecologically important species like *C. frondosa*. Further studies might seek to refine the methodologies necessary to integrate the use of cortisol levels in the coelomic fluid as a rapid, non-invasive biomarker of health in this and other species of invertebrates. Such a tool would greatly assist the design of sustainable harvesting, aquaculture and preprocessing protocols. Insights were also garnered from an ecological standpoint. While the optimal environmental conditions under which feeding, reproduction and development occur in *C. frondosa* are typically oceanic (Hamel and Mercier, 1996, So *et al.*, 2010), this species has apparently developed notable capabilities to cope with harsh, even improbable, conditions in the short term. Such plasticity may explain its high biomasses and broad distribution range throughout a diversity of temperate and polar marine environments (Gianasi *et al.*, 2020).

3.6 Acknowledgments

We would like to thank the members of the Mercier lab for their technical and logistical support, with special thanks to Andrew Tucker for his help with data collection. We would like to acknowledge the invaluable expertise and support of Fabio Zanuzzo in designing a novel ELISA protocol and Kurt Gamperl for allowing use of his equipment to conduct the cortisol analysis.

We would also like to thank Emaline Montgomery and Javier Santander for their contributions during the initial design of this study. This research was partly funded by the Ocean Frontier Institute, through an award from the Canada First Research Excellence Fund to Annie Mercier.

3.7 Literature cited

Ammendolia, J., J.-F. Hamel, and A. Mercier. 2018. Behavioural responses to hydrostatic pressure in selected echinoderms suggest hyperbaric constraint of bathymetric range. *Mar Biol* **165**.

Bang, F. B. 1975. A search in *Asterias* and *Ascidia* for the beginnings of vertebrate immune responses. *Ann N Y Acad Sci* **266**:334-342.

Beck, G., and G. S. Habicht. 1996. Immunity and the Invertebrates. *Sci Am* **275**:60-66.

Binder, A. R. D., M. W. Pfaffl, F. Hiltwein, J. Geist, and S. Beggel. 2019. Does environmental stress affect cortisol biodistribution in freshwater mussels? *Conserv Phys* **7**:coz101.

Branco, P. C., D. A. L. Figueiredo, and J. da Silva. 2014. New insights into innate immune system of sea urchin: Coelomocytes as biosensors for environmental stress. *OA Biol* **18**:1-7.

Brothers, C. J., J. Harianto, J. B. McClintock, and M. Byrne. 2016. Sea urchins in a high CO_2 world: The influence of acclimation on the immune response to ocean warming and acidification. *Proc R Soc B: Biol Sci* **283**:20161501.

Byrne, M. 1986. The ultrastructure of the morula cells of *Eupentacta quinquesemita* (Echinodermata: Holothuroidea) and their role in the maintenance of the extracellular matrix. *J Morphol* **188**:179-189.

Canicatti, C., G. D'Ancona, and E. Farina-Lipari. 1989. The *Holothuria polii* brown bodies. *Ital J Zool* **56**:275-283.

Canicatti, C., and A. Quaglia. 1991. Ultrastructure of *Holothuria polii* encapsulating body. *J Zool* **224**:419-429.

Canicatti, C., and J. Seymour. 1991. Evidence for phenoloxidase activity in *Holothuria tubulosa* (Echinodermata) brown bodies and cells. *Parasitol Res* **77**:50-53.

Caulier, G., J.-F. Hamel, and A. Mercier. 2020. From coelomocytes to colored aggregates: Cellular components and processes involved in the immune response of the holothuroid *Cucumaria frondosa*. *Biol Bull* **239**:95-114.

Chen, J., Y. Ren, Y. Li, and B. Xia. 2018a. Regulation of growth, intestinal microbiota, non-specific immune response and disease resistance of sea cucumber *Apostichopus japonicus* (Selenka) in biofloc systems. *Fish Shellfish Immunol.* **77**:175-186.

Chen, J., Y. Ren, G. Wang, B. Xia, and Y. Li. 2018b. Dietary supplementation of biofloc influences growth performance, physiological stress, antioxidant status and immune response of juvenile sea cucumber *Apostichopus japonicus* (Selenka). *Fish Shellfish Immunol.* **72**:143-152.

Chia, F. S., and J. Xing. 1996. Echinoderm coelomocytes. *Zool Stud* **35**:231-254.

Chiaramonte, M., L. Inguglia, M. Vazzana, A. Deidun, and V. Arizza. 2019. Stress and immune response to bacterial LPS in the sea urchin *Paracentrotus lividus* (Lamarck, 1816). *Fish Shellfish Immunol.* **92**:384-394.

Coteur, G., G. DeBecker, M. Warnau, M. Jangoux, and P. Dubois. 2002. Differentiation of immune cells challenged by bacteria in the common European starfish, *Asterias rubens* (Echinodermata). *Eur J Cell Biol* **81**:413-418.

D'Andrea-Winslow, L., D. W. Radke, T. Utecht, T. Kaneko, and K. Akasaka. 2012. Sea urchin coelomocyte arylsulfatase: A modulator of the echinoderm clotting pathway. *Integr Zool* **7**:61-73.

Dan-Sohkawa, M., M. Morimoto, and H. Kaneko. 1995a. *In vitro* reactions of coelomocytes against sheep red blood cells in the solitary ascidian *Halocynthia roretzi*. *Zool Sci* **12**:411-417.

Dan-Sohkawa, M., M. Morimoto, H. Mishima, and H. Kaneko. 1995b. Characterization of coelomocytes of the ascidian *Halocynthia roretzi* based on phase-contrast, time-lapse video and scanning electron microscopic observations. *Zool Sci* **12**:289-301.

de Freitas Rebelo, M., E. d. S. de Freitas Figueiredo, R. M. Mariante, A. Nóbrega, C. M. de Barros, and S. Allodi. 2013. New insights from the oyster *Crassostrea rhizophorae* on bivalve circulating hemocytes. *PLoS One* **8**:e57384.

Dushoff, J., M. P. Kain, and B. M. Bolker. 2019. I can see clearly now: Reinterpreting statistical significance. *Methods Ecol Evol* **10**:756-759.

Edds, K. T. 1980. The formation and elongation of filopodia during transformation of sea urchin coelomocytes. *Cell Motil.* **1**:131-140.

Eliseikina, M. G., and T. Y. Magarlamov. 2002. Coelomocyte morphology in the holothurians *Apostichopus japonicus* (Aspidochirota: Stichopodidae) and *Cucumaria japonica* (Dendrochirota: Cucumariidae). *Russ J Mar Biol* **28**:6.

Fisher, R. A. 1934. Statistical methods for research workers. *Statistical methods for research workers.*

Fontaine, A. R., and P. Lambert. 1977. The fine structure of the leucocytes of the holothurian, *Cucumaria miniata*. *Can J Zool* **55**:1530-1544.

Franchi, N., and L. Ballarin. 2017. Immunity in protochordates: the tunicate perspective. *Front Immunol* **8**:674.

Galimany, E., M. Baeta, and M. Ramón. 2018. Immune response of the sea cucumber *Parastichopus regalis* to different temperatures: implications for aquaculture purposes. *Aquaculture* **497**:357-363.

Gianasi, B. L., J.-F. Hamel, and A. Mercier. 2016. Experimental test of optimal holding conditions for live transport of temperate sea cucumbers. *Fish Res* **174**:298-308.

Gianasi, B. L., J.-F. Hamel, E. M. Montgomery, J. Sun, and A. Mercier. 2020. Current knowledge on the biology, ecology, and commercial exploitation of the sea cucumber *Cucumaria frondosa*. *Rev Fish Sci Aquac*.

Gianasi, B. L., K. Verkaik, J.-F. Hamel, and A. Mercier. 2015. Novel use of pit tags in sea cucumbers: promising results with the commercial species *Cucumaria frondosa*. *PLoS One* **10**:e0127884.

Gorshkov, A. N., M. I. Blinova, and G. P. Pinaev. 2009. Ultrastructure of coelomic epithelium and coelomocytes of the starfish *Asterias rubens* L. in norm and after wounding. *Cell Tissue Biol* **3**:477-490.

Grantham, B. A., G. L. Eckert, and A. L. Shanks. 2003. Dispersal potential of marine invertebrates in diverse habitats. *Ecol Appl* **13**:108-116.

Gross, P. S., W. Z. Al-Sharif, L. A. Clow, and L. C. Smith. 1999. Echinoderm immunity and the evolution of the complement system. *Dev Comp Immunol* **23**:429-442.

Hamel, J.-F., S. Jobson, G. Caulier, and A. Mercier. 2021. Evidence of anticipatory immune and hormonal responses to predation risk in an echinoderm. *Sci Rep* **11**.

Hamel, J.-F., and A. Mercier. 1996. Early development, settlement, growth, and spatial distribution of the sea cucumber *Cucumaria frondosa* (Echinodermata: Holothuroidea). *Can J Fish Aquat Sci* **53**:253-271.

Hamel, J.-F., J. Sun, B. L. Gianasi, E. M. Montgomery, E. L. Kenchington, B. Burel, S. Rowe, P. D. Winger, and A. Mercier. 2019. Active buoyancy adjustment increases dispersal potential in benthic marine animals. *J Anim Ecol* **88**:820-832.

Hetzel, H. R. 1965. Studies on holothurian coelomocytes. ii. The origin of coelomocytes and the formation of brown bodies. *Biol Bull* **128**:102-111.

Hossain, A., D. Dave, and F. Shahidi. 2020. Northern sea cucumber (*Cucumaria frondosa*): A potential candidate for functional food, nutraceutical, and pharmaceutical sector. *Mar Drugs* **18**:274.

Hou, S., Z. Jin, W. Jiang, L. Chi, B. Xia, and J. Chen. 2019. Physiological and immunological responses of sea cucumber *Apostichopus japonicus* during desiccation and subsequent resubmersion. *PeerJ* **7**:e7427.

Huo, D., L. Sun, X. Ru, L. Zhang, C. Lin, S. Liu, X. Xin, and H. Yang. 2018. Impact of hypoxia stress on the physiological responses of sea cucumber *Apostichopus japonicus*: Respiration, digestion, immunity and oxidative damage. *PeerJ* **6**:e4651.

Huo, D., L. Sun, L. Zhang, X. Ru, S. Liu, X. Yang, and H. Yang. 2019. Global-warming-caused changes of temperature and oxygen alter the proteomic profile of sea cucumber *Apostichopus japonicus*. *J Proteomics* **193**:27-43.

Ince, L. M., J. Weber, and C. Scheiermann. 2019. Control of leukocyte trafficking by stress-associated hormones. *Front Immunol* **9**:3143.

Jans, D., P. Dubois, and M. Jangoux. 1995. Defensive mechanisms of holothuroids (Echinodermata): Formation, role, and fate of intracoelomic brown bodies in the sea cucumber *Holothuria tubulosa*. *Cell Tissue Res.* **283**:99-106.

Kindred, J. E. 1924. The cellular elements in the perivisceral fluid of echinoderms. *Biol Bull* **46**:228-251.

Li, Q., R.-R. Qi, Y.-N. Wang, S.-G. Ye, G. Qiao, and H. Li. 2013. Comparison of cells free in coelomic and water-vascular system of sea cucumber, *Apostichopus japonicus*. *Fish Shellfish Immunol.* **35**:1654-1657.

Li, Q., Y. Ren, L. Luan, J. Zhang, G. Qiao, Y. Wang, S. Ye, and R. Li. 2019. Localization and characterization of hematopoietic tissues in adult sea cucumber, *Apostichopus japonicus*. *Fish Shellfish Immunol.* **84**:1-7.

Majeske, A. J., C. J. Bayne, and L. C. Smith. 2013. Aggregation of sea urchin phagocytes is augmented in vitro by lipopolysaccharide. *PLoS One* **8**:e61419.

Melillo, D., R. Marino, P. Italiani, and D. Boraschi. 2018. Innate immune memory in invertebrate metazoans: A critical appraisal. *Front Immunol* **9**:1915.

Mercier, A., S. C. Battaglene, and J.-F. Hamel. 1999. Daily burrowing cycle and feeding activity of juvenile sea cucumbers *Holothuria scabra* in response to environmental factors. *J Exp Mar Biol Ecol* **239**:125-156.

Nelson, E. J., B. A. MacDonald, and S. M. C. Robinson. 2012. The absorption efficiency of the suspension-feeding sea cucumber, *Cucumaria frondosa*, and its potential as an extractive integrated multi-trophic aquaculture (IMTA) species. *Aquaculture* **370**:19-25.

Pei, S., S. Dong, F. Wang, X. Tian, and Q. Gao. 2012. Effects of density on variation in individual growth and differentiation in endocrine response of Japanese sea cucumber *Apostichopus japonicus* (Selenka). *Aquaculture* **356**:398-403.

Pinsino, A., M. C. Thorndyke, and V. Matranga. 2007. Coelomocytes and post-traumatic response in the common sea star *Asterias rubens*. *Cell Stress Chaperones* **12**:331.

Purcell, S. W., A. Mercier, C. Conand, J.-F. Hamel, M. V. Toral-Granda, A. Lovatelli, and S. Uthicke. 2013. Sea cucumber fisheries: Global analysis of stocks, management measures and drivers of overfishing: Management of sea cucumber fisheries. *Fish Fish* **14**:34-59.

Purcell, S. W., B. A. Polidoro, J.-F. Hamel, R. U. Gamboa, and A. Mercier. 2014. The cost of being valuable: Predictors of extinction risk in marine invertebrates exploited as luxury seafood. *Proc R Soc B: Biol Sci* **281**:20133296.

Qi, H., H. Fu, X. Dong, D. Feng, N. Li, C. Wen, Y. Nakamura, and B. Zhu. 2016. Apoptosis induction is involved in UVA-induced autolysis in sea cucucumber *Stichopus japonicus*. *J Photochem Photobiol B: Biol* **158**:130-135.

Ramírez-Gómez, F., F. Aponte-Rivera, L. Méndez-Castaner, and J. E. García-Arrarás. 2010. Changes in holothurian coelomocyte populations following immune stimulation with different molecular patterns. *Fish Shellfish Immunol.* **29**:175-185.

Ridder, C., and M. Jangoux. 1984. Intracoelomic parasitic: Sporozoa in the burrowing spatangoid echinoid *Echinocardium cordatum*: Coelomocyte reaction and formation of brown bodies. *Helgoländer Meeresuntersuchungen* **37**:225-231.

Rinkevich, B., and W. E. G. Müller. 1996. *Invertebrate immunology*. Springer Berlin Heidelberg, Berlin, Heidelberg.

Russell, M. P. 2013. Echinoderm responses to variation in salinity. *Adv Mar Biol* **66**:171-212.

San Miguel-Ruiz, J. E., and J. E. García-Arrarás. 2007. Common cellular events occur during wound healing and organ regeneration in the sea cucumber *Holothuria glaberrima*. *BMC Dev Biol* **7**:1-19.

Sandner, M., G. Lois, F. Streit, P. Zeier, P. Kirsch, S. Wüst, and M. Wessa. 2020. Investigating individual stress reactivity: High hair cortisol predicts lower acute stress responses. *Psychoneuroendocrinology* **118**:104660.

Satyavathi, V. V., A. Minz, and J. Nagaraju. 2014. Nodulation: An unexplored cellular defense mechanism in insects. *Cell Signal* **26**:1753-1763.

Smith, L. C., V. Arizza, M. A. Barela Hudgell, G. Barone, A. G. Bodnar, K. M. Buckley, V. Cunsolo, N. M. Dheilly, N. Franchi, S. D. Fugmann, R. Furukawa, J. Garcia-Arraras, J. H. Henson, T. Hibino, Z. H. Irons, C. Li, C. M. Lun, A. J. Majeske, M. Oren, P. Pagliara, A. Pinsino, D. A. Raftos, J. P. Rast, B. Samasa, D. Schillaci, C. S. Schrankel, L. Stabili, K. Stensväg, and E. Sutton. 2018. Echinodermata: The complex immune system in echinoderms. Pp. 409-501 in *Advances in Comparative Immunology*, E. L. Cooper, ed. Springer, Cham.

Smith, L. C., and E. H. Davidson. 1992. The echinoid immune system and the phylogenetic occurrence of immune mechanisms in deuterostomes. *Immunol Today* **13**:356-362.

Smith, L. C., and E. H. Davidson. 1994. The echinoderm immune system: Characters shared with vertebrate immune systems and characters arising later in deuterostome phylogeny. *Ann N Y Acad Sci* **712**:213-226.

So, J. J., J.-F. Hamel, and A. Mercier. 2010. Habitat utilisation, growth and predation of *Cucumaria frondosa*: Implications for an emerging sea cucumber fishery. *Fish Manag Ecol* **17**:473-484.

Söderhäll, K. 2010. *Invertebrate Immunity*. Advances in Experimental Medicine and Biology.

Sparks, A. K. 1976. Inflammation and wound repair in oysters. *Mar. Fish. Rev.* **38**:2-4.

Suh, S.-S., J. Hwang, M. Park, S. Y. Park, T. K. Ryu, S. Lee, and T.-K. Lee. 2014. Hypoxia-modulated gene expression profiling in sea urchin (*Strongylocentrotus nudus*) immune cells. *Ecotoxicol Environ Saf* **109**:63-69.

Sun, J., J.-F. Hamel, B. L. Gianasi, M. Graham, and A. Mercier. 2020. Growth, health and biochemical composition of the sea cucumber *Cucumaria frondosa* after multi-year holding in effluent waters of land-based salmon culture. *Aquac Environ Interac* **12**:139-151.

Sun, J., J.-F. Hamel, and A. Mercier. 2018. Influence of flow on locomotion, feeding behaviour and spatial distribution of a suspension-feeding sea cucumber. *J Exp Biol* **221**:jeb189597.

Sun, L., M. Chen, H. Yang, T. Wang, B. Liu, C. Shu, and D. M. Gardiner. 2011. Large scale gene expression profiling during intestine and body wall regeneration in the sea cucumber *Apostichopus japonicus*. *Comp Biochem Physiol D Genomics Proteomics* **6**:195-205.

Toral-Granda, V., A. Lovatelli, and M. Vasconcellos. 2008. *Sea cucumbers: a global review of fisheries and trade*. Food and Agriculture Organization of the United Unations, Rome.

Uren Webster, T. M., D. Rodriguez-Barreto, S. Consuegra, and C. Garcia de Leaniz. 2020. Cortisol-related signatures of stress in the fish microbiome. *Front Microbiol* **11**:1621.

Wang, F., H. Yang, F. Gao, and G. Liu. 2008. Effects of acute temperature or salinity stress on the immune response in sea cucumber, *Apostichopus japonicus*. *Comp. Biochem. Physiol., A: Mol. Integr. Physiol.* **151**:491-498.

Wasserstein, R. L., and N. A. Lazar. 2016. The ASA statement on *p*-values: Context, process, and purpose. *Am Stat* **70**:129-133.

Wasserstein, R. L., A. L. Schirm, and N. A. Lazar. 2019. Moving to a world beyond "p< 0.05". *Am Stat* **73**:1-19.

Wu, H.-T., D.-M. Li, B.-W. Zhu, J.-J. Sun, J. Zheng, F.-L. Wang, K. Konno, and X. Jiang. 2013. Proteolysis of noncollagenous proteins in sea cucumber, *Stichopus japonicus*, body wall: Characterisation and the effects of cysteine protease inhibitors. *Food Chem.* **141**:1287-1294.

Xia, B., Y. Ren, J. Wang, Y. Sun, and Z. Zhang. 2017. Effects of feeding frequency and density on growth, energy budget and physiological performance of sea cucumber *Apostichopus japonicus* (Selenka). *Aquaculture* **466**:26-32.

Xing, K., H. Yang, and M. Chen. 2008. Morphological and ultrastructural characterization of the coelomocytes in *Apostichopus japonicus*. *Aquat Biol* **2**:85-92.

Xu, B., L.-m. Lang, S.-Z. Li, J.-R. Guo, J.-F. Wang, D. Wang, L.-P. Zhang, H.-M. Yang, and S. Lian. 2019. Cortisol excess-mediated mitochondrial damage induced hippocampal neuronal apoptosis in mice following cold exposure. *Cells* **8**:612-612.

Xue, Z., H. Li, X. Wang, X. Li, Y. Liu, J. Sun, and C. Liu. 2015. A review of the immune molecules in the sea cucumber. *Fish Shellfish Immunol.* **44**:1-11.

Yang, H., J.-F. Hamel, and A. Mercier. 2015. *The sea cucumber Apostichopus japonicus: History, biology and aquaculture*. Academic Press.

Yoccoz, N. G. 1991. Use, overuse, and misuse of significance tests in evolutionary biology and ecology. *Bull Ecol Soc Am* **72**:106-111.

Young, C. M., and F. S. Chia. 1982. Factors controlling spatial distribution of the sea cucumber *Psolus chitonoides*: Settling and post-settling behavior. *Mar Biol* **69**:195-205.

Zhang, X., L. Sun, J. Yuan, Y. Sun, Y. Gao, L. Zhang, S. Li, H. Dai, J.-F. Hamel, C. Liu, Y. Yu, S. Liu, W. Lin, K. Guo, S. Jin, P. Xu, K. B. Storey, P. Huan, T. Zhang, Y. Zhou, J. Zhang, C. Lin, X. Li, L. Xing, D. Huo, M. Sun, L. Wang, A. Mercier, F. Li, H. Yang, and J.

Xiang. 2017. The sea cucumber genome provides insights into morphological evolution and visceral regeneration. *PLoS Biol* **15**:e2003790.

3.8 Figures

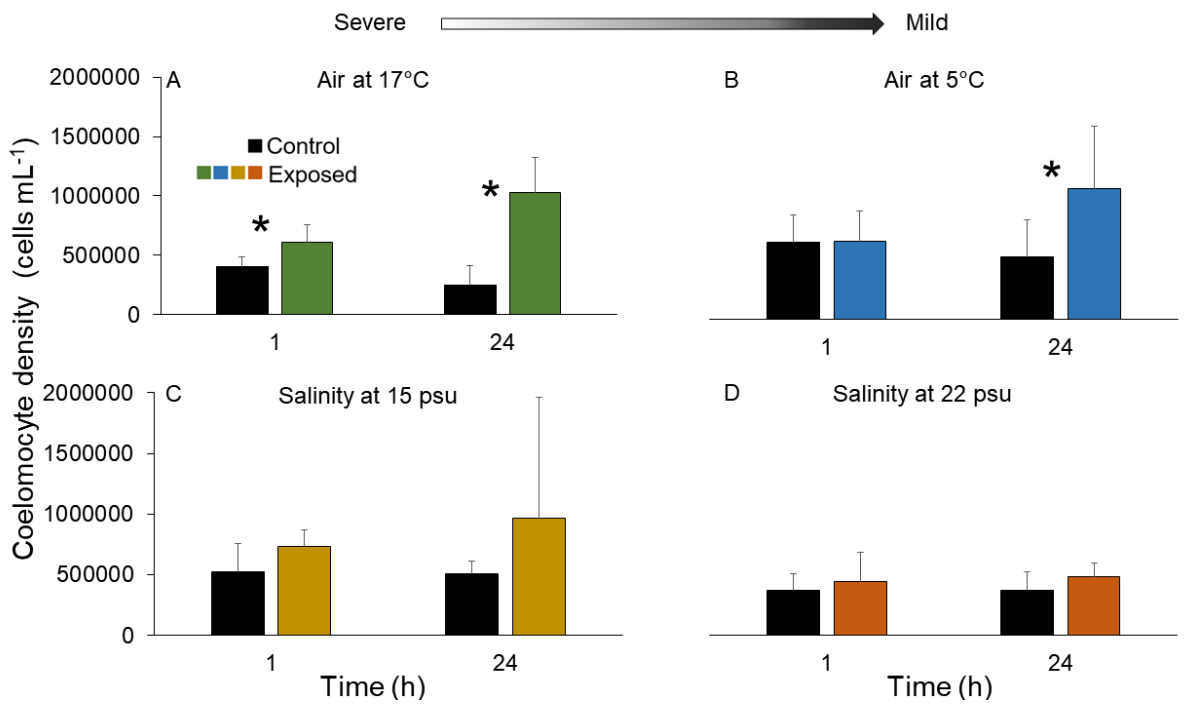

Figure 3-1: Density of free coelomocytes in fluid of the Polian vesicle (mean ± SD, n = 5-10) after exposure of sea cucumbers to A) 17°C air, B) 5°C air, C) 15 psu salinity and D) 22 psu salinity. The asterisk (*) indicates significant differences between control and exposed individuals ($p<0.05$) at each time point. There is no statistical difference between treatment groups at different time points ($p>0.05$). Arrow indicates severe and mild stressors relative to the control. Measurements were made immediately after the exposure (1 h) and after a 23 h recovery period (total of 24 h). Main statistical results are shown in Supplementary Table S3-2.

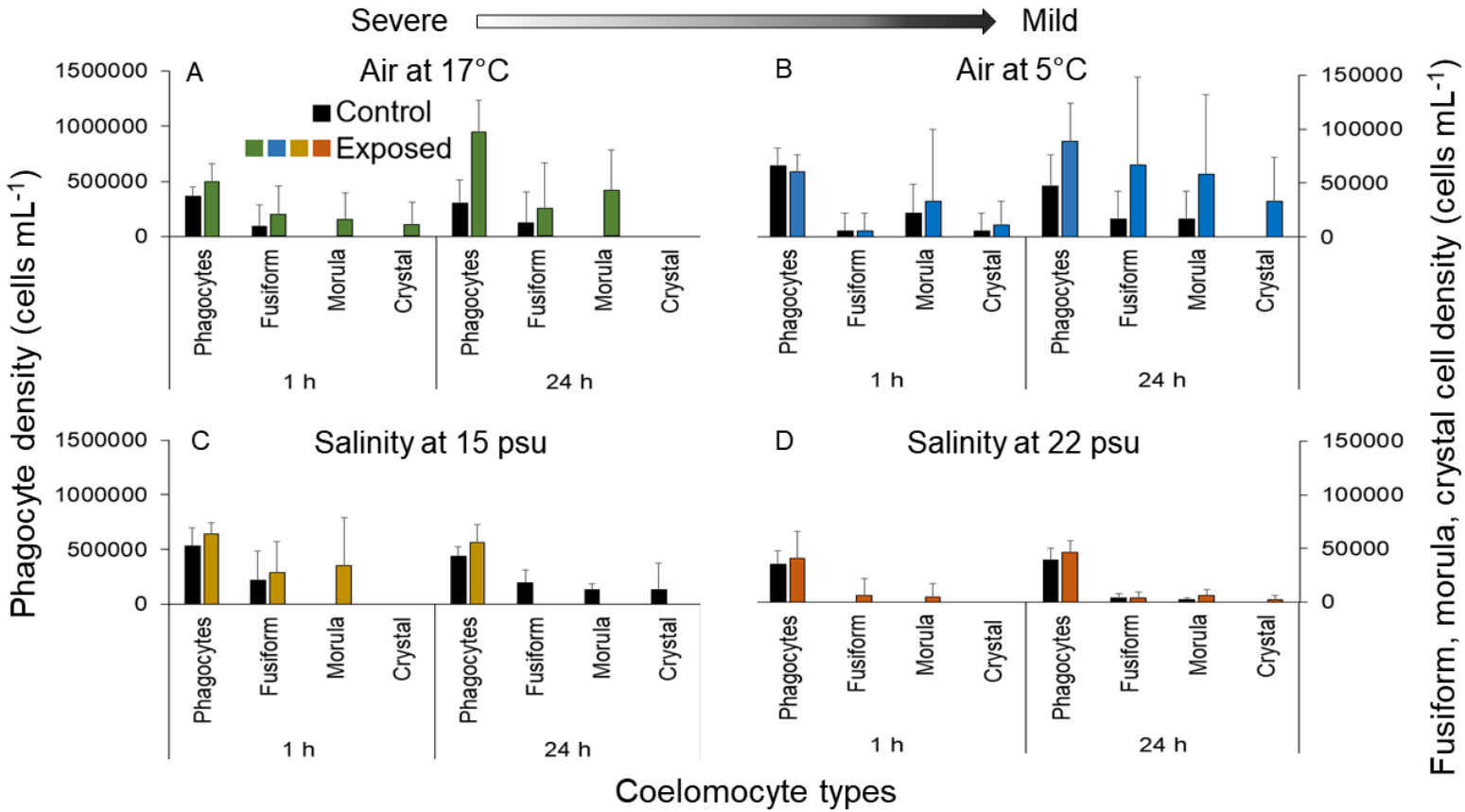

Figure 3-2: Density of free coelomocytes (separated by cell type) per mL of fluid in the Polian vesicle fluid of sea cucumbers (mean ± SD, n = 5-10) following exposure to A) 17°C air, B) 5°C air, C) 15 psu salinity, and D) 22 psu salinity. Arrow indicates severe and mild stressors relative to the control. Measurements were made immediately after the exposure (1 h) and after a 23 h recovery period (total of 24 h).

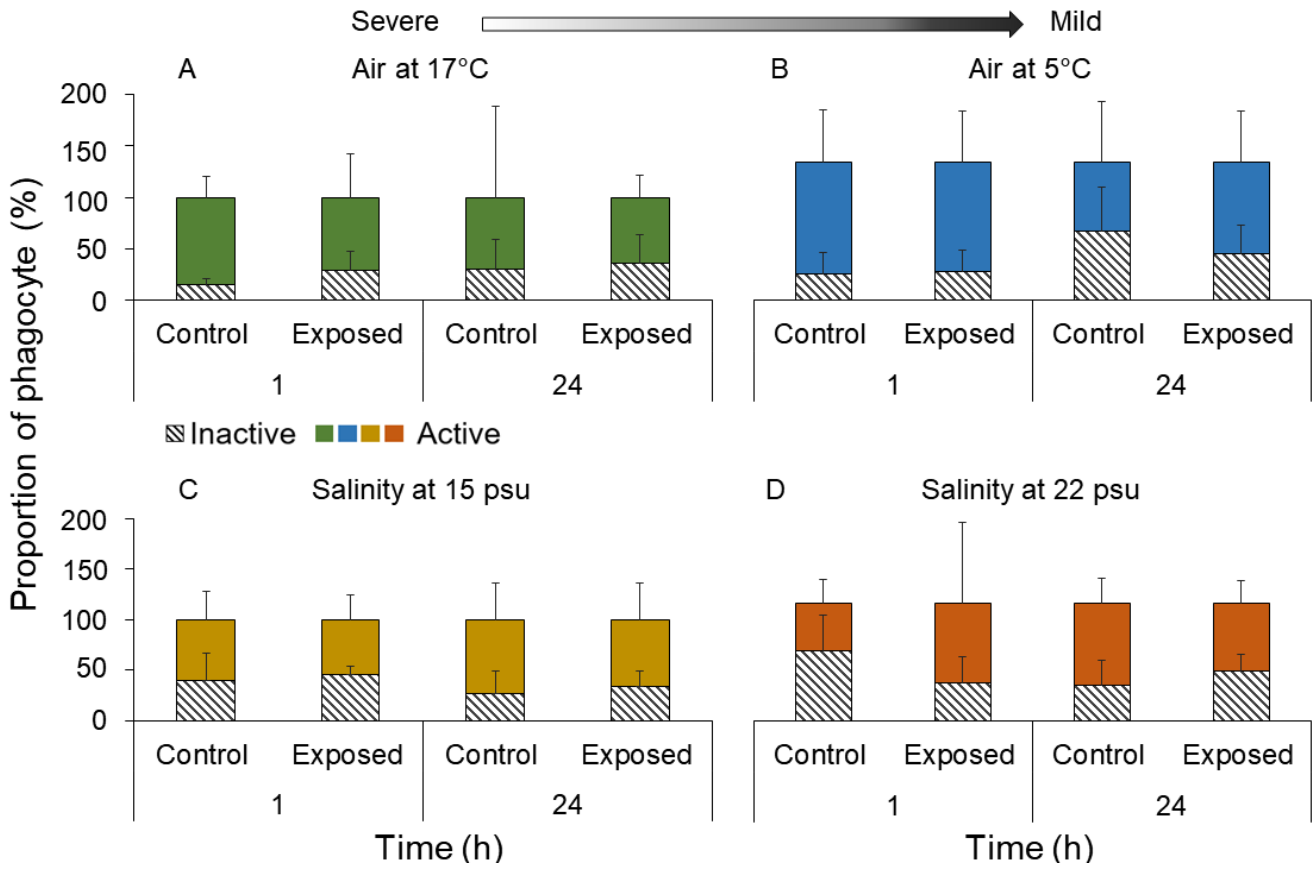

Figure 3-3: Density of phagocytes (active vs. inactive) per mL of Polian vesicle fluid (n = 5-10) following exposure to A) 17°C air, B) 5°C air, C) 15 psu salinity, and D) 22 psu salinity. Arrow indicates severe and mild stressors relative to the control. Measurements were made immediately after the exposure (1 h) and after a 23 h recovery period (total of 24 h).

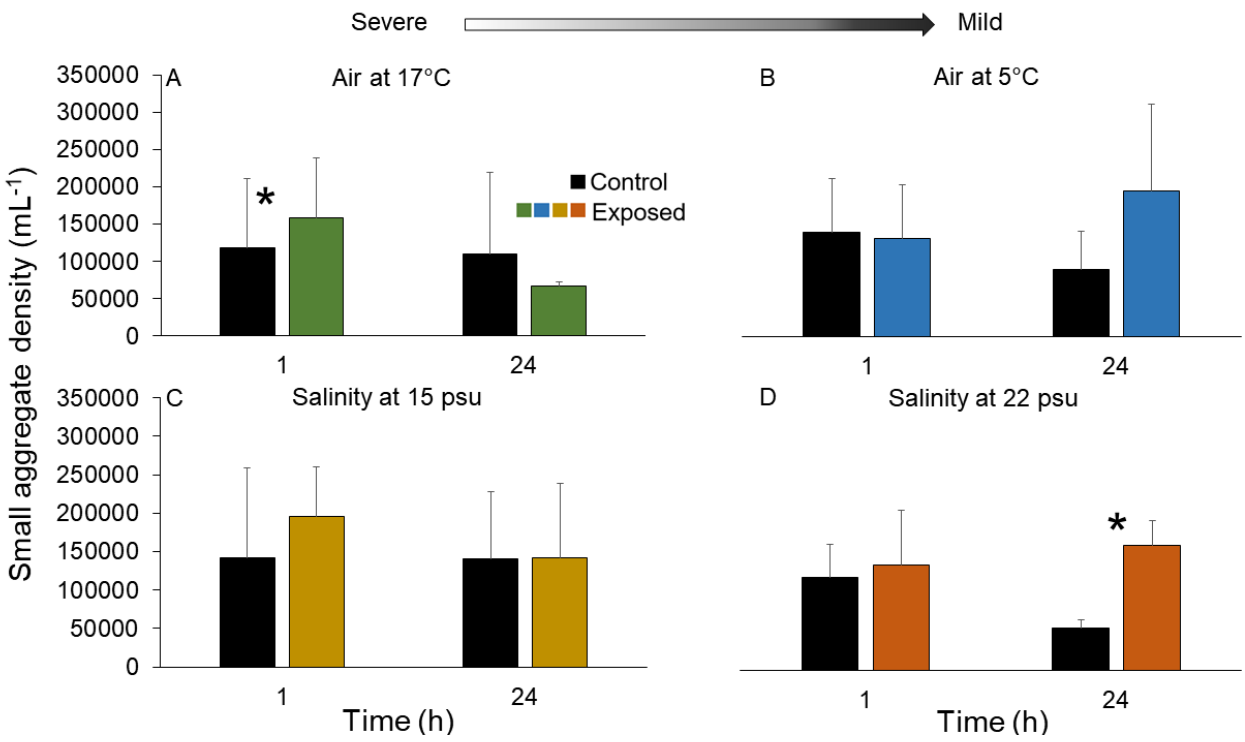

Figure 3-4: Density of small aggregates in fluid of the Polian vesicle (mean ± SD, n = 5-10) after exposure of sea cucumbers to A) 17°C air B) 5°C air C) 15 psu salinity and D) 22 psu salinity. The asterisk (*) indicates significant differences between control and exposed individuals ($p<0.05$) at each time point. There was no statistical difference between treatment groups at different time points ($p>0.05$). Arrow indicates severe and mild stressors relative to the control. Measurements were made immediately after the exposure (1 h) and after a 23 h recovery period (total of 24 h). Main statistical results are shown in Supplementary Table S3-2.

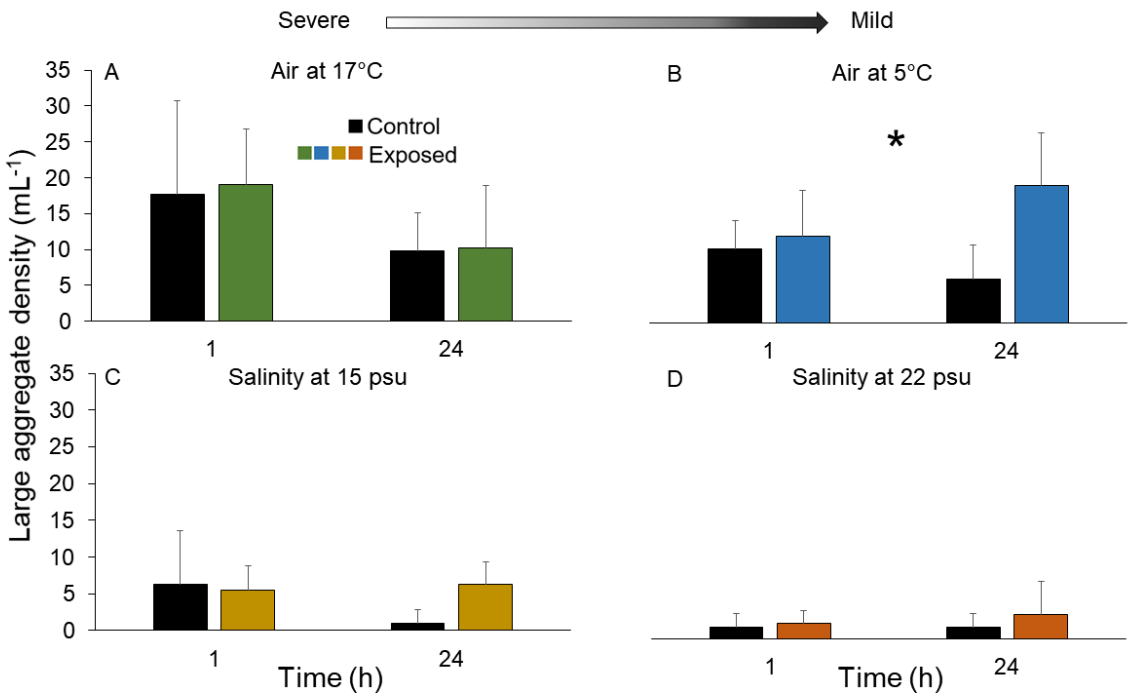

Figure 3-5: Density of large aggregates in fluid of the Polian vesicle (mean ± SD, n = 5-10) after exposure of sea cucumbers to A) 17°C air B) 5°C air C) 15 psu salinity and D) 22 psu salinity. The asterisk (*) indicates significant differences within one treatment group ($p<0.05$), however, pairwise comparisons showed no statistical significance between control and exposed individuals at either time point (1 and 24 h). There was no statistical difference between treatment groups at different time points ($p>0.05$). Arrow indicates severe and mild stressors relative to the control. Measurements were made immediately after the exposure (1 h) and after a 23 h recovery period (total of 24 h). Main statistical results are shown in Supplementary Table S3-2.

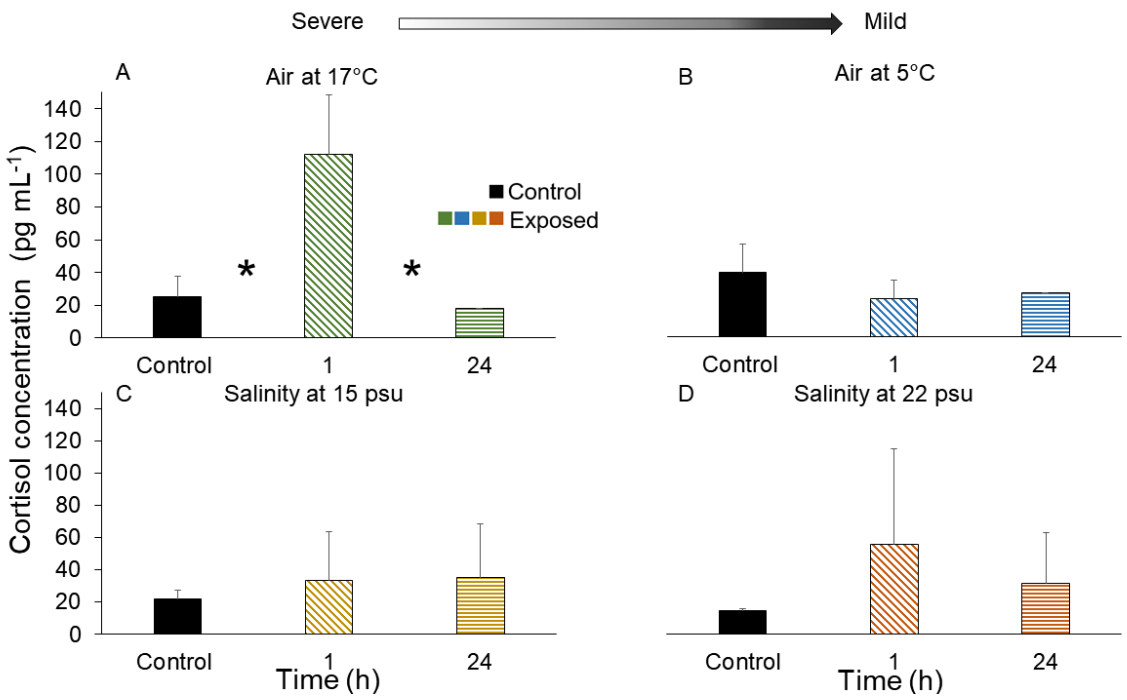

Figure 3-6: Cortisol concentration (pg mL^{-1}) after exposure of sea cucumbers to A) 17°C air B) 5°C air C) 15 psu salinity and D) 22 psu salinity. The asterisk (*) indicates significant differences within one treatment group ($p<0.05$), in this case A) the concentration between control individuals and those sampled at the 1 h mark was significantly different as well as the cortisol concentration between those sampled at 1 and 24 h. There was no statistical difference between the control and exposed individuals after 24 h ($p>0.05$). Arrow indicates severe and mild stressors relative to the control. Measurements were made immediately after the exposure (1 h) and after a 23 h recovery period (total of 24 h). Main statistical results are shown in Supplementary Table S3-2.

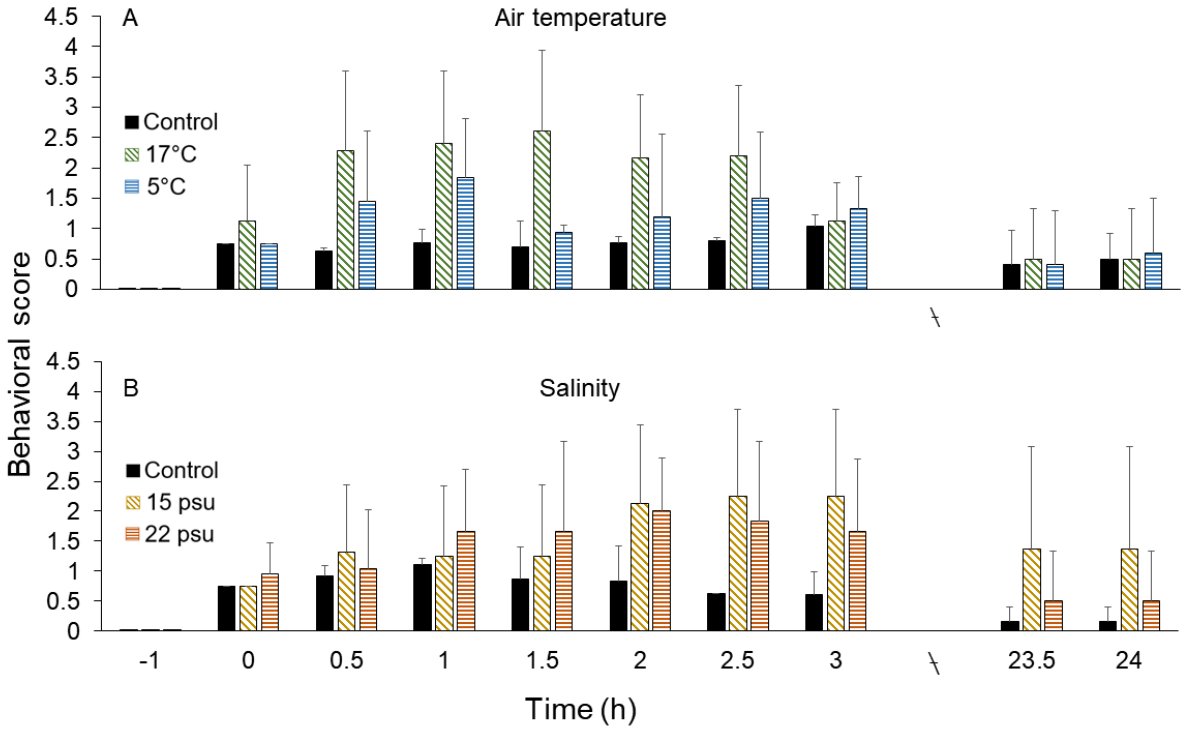

Figure 3-7: Behavioural intensity (0 = resting/baseline state, 4 = maximum stress) in *C. frondosa* at various time points (-0.5 h = negative control, 0-24 h = positive control). A) Comparison between controls and individuals exposed to 17°C and 5°C air (± SD, n = 6). B) Comparison between controls and individuals exposed to 15 and 22 psu salinity (mean ± SD, n = 4-6).

3.9 Supplementary materials

3.9.1 Supplementary Tables

Supplementary Table S3-1: Criteria used to score behaviours indicative of stress in *Cucumaria frondosa* post-exposure to stress conditions.

Behaviour	Score
Full attachment, no movement, tentacles extended or retracted, no body bloating	0
Body is ball shaped, podia extended, attached, tentacles extended or retracted	0.5
Body is ball shaped, podia extended, not attached, tentacles extended or retracted	0.75
Slow movement	1
Fast movement	2
Body is ball shaped, rolling, tentacles sometimes extended but not fluffy	3
Body is ball shaped with severe body contractions (peristaltic motion)	3.5
Full Active buoyancy adjustment	4

Supplementary Table S3-2: Results of two-way ANOVA on density of cellular and hormonal metrics across different treatments (17°C, 5°C, 15 psu, 22 psu). Measurements were made immediately after the exposure (1 h) and after a 23 h recovery period (total of 24 h).

TREATMENT	TWO-WAY ANOVA	HOLM-SIDAK	DF	RESIDUAL	STATISTIC	p-VALUE
Coelomocytes						
Air at 17°C	Exposed vs Control	-	1	20	F = 11.66	0.0030
		1 h	1	20	t = 2.43	0.025
		24 h	1	20	t = 2.40	0.026
	Time (1 h vs 24 h)	-	1	20	F = 1.88	0.19
	Exposed vs Control x Time	-	1	20	F = 0.0072	0.93
Air at 5°C	Exposed vs Control	-	1	18	F = 2.97	0.0080
		1 h	1	18	t = 0.80	0.44
		24 h	1	18	t = 3.40	0.003
	Time (1 h vs 24 h)	-	1	18	F = 3.81	0.067
		Exposure	1	18	t = 2.80	0.012
		Control	1	18	t = 0.063	0.95
	Exposed vs Control x Time	-	1	18	F = 3.4	0.082
Salinity at 15 psu	Exposed vs Control	-	1	12	F = 2.41	0.15
	Time (1 h vs 24 h)	-	1	12	F = 0.050	0.83
	Exposed vs Control x Time	-	1	12	F = 4.67	0.049
Salinity at 22 psu	Exposed vs Control	-	1	19	F = 0.38	0.54
	Time (1 h vs 24 h)	-	1	19	F = 0.076	0.79
	Exposed vs Control x Time	-	1	19	F = 2.26	0.15
Small aggregates						
Air at 17°C	Exposed vs Control	-	1	23	F = 4.38	0.048
		1 h	1	23	t = 2.73	0.012

		24 h	1	23	t = 0.42	0.68
	Time (1 h vs 24 h)	-	1	23	F = 0.082	0.78
	Exposed vs Control x Time	-	1	23	F = 2.093	0.16
Air at 5°C	Exposed vs Control	-	1	16	F = 2.84	0.11
	Time (1 h vs 24 h)	-	1	16	F = 0.0078	0.93
	Exposed vs Control x Time	-	1	16	F = 0.42	0.53
Salinity at 15 psu	Exposed vs Control	-	1	13	F = 0.084	0.78
	Time (1 h vs 24 h)	-	1	13	F = 0.070	0.80
	Exposed vs Control x Time	-	1	13	F = 1.45	0.25
Salinity at 22 psu	Exposed vs Control	-	1	18	F = 8.343	0.010
		1 h	1	18	t = 1.64	0.12
		24 h	1	18	t = 2.39	0.028
	Time (1 h vs 24 h)	-	1	18	F = 0.90	0.36
	Exposed vs Control x Time	-	1	18	F = 6.2	0.44
Large aggregates						
Air at 17°C	Exposed vs Control	-	1	21	F = 0.43	0.52
	Time (1 h vs 24 h)	-	1	21	F = 1.18	0.29
	Exposed vs Control x Time		1	21	F = 0.040	0.84
Air at 5°C	Exposed vs Control	-	1	18	F = 0.11	0.75
	Time (1 h vs 24 h)	-	1	18	F = 4.57	0.047
		Exposure	1	18	t = 1.71	0.10
		Control	1	18	t = 1.30	0.21
	Exposed vs Control x Time	-	1	18	F = 0.15	0.70
Salinity at 15 psu	Exposed vs Control	-	1	12	F = 2.41	0.15

	Time (1 h vs 24 h)	-	1	12	F = 0.049	0.83
	Exposed vs Control x Time	-	1	12	F = 0.049	0.83
Salinity at 22 psu	Exposed vs Control	-	1	17	F = 0.019	0.89
	Time (1 h vs 24 h)	-	1	18	F = 0.088	0.77
	Exposed vs Control x Time	-	1	18	F = 0.11	0.74
Cortisol						
Air at 17°C	Exposed vs Control	-	1	5	F = 4.70	0.082
		1 h	1	5	t = 3.47	0.018
		24 h	1	5	t = 0.019	0.99
	Time (1 h vs 24 h)	-	1	5	F = 10.65	0.022
		Exposure	1	5	t = 3.44	0.018
		Control	1	5	t = 0.91	0.41
	Exposed vs Control x Time	-	1	5	F = 4.58	0.086
Air at 5°C	Exposed vs Control	-	1	5	F = 1.19	0.33
	Time (1 h vs 24 h)	-	1	5	F = 0.44	0.54
	Exposed vs Control x Time	-	1	5	F = 0.12	0.75
Salinity at 15 psu	Exposed vs Control	-	1	7	F = 0.99	0.35
	Time (1 h vs 24 h)	-	1	7	F = 0.62	0.46
	Exposed vs Control x Time	-	1	7	F = 1.46	0.27
Salinity at 22 psu (ranked)	Exposed vs Control	-	1	4	F = 1.78	0.25
	Time (1 h vs 24 h)	-	1	4	F = 1.78	0.25
	Exposed vs Control x Time	-	1	4	F = 1.78	0.25

Supplementary Table S3-3: Number of free coelomocytes (separated by cell type) per mL of fluid in the Polian vesicle fluid of sea cucumber measured across different treatments (17°C, 5°C, 15 psu 22 psu).

Treatment			Coelomocyte types			
			Phagocytes	**Fusiform cells**	**Morula cells**	**Crystal cells**
17°C air	*1 h*	*Control*	366667	8333	0	0
		Exposed	500000	20000	15000	10000
	24 h	*Control*	300000	11667	0	0
		Exposed	950000	25000	41667	0
5°C air	*1 h*	*Control*	657143	5556	22222	5556
		Exposed	600000	5556	33333	11111
	24 h	*Control*	470000	16667	16667	0
		Exposed	883333	66667	58333	33333
15 psu	*1 h*	*Control*	533500	22083.33	0	0
		Exposed	644000	29000	16875	0
	24 h	*Control*	438125	19350	13250	13500
		Exposed	566875	0	0	0
22 psu	*1 h*	*Control*	353929	0	0	0
		Exposed	408107	5964	14286	4750
	24 h	*Control*	389500	3750	2083	0
		Exposed	459500	4000	6000	2000

3.9.2 Supplementary Figures

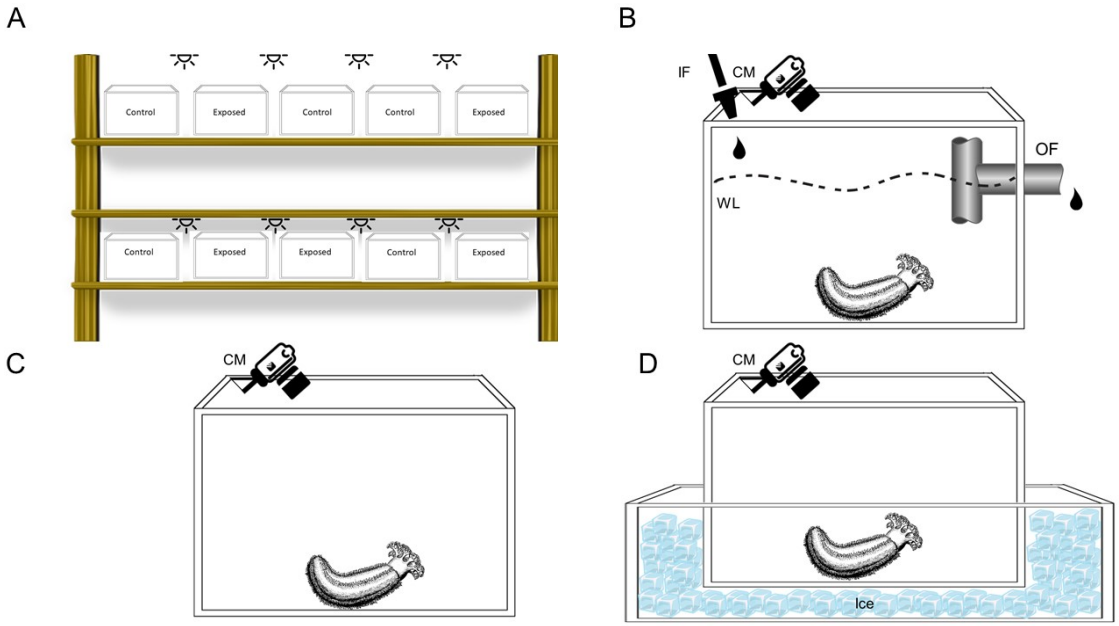

Supplementary Figure S3-1: Experimental tank setup: A) Random distribution of tanks/treatments in the experimental setup. B) Tanks used for controls and exposures to low salinity received flow at the desired salinity (35 and 22/15 psu, respectively). CM = camera, IF = inflow, OF = outflow, WL = waterline. C) Tanks used for exposure to 17°C air were empty and exposed to ambient temperature. D) Tanks used for exposure to 5°C air were empty and placed on ice to achieve the desired temperature. All tanks held one sea cucumber and empty tanks had a lid.

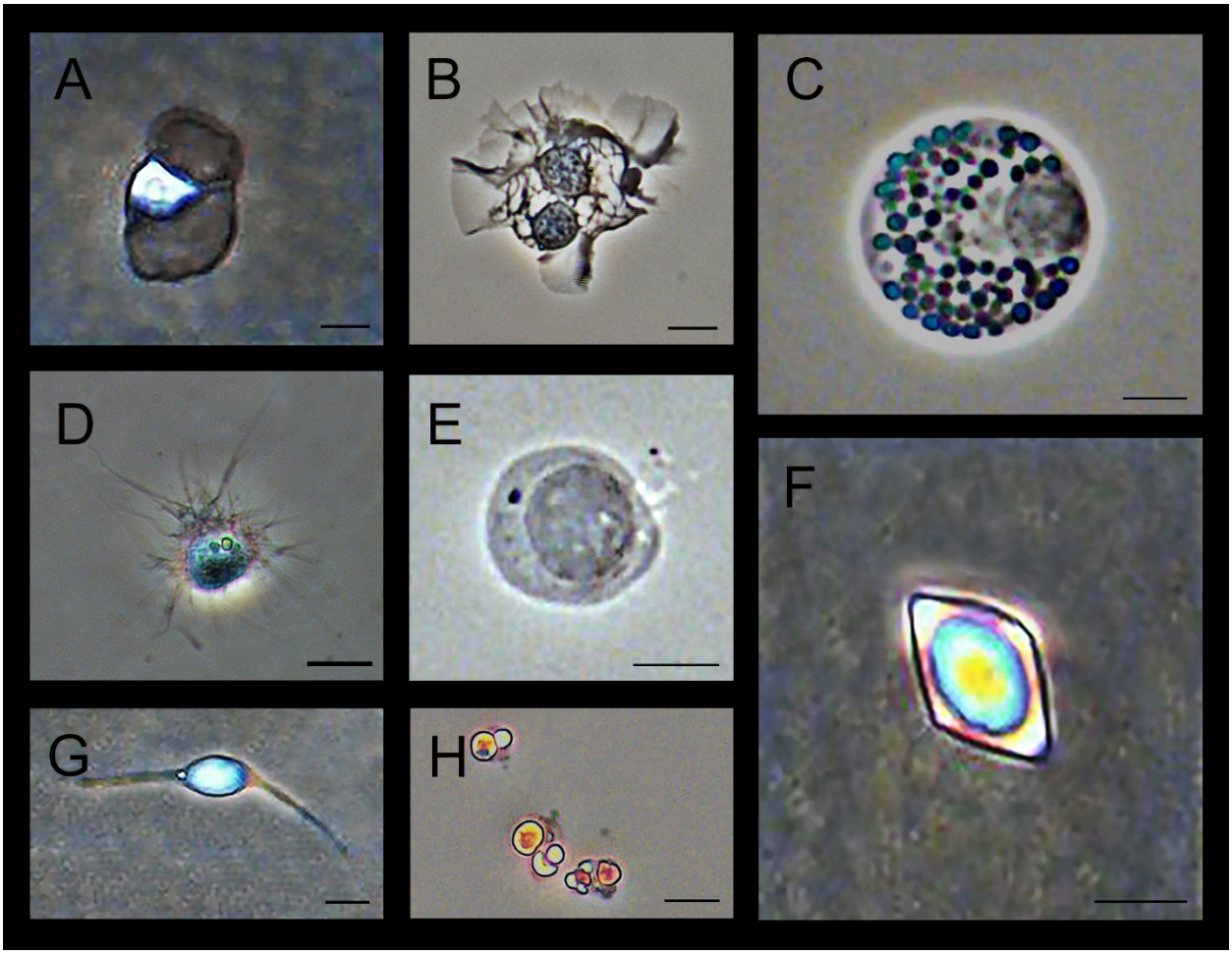

Supplementary Figure S3-2: Different coelomocyte types found in *C. frondosa.* A) Inactive (bladder) phagocyte (scale bar = 5 µm). B) Two active (petaloid) phagocytes (scale bar = 10 µm). C) morula cell (scale bar = 5 µm). D) Active (filopodial) phagocyte (scale bar = 10 µm). E) progenitor cell (scale bar = 5 µm). F) crystal cell (scale bar = 9 µm). G) fusiform cell (scale bar = 4 µm). H) a cluster of hemocytes (scale bar = 8 µm).

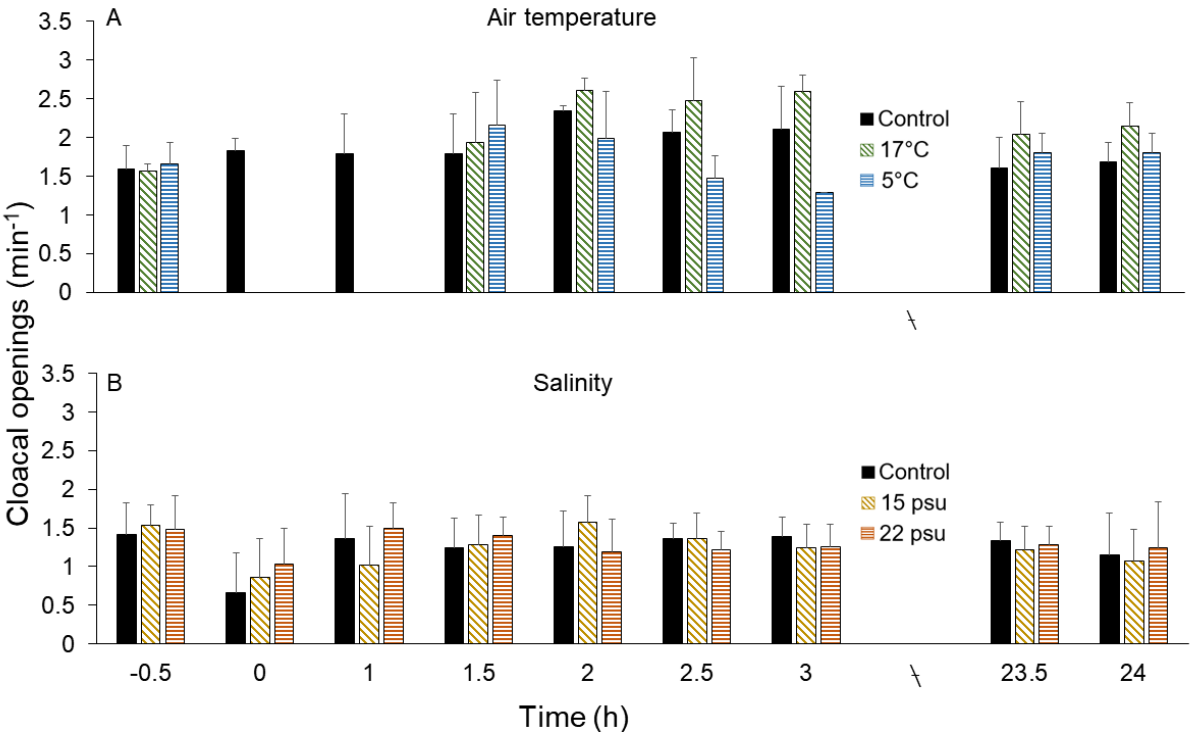

Supplementary Figure S3-3: Frequency of cloacal openings (min^{-1}) in *C. frondosa* at various time points before exposure (time 0 h, negative control), after the 1-h exposure (time 1 h) and over a subsequent recovery period of 23 h (until time 24 h; positive control). A) Comparison between controls and individuals exposed to 17°C and 5°C air. B) Comparison between controls and individuals exposed to 15 and 22 psu salinity. Data shown as mean ± SD (n = 5-11).

Chapter 4 - General Discussion and Conclusion

4.1 Background and overview of results

Echinoderms possess intuitive and resilient immune systems and their position next to chordates in the deuterostome clade validates the exploration of these systems towards improving our understanding of the evolution of vertebrate immunology (Smith *et al.*, 2018, Smith and Davidson, 1994). Coelomocytes are believed to be the main cellular agents of echinoderm immune systems, yet they are still poorly understood in terms of their origin, function, and inter-cellular interactions (Chia and Xing, 1996, Ramírez-Gómez and García-Arrarás, 2010). Previous studies have proposed that various coelomocytes are involved in allograft rejection, cytotoxic responses, neutralization/removal of bacteria and foreign particles, wound healing, and various other functions within echinoderms (Branco *et al.*, 2014, Chia and Xing, 1996). The behaviour of coelomocytes, their conservation, and their relationship with other mechanisms of immune defense have been largely overlooked in echinoderms when compared to similar work done on vertebrates. This research gap, partnered with echinoderms being considered keystone species around the world and sea cucumbers specifically being a lucrative seafood product, highlights the need for further work in this area.

4.1.2 Chapter 2

Chapter 2 of this thesis investigated the presence of coelomocyte aggregates in direct response to the injection of carbon particles across 23 species of echinoderms belonging to Holothuroidea, Echinoidea, Asteroidea, Ophiuroidea, and Crinoidea. Each species was evaluated for the presence of aggregates 96 h after injection. The cellular catalyst of aggregate formation and the eventual expulsion of packaged particles were also assessed.

The formation of coelomocyte aggregates was observed in every echinoderm class studied, although many species presented diverse aggregate phenotypes. The most striking

variation, i.e., colour, was linked to phylogeny. For example, holothuroids presented bright red aggregates, echinoids chiefly green to purple, asteroids variations of blue, green, beige and brown, ophiuroids beige and light green and crinoids presented beige to red-brown. As red colour in aggregates has previously been linked to antibacterial defense (Płytycz and Seljelid, 1993) it is possible that the range of colours described by this study provides baseline data for uncovering further defense capacities, cytotoxic or otherwise. It is possible that other factors beyond phylogeny (e.g., physiology) also affect the phenotypes of aggregates, however, the design of this study did not allow us to accurately assess them.

The composition of these aggregates was also diverse, with various coelomocyte types participating in the catalysis and development of aggregates. At the early stage of formation, it was possible to identify a variety of coelomocyte types, both actively involved in aggregation and freely circulating within the coelomic fluid. A number of the coelomocytes identified had only been previously described in holothuroids but here they were found across various classes (i.e., to my knowledge, fusiform cells were previously only documented in holothuroids but here, were found also within echinoids and ophiuroids).

Among the coelomocytes collected through this study, some had not been completely characterized (or even described) before. Globally, the different cell types have been named on the basis of their general morphology (e.g., morula), activity (e.g., phagocyte), or colour (e.g., red spherule cells; Ramírez-Gómez and García-Arrarás, 2010). In echinoderms, coelomocytes are classified into six main categories, namely, phagocytes (i.e., leukocytes, amoebocytes, bladder amebocytes, filiform amoebocytes), spherulocytes (i.e., amoebocytes, morula cells, white spherule cells), hemocytes, progenitor cells (i.e., lymphocytes, hyaline cells, dedifferentiated cells, undifferentiated cells, amoebocytes), crystal cells and fusiform cells. This

terminology is mainly based on studies in sea cucumbers (Caulier *et al.*, 2020, Eliseikina and Magarlamov, 2002, Hetzel, 1963) and sea urchins (Branco *et al.*, 2014, Brothers *et al.*, 2016, Smith *et al.*, 2019). Coelomocytes are rather conserved in these classes (i.e., different species present similar cell types and relative quantities in different compartments; Smith *et al.*, 2018), but holothuroid coelomocytes differ widely among orders. For example, some cell types, like hemocytes, are reported only from the Dendrochirotida and Molpadida orders (Baker and Terwilliger, 1993, Terwilliger and Terwilliger, 1988) and they often exhibit marked interspecific diversity in colour and shape (Chia and Xing, 1996). In the present study, the diversity of coelomocytes across different echinoderm classes was indeed maximal in holothuroids, followed by echinoids, while the other three classes showed comparable diversity in coelomocyte types (Supplementary Table S2-2). As expected, phagocytes were among the most common, appearing in every species. The literature is consistent in its description of the prolific expression of phagocytes (i.e., leukocytes, amebocytes, bladder amoebocytes, filiform amoebocytes). Given their involvement in phagocytosis and the early stages of aggregate formation, it makes sense that they would appear universally across the phylum. Throughout the literature, phagocytes are documented as having three morphologies (bladder, petaloid and filapodial). While there is a wide consensus that the final stage of transformation is the filapodial stage (Boolootian and Giese, 1958, Smith and Davidson, 1992), the bladder and petaloid phases have often been synonymized in the literature (Chia and Xing, 1996, Smith *et al.*, 2018) when they are, in fact, two distinct phases of transformation. The transformation from one form to the other can be spontaneous or triggered by environmental shock and involve pseudopodia, which have been tightly wrapped around the nucleus (bladder or inactive form), fanning outward to create a "halo" of actin filaments (petaloid or active form) followed by the cytoplasm gradually retracting

back towards the nucleus, leaving a network of microtubule tendrils free (filapodial form also considered to be the active form; Chia and Xing, 1996, Matranga, 2005, Noble, 1970, Smith and Davidson, 1992, 1994, Söderhäll, 2010).

The expulsion of aggregates at a mature stage of formation was also noted in four of the five classes (holothuroids, echinoids, asteroids, and ophiuroids). Within holothuroids and asteroids, it was possible to track this process directly, and aggregates were seen exiting the body through the anus and dermal papillae, respectively. While active expulsion of aggregates was not observed in echinoids and ophiuroids, recently expelled aggregates were discovered on the bottom of holding tanks, confirming that expulsion does occur.

Overall, findings in Chapter 2 confirm that, while aggregation is a conserved cellular phenomenon across Echinodermata, the catalysts (e.g., foreign particles, pathogens, environmental stress) and coelomocytes involved vary among species and classes. This diversity is also seen in cellular phenotypes and possibly in their mode of action and defense capabilities.

4.1.3 Chapter 3

Sea cucumbers experience high levels of harvesting pressures due to their lucrative value in global seafood markets. Understanding the health and well-being of these commercial species is therefore invaluable to designing an ethical, sustainable, and high-quality industry. Unfortunately, our current social and scientific perception of how sea cucumbers experience stress is negligible, resulting in an industry with minimal and non-specific health and safety guidelines. To expand our understanding of how sea cucumbers respond to common harvesting practices, Chapter 3 investigated the response of cellular (coelomocytes and aggregates), hormonal (cortisol), and behavioural (cloacal openings, force of attachment, and behavioural score) biomarkers in *Cucumaria frondosa* exposed to temperature- and pH-induced stress.

Individuals were exposed to air at varying intensities of increased temperature (5, 17°C) and lowered salinity (15, 22 psu). After different lengths of time (1 h of exposure and 1 h of exposure plus 23 h of recovery), individuals were evaluated for levels of coelomocytes, cellular aggregates, cortisol and for behavioural metrics, in comparison to control (baseline) results. Cellular and hormonal markers were measured in the fluid collected from the Polian vesicle. As this vesicle offers a discreet and clean subsample of fluid, it is a way to standardize methodology and avoid artifacts that come from accidentally puncturing organs like the gonad or digestive tract.

All the biomarkers measured during the study fluctuated proportionally to the severity of the stressor (as a measure of departure from natural conditions). As expected, air exposure at 17°C and salinity at 15 psu prompted the strongest responses while air at 5°C and water at 22 psu produced milder responses. However, the fact that seemingly mild stressors did continue to elicit a stress response even after 23 h of recovery post-exposure, suggests these individuals may be more sensitive to environmental changes than previously believed. Interpreted together, the biomarkers examined in this study provide a more comprehensive look at how harvesting impacts sea cucumbers and potentially modulates the quality of the commercially traded products.

4.2 Future directions

Chapter 2 focused on providing comprehensive baseline data for the cellular agents of echinoderm immunity. Among the main challenges was inconsistencies in the existing nomenclature, which differed among studies and taxa, sometimes referring to the same or similar elements. Many previously undescribed coelomocyte morphologies were documented for the first time during the present study (Table S4-1), and it was difficult to adequately insert them in

this messy nomenclature. A helpful area of future research could thus include standardizing and expanding nomenclature to compile more coelomocyte types and streamline the terminology across taxa. Table 1-1 is a first attempt at standardizing the names of cells to hopefully help readers compare the results of this study to previous work. Furthering this would allow interdisciplinary researchers to collaborate more readily. It would also be beneficial to confirm the presence or absence of vibratile cells within echinoderms. While these cells are documented in the literature, I have not included them in my studies, due to growing evidence that they may not be a type of coelomocyte and that their presence within the coelomic fluid is an artifact (the methodology I used tends to confirm this). As an additional follow-up, it would be valuable to characterize the humoral elements secreted by each cell type involved in the aggregation process. This would hopefully help explain the phenotypic differences seen across the mature coelomocyte aggregates of different echinoderm classes, as well as their individual roles. Finally, it would benefit our understanding of echinoderm physiology if further work was done to examine the process of aggregate expulsion within echinoids, ophiuroids and crinoids. Based on the size of expelled aggregates and their anatomy, it is possible that all echinoderm classes are able to expel aggregates through the anus or coelo-rectal canal in a process similar to sea cucumbers. Characterizing this process would not only provide novel information to the field but also offer insight into possible evolutionary divergence within asteroids.

The results of Chapter 3 outlined sensitive biomarkers to evaluate the health of sea cucumbers exposed to selected stressors. Future work could use the same approach to examine other echinoderm taxa and different anthropogenic stressors like agricultural pollution, ocean acidification, noise pollution, hydrocarbon pollution, etc. While the current method of testing hormone levels proved effective, refining the methodology would improve its sensitivity and

possibly expand cortisol monitoring to other marine invertebrates. This would be a valuable research area, as current methods of hormone analysis in invertebrates are not easily accessible to the majority of researchers, whereas ELISA assays are safe and affordable by comparison.

The research outlined in Appendix 1 and Appendix 2 directly supplemented the work conducted in this thesis. Appendix 1 provided insight into a unique behavioural strategy of the apodid sea cucumber *Chiridota laevis*, which was discovered while gathering data for Chapter 2. Spontaneous and rapid transversal fission occurred in this species when presented with a physical stressor, offering novel insight into how some holothuroids cope with stress and as mentioned in Chapter 2, may help explain some of the cellular immune results found here. I plan to look further into this remarkable fissiparous reaction and the physiological and immune mechanisms that underlie it. Appendix 2 is closely linked to the work outlined in Chapter 3 in showing how the immune response of sea cucumbers might be used as an indicator of cognitive appraisal, or anticipatory reaction to stress. This study also helped to refine the methodology used to detect cortisol and allowed researchers to make parallels between the cellular and hormonal markers of stress. While Chapter 3 focused on measuring bioindicators immediately following stress and after recovery, the work done in Appendix 2 allowed for monitoring at regular intervals over several hours. This highlights the importance of selecting appropriate time frames, and underscores the logistical difficulties associated with studying live coelomocytes (which are constantly morphing and prone to forming clumps). The use of combined techniques that make use of live and preserved cells may lead to more integrative approaches in the future.

4.3 Literature cited

Baker, S. M., and N. B. Terwilliger. 1993. Hemoglobin structure and function in the rat-tailed sea cucumber, *Paracaudina chilensis*. *Biol Bull* **185**:115-122.

Boolootian, R. A., and A. C. Giese. 1958. Coelomic corpuscles of echinoderms. *Biol Bull* **115**:53-63.

Branco, P. C., D. A. L. Figueiredo, and J. da Silva. 2014. New insights into innate immune system of sea urchin: Coelomocytes as biosensors for environmental stress. *OA Biol* **18**:1-7.

Brothers, C. J., J. Harianto, J. B. McClintock, and M. Byrne. 2016. Sea urchins in a high CO_2 world: The influence of acclimation on the immune response to ocean warming and acidification. *Proc R Soc B: Biol Sci* **283**:20161501.

Caulier, G., J.-F. Hamel, and A. Mercier. 2020. From coelomocytes to colored aggregates: Cellular components and processes involved in the immune response of the holothuroid *Cucumaria frondosa*. *Biol Bull* **239**:95-114.

Chia, F. S., and J. Xing. 1996. Echinoderm coelomocytes. *Zool Stud* **35**:231-254.

Eliseikina, M. G., and T. Y. Magarlamov. 2002. Coelomocyte morphology in the holothurians *Apostichopus japonicus* (Aspidochirota: Stichopodidae) and *Cucumaria japonica* (Dendrochirota: Cucumariidae). *Russ J Mar Biol* **28**:6.

Hetzel, H. R. 1963. Studies on holothurian coelomocytes. i. A survey of coelomocyte types. *Biol Bull* **125**:289-301.

Matranga, V. 2005. *Echinodermata*. Springer, Berlin ; New York.

Noble, P. B. 1970. Coelomocyte aggregation in *Cucumaria frondosa*: Effect of ethylenediaminetetratraacetate, adenosine and adenosine nucleotides. *Biol Bull* **139**:549-556.

Ramírez-Gómez, F., and J. García-Arrarás. 2010. Echinoderm immunity. *Invert Surv J* **7**:211-220.

Smith, L. C., V. Arizza, M. A. Barela Hudgell, G. Barone, A. G. Bodnar, K. M. Buckley, V. Cunsolo, N. M. Dheilly, N. Franchi, S. D. Fugmann, R. Furukawa, J. Garcia-Arraras, J. H. Henson, T. Hibino, Z. H. Irons, C. Li, C. M. Lun, A. J. Majeske, M. Oren, P. Pagliara, A. Pinsino, D. A. Raftos, J. P. Rast, B. Samasa, D. Schillaci, C. S. Schrankel, L. Stabili, K. Stensväg, and E. Sutton. 2018. Echinodermata: The complex immune system in echinoderms. Pp. 409-501 in *Advances in Comparative Immunology*, E. L. Cooper, ed. Springer, Cham.

Smith, L. C., and E. H. Davidson. 1992. The echinoid immune system and the phylogenetic occurrence of immune mechanisms in deuterostomes. *Immunol Today* **13**:356-362.

Smith, L. C., and E. H. Davidson. 1994. The echinoderm immune system: Characters shared with vertebrate immune systems and characters arising later in deuterostome phylogeny. *Ann N Y Acad Sci* **712**:213-226.

Smith, L. C., T. S. Hawley, J. H. Henson, A. J. Majeske, M. Oren, and B. Rosental. 2019. Methods for collection, handling, and analysis of sea urchin coelomocytes. *Methods Cell Biol* **150**:357-389.

Söderhäll, K. 2010. *Invertebrate Immunity*. Advances in Experimental Medicine and Biology.

Terwilliger, R., and N. B. Terwilliger. 1988. Structure and function of holothurian hemoglobins. P.^Pp. 589-595 in *Echinoderm Biology: Proceedings from the Sixth International Echinoderm Conference* Balkema, Rotterdam.

4.4 Supplementary Tables

Supplementary Table S4-1: Undescribed coelomocytes from all classes of echinoderms.

Minute corpuscles /Unidentified cells	Appears in: **A = Asteroids E = Echinoids H = Holothuroids O = Ophiuroids**	Size (µm)	Species
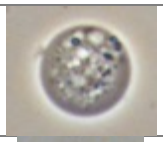	A, E, H, O	~15	*Asterias rubens*
	A, E, H, O	~10	*Asterias rubens*
	A, E, H, O	~25	*Asterias rubens*
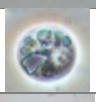	A	~6	*Asterias rubens*
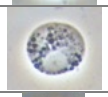	H,	~7	*Chiridota laevis*
	A, E, H, O	~4	*Chiridota laevis*
	H, O	~23	*Chiridota laevis*
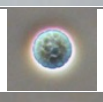	A, E, H, O	~5	*Ceramaster granularis*
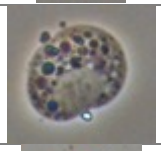	A	~17	*Ceramaster granularis*
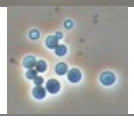	A, E, H, O	~1-5	*Ceramaster granularis*

	A, E, H, O	~10	*Crossaster papposus*
	A	~5	*Crossaster papposus*
	O	~15	*Gorgonocephalus arcticus*
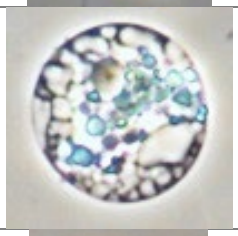	A	~25	*Henricia lisa*
	A	~15	*Henricia lisa*
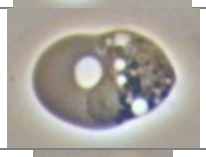	A	~20	*Henricia lisa*
	A	~11	*Henricia lisa*
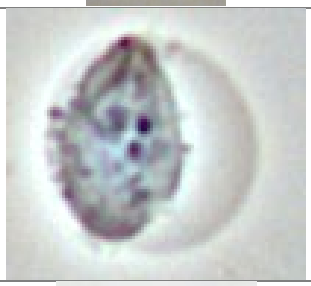	A	~30	*Henricia perforata*
	A	~18	*Henricia perforata*
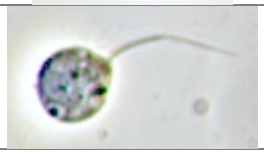	A	~20	*Henricia perforata*

	A, E, H, O	~23	*Hippasteria phrygiana*
	A	~40	*Hippasteria phrygiana*
	A	~23	*Hippasteria phrygiana*
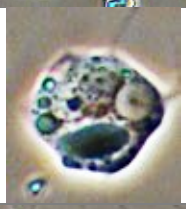	A	~20	*Hippasteria phrygiana*
	A	~25	*Hippasteria phrygiana*
	A	~17	*Hippasteria phrygiana*
	A	~12	*Leptasterias polaris*
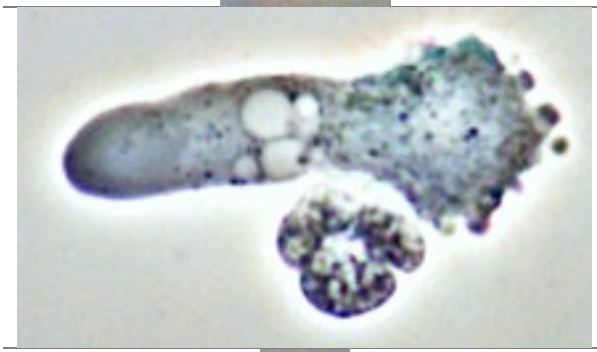	A	~58	*Leptasterias polaris*
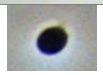	A, E, H, O	~4	*Leptasterias polaris*

	A	~12	*Leptasterias polaris*
	O	~20	*Ophiopholis aculeata*
	H	~28	*Psolus fabricii*
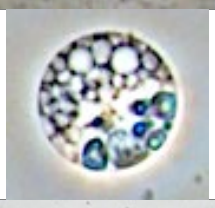	H	~20	*Psolus fabricii*
	A	~22	*Solaster endeca*
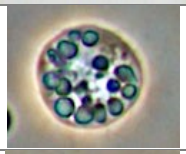	A	~13	*Solaster endeca*
	A	~13	*Strongylocentrotus droebachiensis*

Appendix 1

FrontiersEcoPics

Split personality

Survival is the greatest imperative of any life form, and the apodid holothuroid echinoderm (*Chiridota laevis*) exemplifies this in a remarkable manner. This small, 40–50 mm long, soft-bodied sea cucumber (top) normally spends its time hidden underneath rocks in the shallow waters of the North Atlantic. However, a recent discovery showed that *C laevis* is resourceful in the face of danger. When sensing a threat to the integrity of its body, such as a bite or a tear, the sea cucumber can quickly pinch itself and split apart in a matter of seconds. This response begins with an anterior inflation, followed by the appearance of a constriction collar that rapidly elongates and thins, ultimately leading to the physical separation of the front and back body segments (bottom) in less than 30 seconds.

Although potentially costly (from an energetic perspective), this reaction presumably acts either as a countermeasure or as wound limitation, shifting the threat away from the vital anterior body section. The rapidity of the process makes it an autotomic response rather than the much slower process of fissiparous (asexual) reproduction, which has been documented in echinoderms. However, autotomy usually involves the defensive shedding of non-essential body parts (a tail or arm, for example) in a controlled manner, whereas mid-body autotomy has – to the best of our knowledge – never been previously reported in unsegmented animals. The mechanisms and evolutionary advantages behind this impressive behavior remain an enigma.

Sara Jobson[1], Heather D Penney[1], Jean-François Hamel[2], and Annie Mercier[1]

[1]Memorial University, St John's, Canada; [2]SEVE, St Philips, Canada

doi:10.1002/fee.2281

Jobson, S., Penney, H.D., Hamel, J.-F. & Mercier, A. (2020). Split personality. *Frontiers in Ecology and the Environment*, 18, 557-557.

Appendix 2

www.nature.com/scientificreports

scientific reports

Check for updates

OPEN

Evidence of anticipatory immune and hormonal responses to predation risk in an echinoderm

Jean-François Hamel[1], Sara Jobson[2], Guillaume Caulier[2] & Annie Mercier[2]✉

Recent efforts have been devoted to the link between responses to non-physical stressors and immune states in animals, mostly using human and other vertebrate models. Despite evolutionary relevance, comparatively limited work on the appraisal of predation risk and aspects of cognitive ecology and ecoimmunology has been carried out in non-chordate animals. The present study explored the capacity of holothuroid echinoderms to display an immune response to both reactive and anticipatory predatory stressors. Experimental trials and a mix of behavioural, cellular and hormonal markers were used, with a focus on coelomocytes (analogues of mammalian leukocytes), which are the main components of the echinoderm innate immunity. Findings suggest that holothuroids can not only appraise threatening cues (i.e. scent of a predator or alarm signals from injured conspecifics) but prepare themselves immunologically, presumably to cope more efficiently with potential future injuries. The responses share features with recently defined central emotional states and wane after prolonged stress in a manner akin to habituation, which are traits that have rarely been shown in non-vertebrates, and never in echinoderms. Because echinoderms sit alongside chordates in the deuterostome clade, such findings offer unique insights into the adaptive value and evolution of stress responses in animals.

Stress has been defined in various ways but can be viewed as the response of an organism subjected to a challenge that may result in real or possible danger to its integrity[1]. Stressors may be distinguished based on whether they are reactive (direct challenge to homeostasis, like an injury or predator attack) or anticipatory (perceived threat requiring cognitive appraisal, like a cue of predation risk)[2]. While fear in animals is in response to the former, anxiety is in response to the latter[3]. The stress response to both situations may involve a wide range of mechanisms, including changes in genetic, metabolic, energetic, immune, endocrine, neural and behavioural processes aiming to overcome and compensate for the imbalances produced by the stressor. With these reactions, the animal tries to avoid dangerous situations and any threats to its survival or integrity and ultimately to reintegrate a state of balance[1].

While perceptible physical stressors (direct challenges) elicit a direct stress response, non-physical stressors first need to be appraised before eliciting a response[4]. Current knowledge on appraisal of non-physical stressors is almost entirely based on work conducted on humans (e.g. emotional/psychological stress) and in other members of the Chordata phylum (mammals and fishes), including in the context of predation risk[5]. More basal animals (non-vertebrates) are often not considered to have the necessary neural requirements to trigger anticipatory reactions; instead they are assumed to undergo strictly sensorimotor responses[6]. However, there is increasing evidence to support a re-evaluation of this assumption[7,8], circling back to Darwin's initial suggestion that insects have emotions[9]. For instance, research has shown that members of the phyla Arthropoda (insects, malacostracan decapods) and Mollusca (gastropods) may exhibit a variety of cognitive phenomena that were previously thought to be restricted to vertebrates or even to be unique to humans[8]. A new framework has been proposed for studying emotions across all animal species, based on a central emotion state with properties that are expressed through cognitive, behavioural, physiological and subjective components[10]. This approach disentangles emotions and their precursors from feelings (the conscious experience of emotional reactions), and moves away from comparisons with humans in favour of defining common features like scalability, persistence, valence and generalization to multiple contexts. While measuring cognitive responses in non-vertebrates represents a challenge[11], the last decade has seen breakthroughs. For instance, aversive taste stimuli were suggested to elicit behavioural reactions analogous to conditioned fear in pond snails[12] and cognitive bias was shown in honey bees exposed to vigorous shaking (mimicking danger), which subsequently interpreted ambiguous olfactory cues in

[1]Society for the Exploration and Valuing of the Environment (SEVE), St. Philips, NL A1M 2B7, Canada. [2]Department of Ocean Sciences, Memorial University, St. John's, NL A1C 5S7, Canada. ✉email: amercier@mun.ca

EVIDENCE OF ANTICIPATORY IMMUNE AND HORMONAL RESPONSES TO PREDATION RISK IN AN ECHINODERM

[1]Jean-François Hamel, [2]Sara Jobson, [2]Guillaume Caulier, and [2*]Annie Mercier

[1]Society for the Exploration and Valuing of the Environment (SEVE), 21 Phils Hill Road, St. Philips (Newfoundland), A1M 2B7, Canada;

[2]Department of Ocean Sciences, Memorial University, St. John's (Newfoundland), A1C 5S7, Canada

*Corresponding author: amercier@mun.ca

Keywords: anticipatory stress, coelomocytes, emotional state, holothuroid, immunity, indirect predator effects, response to threat, sea cucumber

Abstract

Recent efforts have been devoted to the link between responses to non-physical stressors and immune states in animals, mostly using human and other vertebrate models. Despite evolutionary relevance, comparatively limited work on the appraisal of predation risk and aspects of cognitive ecology and ecoimmunology has been carried out in non-chordate animals. The present study explored the capacity of holothuroid echinoderms to display an immune response to both reactive and anticipatory predatory stressors. Experimental trials and a mix of behavioural, cellular and hormonal markers were used, with a focus on coelomocytes (analogues of mammalian leukocytes), which are the main components of the echinoderm innate immunity. Findings suggest that holothuroids can not only appraise threatening cues (i.e., scent of a predator or alarm signals from injured conspecifics) but prepare themselves immunologically, presumably to cope more efficiently with potential future injuries. The responses share features with recently defined central emotional states and wane after prolonged stress in a manner akin to habituation, which are traits that have rarely been shown in invertebrates, and never in echinoderms. Because echinoderms sit alongside chordates in the deuterostome clade, such findings offer unique insights into the adaptive value and evolution of stress responses in animals.

Introduction

Stress has been defined in various ways but can be viewed as the response of an organism subjected to a challenge that may result in real or possible danger for its integrity[1]. Stressors may be distinguished based on whether they are reactive (direct challenge to homeostasis, like an injury or predator attack) or anticipatory (perceived threat requiring cognitive appraisal, like a cue of predation risk)[2]. While fear in animals is in response to the former, anxiety is in response

to the latter[3]. The stress response to both situations may involve a wide range of mechanisms, including changes in genetic, metabolic, energetic, immune, endocrine, neural and behavioural processes aiming to overcome and compensate for the imbalances produced by the stressor. With these reactions, the animal tries to avoid dangerous situations and any threats to its survival or integrity and ultimately to reintegrate a state of balance[1].

While perceptible physical stressors (direct challenges) elicit a direct stress response, non-physical stressors first need to be appraised before eliciting a response[4]. Current knowledge on appraisal of non-physical stressors is almost entirely based on work conducted on humans (e.g., emotional/psychological stress) and in other members of the Chordata phylum (mammals and fishes), including in the context of predation risk[5]. More basal animals (invertebrates) are often not considered to have the necessary neural requirements to trigger anticipatory reactions; instead they are assumed to undergo strictly sensorimotor responses[6]. However, there is increasing evidence to support a re-evaluation of this assumption[7,8], circling back to Darwin's initial suggestion that insects have emotions[9]. For instance, research has shown that members of the phyla Arthropoda (insects, malacostracan decapods) and Mollusca (gastropods) may exhibit a variety of cognitive phenomena that were previously thought to be restricted to vertebrates or even to be unique to humans[8]. A new framework has been proposed for studying emotions across all animal species, based on a central emotion state with properties that are expressed through cognitive, behavioural, physiological and subjective components[10]. This approach disentangles emotions and their precursors from feelings (the conscious experience of emotional reactions), and moves away from comparisons with humans in favour of defining common features like scalability, persistence, valence and generalization to multiple contexts. While measuring cognitive responses in non-vertebrates represents a challenge[11], the last decade has seen

breakthroughs. For instance, aversive taste stimuli were suggested to elicit behavioural reactions analogous to conditioned fear in pond snails[12] and cognitive bias was shown in honey bees exposed to vigorous shaking (mimicking danger), which subsequently interpreted ambiguous olfactory cues in a 'pessimistic' way similar to negative emotional states seen in vertebrates[13]. Similarly, bumblebees were shown to exhibit cognitive bias analogue to optimism[14].

Interpreting such reactions in slow-moving aquatic organisms with few recognizable features (no eyes or limbs) relies on the development of suitable behavioural, physiological, or immunological proxies, which may be explored in the context of adaptive stress responses. The fight or flight response first described 80 years ago[15], also called acute stress response, is triggered by a perceived (not necessarily actual) harmful event, attack, or threat to survival, to prepare the animal for fighting or fleeing[16]. A chain of reactions inside the body mobilises resources to deal with threatening circumstances, i.e., releasing hormones like adrenalin and cortisol, speeding the heart rate, slowing digestion, shunting blood flow to major muscle groups, giving the body a burst of energy and strength[15]. Burnovicz, et al.[17] studied the cardiac response of a crab exposed to various stimuli: light pulse, air puff, virtual looming and a real visual danger. The first two did not trigger observable behaviour, but the last two elicited a clear escape response and a change in heart rate upon sensory stimulation. The correlation found between escape and cardiac responses supports that the crab triggered several defensive reactions in the face of impending danger[17].

Where physiological metrics like cardiac responses cannot be measured (in the absence of a heart or circulatory system), immune responses provide a promising alternative[18]. Interestingly, Höglund, et al.[19] showed that regulatory T cells (lymphocytes that control the activity of other types of immune cell), appear to increase sharply in number in response to

psychological stress in humans. Terrestrial and aquatic invertebrates exhibit innate immunity comprised of cell-mediated phagocytosis, activation of cellular responses, and production of humoral antimicrobial compounds[20]. Their immune system is based on the presence of a group of cells called coelomocytes, which are abundantly described in the literature from different taxa (see reviews[21-24]) as the first line of defence, with their number and type varying dramatically during infections or following injury. Coelomocytes are found in the cavities of all echinoderm classes, including in the perivisceral coelom, the hydrovascular system, and the haemal system, as well as in the connective tissues and amongst various organs[25,26]. Their functions are similar to their leukocyte analogues in the immune system of vertebrates, such as formation of cellular clots, phagocytosis, encapsulation and clearance of parasites, bacteria and other foreign materials[27,28]. Encapsulation in echinoderms has been documented in classes Ophiuroidea, Echinoidea, and Holothuroidea, and its products are conventionally referred to as brown bodies or aggregates[29-31]. The latter are composed of various coelomocytes that can have different functions[22]. Based on work conducted on two echinoids (sea urchins), coelomocytes are considered sensitive biomarkers of marine environmental stress[32]. Apart from the immune response, the hormonal response offers other potential biomarkers of the stress response. For instance, cortisol is a steroid often referred to as the 'stress hormone' that is well known in aquatic vertebrates such as fishes[33]. It is also detected in non-chordate groups, including echinoderms[34], and a spike in cortisol was recently determined to be an expression of stress in bivalves[35] and holothuroids[36,37].

The present study used levels of coelomocytes and cortisol to explore the capacity of holothuroid echinoderms, more precisely the species *Cucumaria frondosa*, to display an immune response to both reactive and anticipatory stressors (physical attack vs cues of predation risk).

The approach mixed behavioural, immune and hormonal markers to test the following hypotheses: (i) if acute predation-related stress enhances the immune response, coelomocyte counts and cortisol levels will increase upon short-term acute exposure (<3 h) to a threat; (ii) if appraisal and perception of imminent threat is enough to trigger the stress response, direct contact with the stressor (predator) will not be necessary; (iii) when the non-physical cue is prolonged without the threat (attack) materializing, chronic stress will translate into a decrease of coelomocyte counts back to baseline levels (i.e., habituation). Ultimately, the study seeks to build the knowledge base on cognitive ecology by assessing whether non-vertebrate deuterostomes can react to potential threats before they materialize by preparing their immune line of defence in anticipation. Identifying markers of non-physical stress in a basal deuterostome clade that shares closes ancestors with chordates[38] provides an exciting tool for studying the adaptive value and early evolution of stress responses like anxiety inside the animal kingdom.

Results

Chronic exposure to direct and indirect stressors

All controls across treatments showed a baseline density of coelomocytes (all types combined) between 1.0 and 1.7 X 10^6 cells ml^{-1} from the beginning to the end of the 72-h trial (global mean of 1.4 X 10^6 cells ml^{-1}; Figure 1a). The control holothuroids remained firmly attached to the substrate (no displacement) with their tentacles extending periodically in the water column for feeding, corresponding to a resting state and a behaviour score <0.3 (Figure 1b).

In experiment 1, representing direct physical contact with the predatory asteroid (including predatory attacks), the total density of free coelomocytes rose from baseline values at time 0 to 11.6 X 10^6 cells ml^{-1} after 3 h, representing an increase of about 730% (Figure 1a).

Coelomocyte densities decreased after 6 h but remained higher than baseline, between 9-10 X 10^6 cells ml^{-1}, until the end of the trial (Figure 1a). From the onset (≤10 min), the exposed holothuroids displayed an increase in locomotory movement (92 cm min^{-1}) and the typical escape response (detachment, rolling and muscular contractions), occasionally combined with active buoyancy adjustment (ABA)[39], until the end of the experiment (72 h), corresponding to a mean behaviour score of 2.8-3.0 (Figure 1b).

In experiment 2 (contactless treatment), holothuroids received only the chemical cue (i.e., 'scent') from the predator without any physical or visual cue (no actual physical threats for their physical integrity). The density of coelomocytes rose to 5.6 X 10^6 cells ml^{-1} after 3 h, representing about 300% increase from baseline, which was lower than upon direct contact with the predator (Figure 1a). Coelomocyte densities remained comparably high at 6.3 X 10^6 cells ml^{-1} and 5.3 X 10^6 cells ml^{-1} after 6 and 24 h, respectively, before falling back to baseline values below 1.7 X 10^6 cells ml^{-1} after 72 h (Figure 1a). The behaviour of holothuroids exposed to the predator scent was similar to the one recorded following direct contact during the first 6 h, i.e., rapid displacement (80–85 cm min^{-1}), escape response and retraction of the tentacles, yielding a mean behaviour score of 2.7 (Figure 1b). However, an increasing number of individuals returned to a resting state after 24 h, whereby a more static posture was adopted (decreased locomotion to ≤10 cm min^{-1}, tentacles periodically extended, and no escape response), with a mean behaviour score of 0.8 (Figure 1b). After 72 h, all exposed holothuroids had resumed normal behaviour (mean score of 0.1; Figure 1b).

Experiment 3 (exposure to the scent of an injured conspecific) produced intermediate results, with overall sharper responses, but an eventual return to baseline. After 3 h of exposure, the density of coelomocytes rose sharply to 11.2 X 10^6 cells ml^{-1}, comparable to values in the

treatment involving contact with the predator (about 700% increase; Figure 1a). However, values continued to rise, reaching 14.8 X 10^6 cells ml^{-1} after 6 h, which was higher than in the response to direct contact with the predator. Coelomocyte densities decreased to 6.8 X 10^6 cells ml^{-1} after 24 h, mirroring values of the contactless treatment, before returning to values close to baseline, i.e., 1.9 X 10^6 cells ml^{-1}, after 72 h (Figure 1a). Similar to the contactless treatment, behaviour scores rose markedly to 1.8-2.2 after 3-24 h and decreased back to near-baseline values (score of 0.4) after 72 h (Figure 1b) and displacement peaked between 71–88 cm min^{-1}.

Statistical analysis highlighted the interaction between the effects of treatment and time on coelomocyte density ($F_{12,252} = 112.4$, $p < 0.001$) and behaviour score ($F_{12,252} = 84.5$, $p < 0.001$). Further analyses conducted independently for each factor confirmed the clear effect of time ($F_{4,38} = 23.2$, $p < 0.001$); with spikes in coelomocyte density between 3-24 h followed by a return to baseline after 72 h in all treatments, except contact with the predator (Figure 1a). An identical pattern was also statistically clear in the behaviour scores (Figure 1b; $H = 42.4$, $df = 4$, $p < 0.001$). A clear effect of treatment on the coelomocyte density (Figure 1c; $H = 137.3$, $df = 3$, $p < 0.001$) and behaviour score (Figure 1d; $H = 162.6$, $df = 3$, $p < 0.001$) was also shown. When integrated over the 72-h response, coelomocyte densities deviated from controls inside treatments, but were similar among treatments; whereas behaviour scores showed full pairwise differences, except between the two contactless treatments (scent of predator and scent of injured conspecifics).

Short-term contactless exposure to predator

From 0 to 150 min, the total number of free coelomocytes increased steadily by steps, from 1.3 X 10^6 cells ml^{-1} to a maximum of 9.2 X 10^6 cells ml^{-1} after 150 min (an increase of 770%), which was maintained after 180 min (Figure 2a). Upon examination of coelomocyte types, a

progressive increase in phagocytes was detected during the first 150 min, from 1.3 to 8.9 X 10^6 cells ml^{-1}, followed by a decrease over the next 30 min to 3.8 X 10^6 cells ml^{-1} after 180 min (Figure 2b). The morula cells remained low until 120 min (≤0.2 X 10^6 cells ml^{-1}) and increased to >0.2 X 10^6 cells ml^{-1} after 150 min, before decreasing back to 0.1 X 10^6 cells ml^{-1} after 180 min (Figure 2c). Moreover, the hemocyte counts increased drastically from near zero to 5.3 X 10^6 cells ml^{-1} after 180 min (an increase of ~2500%; Figure 2d). After 180 min, the hemocytes represented 20-93% of all coelomocytes present (Figure 2d), at a time when phagocyte counts were decreasing back to baseline values in some individuals. The statistical analysis of coelomocyte density (pooled types) confirmed the clear effect of time ($F_{6,14} = 3.36$, $p = 0.029$), including a clear departure from baseline (time 0) after 150 min and 180 min (post-hoc test, $p =$ 0.032 and 0.031, respectively). Phagocytes also displayed a clear stepwise increase ($F_{6,14} =$ 13.07, $p < 0.001$), with departure from baseline becoming clear from 90 min onward (post-hoc test, $p < 0.004$). Morula cells peaked at 150 min (Figure 2c; post-hoc test, $p = 0.006$) and hemocytes peaked at 180 min (Figure 2d; post-hoc test, $p = 0.004$).

Individuals in the control group and those assessed at time 0 exhibited cloacal opening rates (respiration) around 1 min^{-1} while their force of attachment to the substrate was ~14.7 N. All remained firmly attached to the substrate and ~65% of them had their tentacles extended at any time point. After 30 min of exposure to the stressor, cloacal openings increased to 4.3 min^{-1}, reaching a maximum of 7 min^{-1} after 60 min, thereafter remaining steady until the end (180 min). The force of attachment to the substrate dropped to ~0.2 N after 30 min and to almost 0 N thereafter. Concurrently, the locomotor activity increased from 0 to 35 cm min^{-1} inside the first 60 min, and up to 80 cm min^{-1} after 90 min, with 46% of individuals showing the typical escape

response. Some 33% of individuals showed excessive production of mucus on the surface of the body wall after 60 min and some of them were also showing clear ABA after 120 min. Individuals in the short-term exposure to the scent of the predator showed levels of cortisol that spiked after 30 min at levels that were clearly higher than at time 0 ($H = 13.31$, $df = 6$, $p = 0.038$) and decreased subsequently, although levels after 120 min remained higher than baseline (post-hoc test, $p = 0.031$; Figure 3). Overall, interindividual variability showed that the hormonal response was not uniform or consistent (Figure 3).

Discussion

The present study of the holothuroid echinoderm *Cucumaria frondosa* compared the effects of reactive versus anticipatory stressors (direct predator attacks versus cues of predation risk) on behavioural, immune and hormonal markers. It revealed that chemical cues (scent) from a nearby predator or injured conspecifics triggered all markers. Cortisol spiked within 30 minutes and cell counts in the hydrovascular fluid increased steadily over 3 hours to levels up to 700-770% greater than baseline levels measured in undisturbed individuals. In addition, chronic exposure to contactless stress for 3 days eventually led to a decrease in the immune markers, providing evidence of something akin to habituation[40]. Such findings of adaptive stress responses also intersect with two transformative fields of research; one seeking to explore analogues of emotions in non-vertebrates through behavioural, neural and physiological approaches[8], and the other devoted to the link between emotional and immune states in animals, mainly humans[18,41]. The anticipatory immune response to imminent threat seen here in a holothuroid, paralleling hormonal and behavioural responses, adds to recent breakthroughs on analogues of anxiety reported in other phyla (recently reviewed[8]). Because echinoderms are the closest non-chordate

invertebrate clade to mammals/humans[38], data on their cognitive-like processes offer interesting perspectives in the study of anxiety and other stress responses.

A substantial body of literature on brain circuitry and other aspects of neuroscience have historically drawn from studies of invertebrate biology and physiology[42], while research on cognitive phenomena in invertebrates is gaining interest[8,43]. A common framework for the study of emotions across species, including invertebrates, has also been recently proposed[10]. To date, studies on invertebrate models have typically centred on species with a distinct cephalic region (including two eyes) and recognizable behavioural reactions (agitation), such as bees, flies, crabs and snails. Echinoderms have remained largely unstudied despite their pivotal position in the deuterostome clade, possibly due to technical difficulties; they have no head and their nervous system is among the least studied[44]. Work on learning abilities in echinoderms is also scarce[45,46] and it was recently suggested that this paucity of information prevented a clear understanding of the role of neural centralization in the evolution of associative learning[47]. It was also recently demonstrated that even single-celled organisms can display simple learning[48].

Moving away from anthropocentric analogy, the unifying framework proposed in 2014 to study emotions across species[10] outlined behavioural, neural and physiological (including hormonal) underpinnings of central emotional states. The building blocks of emotional responses, which set them apart from simple reflexes, were defined as scalability (intensity), valence (antithesis), persistence and generalization[10]. While humoral/cellular immunity pathways were not covered in that study, the responses measured here in *C. frondosa* possess some of the features of these building blocks, such as scalability and persistence. The nature of the signal clearly influenced the severity of the response, i.e., maximum upon direct contact with the predator, mildest when only the scent of a predator was perceptible, and intermediate when

injured conspecifics could be sensed (evoking alarm signals triggered by active predatory events[49]). These results are also akin to stimulus decoupling in humans, which involves the anticipation or recollection of a stimulus instead of a direct confrontation with it, exemplified by the direct versus anticipated encounter with a predator[10]. Although it was not explicitly measured here, the response of holothuroids was almost certainly persistent (lasting hours after the stimulus was applied) since cortisol level was still elevated after 3 hours and coelomocyte counts take a long time to decrease, based on a previous study[31]. Valence is more difficult to assess since opposites states are hard to define in holothuroids beyond behavioural approach vs avoidance, for which neurobiological underpinnings have yet to be understood.

Regardless of whether the response of *C. frondosa* to direct and indirect indicators of a predator qualifies as anxiety or apprehension, it belies anticipation of injury by triggering an immune reaction. This is a useful adaptive response because, while the escape behaviour of *C. frondosa* is often successful, sublethal predation by the asteroid *S. endeca* can generate lesions on the body wall. In exposures to predator scent only, the counts of phagocytes rose first, whereas morula cells and hemocytes spiked only after 150-180 minutes, as phagocytes counts started to decrease. Phagocytes represent the frontline of the immune response; they are primarily designed to engulf pathogens or dead cells[31]. Morula cells are hypothesized to secrete humoral effectors and provide the foundation for tissue repair[50,51], whereas hemocytes are presumed to provide oxygen and nutrients to tissues regenerating tissues[52], and they are also linked to packaging and oxidation of material captured in cellular aggregates[31]. After the first spike, the coelomocyte counts returned to normal when the stress became chronic (>24 h) without materializing in terms of physical encounter/attack. Hence, to balance energetic costs with survival, the holothuroid was apparently able to assess when danger was high/imminent and

react by developing an anticipatory immune reaction, which eventually waned after prolonged/repeated stimulation without direct finality. In addition, *C. frondosa* exhibited a clear (slightly more pronounced) increase in immune responses when exposed to the scent of injured conspecifics. Research has shown that both animals and plants produce secondary metabolites in response to signals from wounded neighbours[49]. The present study indicates that holothuroids can stand ready for injuries when sensing cues both from the predator and from conspecifics, helping to maximize survival at the population level.

While predator-induced stress is a long-standing field of study, novel perspectives on the ecology of fear are emerging[5]. Moreover, the link between stress and immunity in prey species has only recently been explored in non-vertebrates (i.e., insects), indicating that predation risk modulates defence against pathogens and, inversely, that immune challenge increases predation risk. In larval Lepidoptera, predator-induced stress compromised immunity to bacteria and had physiological outcomes, including reduced body mass[53]. On the other hand, immune-challenged crickets were slower to react to predators[54]. Here, the predation risk itself seemed to trigger the innate immune response of holothuroids. It would be interesting to investigate the metabolic and fitness costs of this response. Another question is whether individuals of *C. frondosa* already undergoing an immune challenge (e.g., presence of foreign particles in the hydrovascular system) would display a different (e.g., slower, incomplete) response to predation, similar to crickets[54].

Upon exposure to a perceived threat emanating from the scent of a predator, cortisol levels in *C. frondosa* rose above baseline level measured pre-trial and in control individuals. The exact role of cortisol in holothuroids remains incompletely understood, but in vertebrates it has been shown to mobilize energy to meet excessive metabolic demands and trigger a broad range of responses

working towards resumption of homeostasis[55]. The cortisol spike in *C. frondosa* paralleled the rise in coelomocyte counts, similar to what has been described in humans[56,57]. A hormonal cue for the release of coelomocytes in the hydrovascular system might thus be present. Since there was no loss of tissue integrity, the increase in both cortisol and coelomocytes evokes preparatory actions in the face of a potential injury, i.e., the holothuroid can detect an imminent attack and react to increase its chance of survival to nonlethal predatory events. The ability to stay alert to environmental cues and to react to predators (freeze, fight or flight) relies on the integration of sensory information and its translation into motor output via the nervous system[58]. Such reactions are usually ascribed to vertebrates but invertebrates may possess comparable counterparts, as recently highlighted by a review which showed that features of neuroautonomic regulation of the cardiac function appeared early in the evolution of decapod crustaceans[58].

Future studies that could build on the present findings include assessments of how stress affects cognitive processes and appraisal of the environment, which is a fairly new branch of non-human research on emotions, dating back less than 20 years[59], even though Darwin drew attention to it long ago[9]. The holothuroid *C. frondosa* could be used to study how individuals, whether undisturbed or recently exposed to stressful conditions that stimulated their immune responses, react to the presence of food, knowing that feeding requires the extension of vulnerable body parts (tentacles). A difference in the number of feeding individuals would provide evidence of "cognitive bias", as recently shown in shaken bees[11-13]. Measurements of biogenic amines (e.g., dopamine, serotonin) could also be attempted. Ultimately, further research with echinoderms like *C. frondosa* may offer clues into how cognition and emotion interact in ecological contexts, how the simplest neural networks can underpin complex assessments and responses, and how central emotion states evolved in higher deuterostomes, all the way to

humans. More pragmatic outcomes include a refined understanding of stress, pain and fear in non-vertebrate species, ultimately leading to the design of suitable animal care protocols.

Methods

Choice of focal species

The sea cucumber *Cucumaria frondosa* belongs to class Holothuroidea of phylum Echinodermata, and is thus a member of the lowest deuterostome clade (sitting closer to humans than nearly all other non-vertebrates[38]). Its feeding ecology, reproduction, larval development, behavioural response to stressors and most aspects of its anatomy, general biology, biochemical composition and metabolites are well known[60]. Investigations of its immune system and how it responds to the presence of foreign particles in its tissues or cavities and to injuries have recently been published[31].

Collection and maintenance

Adult holothuroids (12-15 cm contracted length) were collected by divers between 10-15 m depths in eastern Newfoundland, Canada (47°12'45.7"N, 52°50'41.3"W) in January 2018 and September 2019. They were carefully detached from their substrates to avoid damaging the tissues, especially the ambulacral podia. Individuals were maintained in a 200-L tank with running unfiltered seawater (60 L h^{-1}) that provided them with planktonic food (their natural diet) at ambient temperatures ranging from -1 to 5°C. Light was supplied to a maximum intensity of 200 lux following natural photoperiod. Only healthy individuals acclimated for a minimum of eight weeks that were firmly attached and showed no sign of stress behaviour[39] or physical damage were used. Sex was determined based on the external sexual dimorphism of the genital papilla[61].

Four individuals of the predatory asteroid *Solaster endeca* (about 24 cm in diameter) were collected in Bay Bulls (47°18'41.8"N, 52°48'33.1"W) in July 2018 and maintained separately under the same conditions as the holothuroids. They were fasted for a month to standardize their hunger level before the experiment[62].

Chronic exposures to direct and indirect stressors

Treatments and experimental design

Twelve 20-L tanks were dedicated to each experiment consisting of 6 header thanks flowing unidirectionally into 6 other tanks to create 6 independent paired units. All units received similar flows (about 19 L h^{-1}) and were randomly oriented to minimize tank effects. Fluorescein sodium salt was used to verify that water entering the experimental tank was well mixed. In each experiment, 3 of the paired units were used for one of three treatments: 1) Direct physical contact between the holothuroids and their predator, the asteroid *S. endeca* (involving sublethal predation attempts and/or injuries); 2) exposure to the predator cues through water (contactless); and 3) exposure to cues from an injured conspecific through water. The 3 other paired units were used for controls, whereby holothuroids were exposed to natural seawater flowing from bare headers. Experimental tanks that had to be reused were emptied and scrubbed to prevent any sensory bias.

At the onset of an experiment, 6 holothuroids (3 of each sex per experimental tank) of a similar size (89.1 ± 11.7 g body-wall weight) were distributed in each of the 6 downflow tanks (i.e., 18 experimental sea cucumbers and 18 control sea cucumbers per treatment). They were left to acclimate for at least a week [31]. In experiment 1, one asteroid was introduced in each of 3 downflow tanks alongside the holothuroids; in experiment 2 one predatory asteroid was placed in each of 3 header tanks (running into the downflow tanks); and in experiment 3, one injured

holothuroid was placed in each of 3 headers. The injured individual had a 3-cm long cut in the body wall; rapid healing occurred inside 10 d, as is common in this species[60].

Behavioural responses

A Brinno MAC200 camera placed above the tanks to capture the entire experimental arena with an automated infrared light allowing recording to continue at night. A picture every 30 s (aligned with the slow movements of sea cucumbers), which the camera software stitched into a video clip. Behavioural scores were established at 10-min intervals, i.e., ± 5 min around times 0, 3, 6, 24 and 72 h, based on three criteria: evidence of an escape response (defined below); displacement speed; and cycles of deployment and extension of tentacles. A score of 0 corresponded to the relaxed/resting state, i.e., no escape response, no movement, and normal tentacle state; while a score of 3 meant a full-fledged escape response, which consists of detaching from the substrate, contracting and elongating the body[63] and undergoing active buoyancy adjustment (ABA)[39]. See Table 1 for detailed definitions. Scores of individuals inside a tank were averaged, and the proportion of individuals with visible mucus was also noted.

Sample collection and analysis of coelomocytes

One holothuroid was collected from each tank after 0, 3, 6, 24 and 72 h (terminal procedure). It was opened dorsally using a scalpel, avoiding the radial canals and row of ambulacral podia, keeping the Polian vesicle intact. The latter holds uncontaminated hydrovascular fluid in *C. frondosa*[31]. A small opening at the base of the Polian vesicle allowed the entire fluid to leak into 50-ml Falcon tubes. The fluid was immediately mixed and inverted six times to resuspend and homogenize any free coelomocytes. A subsample of 1 ml was collected and placed into a Neubauer counting chamber, which was examined under a light microscope. Images were taken at 400X using an Olympus DP73 digital camera to count and

identify coelomocytes in grid cells selected using a random integer set generator (random.org). For each time point, the dominant coelomocyte types (phagocytes, morula, hemocytes) and the coelomocyte count (all types pooled) were scored in 3-4 replicate cells. The mean density of coelomocyte (ml^{-1}) established from replicates was compared among treatments over time.

Short-term contactless exposure to predator

The short-term experiment (3 h) was conducted using the same general set up as the chronic exposures outlined earlier. It tested contactless exposure to the predator only, and it was monitored directly rather than through video analysis. One holothuroid per experimental tank was assessed after 0, 30, 60, 90, 120, 150 and 180 min, along with controls at the first and last time points. The cloacal opening (respiration) and the force of attachment to the substrate were established at each time points. These parameters are behavioural indicators of the level of stress in holothuroids[39,64]. The number of cloacal openings inside a period of 2 min was measured three times in close succession. Attachment strength was measured by wrapping a zip-tie around the middle of each individual, attaching the loop to a hand-held precision spring balance, and measuring the force required to perpendicularly pull the individual off[39].

After the above assessment, individuals were sampled (terminally) for analysis of free coelomocytes as described for the chronic exposures. In addition, cortisol levels were measured. For the latter, 1-ml samples of Polian vesicle fluid were placed in vials and frozen undiluted at -80°C within 10 min of collection. For processing, the fluid was thawed, and the pH lowered to 1.5 - 2.0 using 0.5 M HCL. Samples were washed once with 4 ml of dichloromethane following the procedure provided for a competitive cortisol ELISA assay (Cayman Chemical 500360). Dichloromethane was evaporated out of the washed sample using a nitrogen stream. Preparation of assay-specific reagents followed standard ELISA kit protocol. Before plating, each sample

was centrifuged at 4000 rpm for 5 min. The incubation and development of the plate was completed as per vendor instructions. The 8-point standard curve, blank, total activity, non-specific binding and maximum binding wells were all run in duplicate. The plate was shaken mechanically for 3 s and read at 420 nm using a microplate reader (Molecular Devices SpectraMax® M5) and the software SoftMax® Pro v6.4. Data were processed using the publicly available Excel program designed for this ELISA kit.

Data analysis

In chronic exposure trials, two-way analysis of variance (ANOVA) followed by pairwise comparison (Holm-Sidak) was used to assess the effect of treatment (contact, contactless, injured conspecific; and their three respective controls) and time (0, 3, 6, 24, 72 h) on the dependent variables (coelomocyte densities and behaviour scores). Because controls for both variables (representing baseline metrics) were not statistically different across treatments at any time point (Holm-Sidak, $p > 0.20$), they were pooled to generate four treatment categories (i.e., contact, contactless, injured conspecifics, control). To subsequently deal with interactions between treatment and time, analyses were conducted at each level of the two factors using one-way ANOVA or ANOVA on ranks, depending on data homoscedasticity, followed by pairwise comparisons with Holm-Sidak or Dunn's methods, respectively. In the short-term contactless exposure trials, cortisol levels over time were not normally distributed and were analysed using a one-way ANOVA on ranks followed by Dunn's pairwise tests. All tests used $\alpha = 0.05$, although the analyses were interpreted cautiously, following calls to move away from arbitrary thresholds (including by the American Statistical Association[65]); hence, the principles of statistical clarity[66] were followed.

Data availability

The datasets generated during and/or analysed during the current study are available from the corresponding author on reasonable request.

References

1 Tort, L. Stress and immune modulation in fish. *Dev. Comp. Immunol.* **35**, 1366-1375 (2011).

2 Boonstra, R. Reality as the leading cause of stress: rethinking the impact of chronic stress in nature. *Funct. Ecol.* **27**, 11-23, doi:https://doi.org/10.1111/1365-2435.12008 (2013).

3 Öhman, A. Fear and anxiety: Overlaps and dissociations. in *Handbook of Emotions* (eds M. Lewis, J. M. Haviland-Jones, & L. F. Barrett) 709–728 (The Guilford Press, 2008).

4 Maydych, V. *et al.* Impact of chronic and acute academic stress on lymphocyte subsets and monocyte function. *PLoS One* **12**, e0188108 (2017).

5 Clinchy, M., Sheriff, M. J. & Zanette, L. Y. Predator-induced stress and the ecology of fear. *Funct. Ecol.* **27**, 56-65, doi:https://doi.org/10.1111/1365-2435.12007 (2013).

6 Allen-Hermanson, S. Insects and the problem of simple minds: Are bees natural zombies? *J. Philos.* **105**, 389-415 (2008).

7 Loukola, O. J., Perry, C. J., Coscos, L. & Chittka, L. Bumblebees show cognitive flexibility by improving on an observed complex behavior. *Science* **355**, 833-836 (2017).

8 Perry, C. J. & Baciadonna, L. Studying emotion in invertebrates: what has been done, what can be measured and what they can provide. *J. Exp. Biol.* **220**, 3856-3868 (2017).

9 Darwin, C. *The Expression of the Emotions in Man and Animals*. (John Murray, 1872).

10 Anderson, D. J. & Adolphs, R. A framework for studying emotions across species. *Cell* **157**, 187-200 (2014).

11 Mendl, M., Paul, E. S. & Chittka, L. Animal behaviour: emotion in invertebrates? *Curr. Biol.* **21**, R463-R465 (2011).

12 Kita, S. *et al.* peiDoes conditioned taste aversion learning in the pond snail *Lymnaea stagnalis* produce conditioned fear? *Biol. Bull.* **220**, 71-81 (2011).

13 Bateson, M., Desire, S., Gartside, Sarah E. & Wright, Geraldine A. Agitated honeybees exhibit pessimistic cognitive biases. *Curr. Biol.* **21**, 1070-1073, doi:https://doi.org/10.1016/j.cub.2011.05.017 (2011).

14 Perry, C. J., Baciadonna, L. & Chittka, L. Unexpected rewards induce dopamine-dependent positive emotion–like state changes in bumblebees. *Science* **353**, 1529, doi:10.1126/science.aaf4454 (2016).

15 Cannon, W. B. *The Wisdom of the Body*. (Norton & Co., 1939).

16 Jansen, A. S. P., Van Nguyen, X., Karpitskiy, V., Mettenleiter, T. C. & Loewy, A. D. Central command neurons of the sympathetic nervous system: basis of the fight-or-flight response. *Science* **270**, 644-646 (1995).

17 Burnovicz, A., Oliva, D. & Hermitte, G. The cardiac response of the crab *Chasmagnathus granulatus* as an index of sensory perception. *J. Exp. Biol.* **212**, 313-324 (2009).

18 Brod, S., Rattazzi, L., Piras, G. & D'Acquisto, F. 'As above, so below'examining the interplay between emotion and the immune system. *Immunology* **143**, 311-318 (2014).

19 Höglund, C. O. *et al.* Changes in immune regulation in response to examination stress in atopic and healthy individuals. *Clin. Exp. Allergy* **36**, 982-992 (2006).

20 Mydlarz, L. D., Jones, L. E. & Harvell, C. D. Innate immunity, environmental drivers, and disease ecology of marine and freshwater invertebrates. *Annu. Rev. Ecol. Evol. S.* **37**, 251-288 (2006).

21 Beck, G. & Habicht, G. S. Immunity and the invertebrates. *Sci. Am.* **275**, 60-66 (1996).

22 Chia, F.-S. & Xing, J. Echinoderm coelomocytes. *Zool. Stud.* **35**, 231-254 (1996).

23 Pinsino, A. & Matranga, V. Sea urchin immune cells as sentinels of environmental stress. *Dev. Comp. Immunol.* **49**, 198-205 (2015).

24 Smith, A. B. Fossil evidence for the relationships of extant echinoderm classes and their times of divergence. in *Echinoderm Phylogeny and Evolutionary Biology* (eds C.R.C. Paul & A.B. Smith) 85-97 (Clarendon Press, 1988).

25 Gliński, Z. & Jarosz, J. Immune phenomena in echinoderms. *Arch. Immunol. Ther. Ex.* **48**, 189-193 (2000).

26 Muñoz-Chápuli, R., Carmona, R., Guadix, J. A., Macías, D. & Pérez-Pomares, J. M. The origin of the endothelial cells: an evo-devo approach for the invertebrate/vertebrate transition of the circulatory system. *Evol. Develop.* **7**, 351-358 (2005).

27 Matranga, V., Pinsino, A., Celi, M., Di Bella, G. & Natoli, A. Impacts of UV-B radiation on short-term cultures of sea urchin coelomocytes. *Mar. Biol.* **149**, 25-34 (2006).

28 Matranga, V. *et al.* Monitoring chemical and physical stress using sea urchin immune cells. in *Echinodermata* Vol. 39 (ed V. Matranga) 85-110 (Springer, 2005).

29 Canicattì, C., D'Ancona, G. & Farina-Lipari, E. The *Holothuria polii* brown bodies. *Ital. J. Zool.* **56**, 275-283 (1989).

30 Canicatti, C. & Quaglia, A. Ultrastructure of *Holothuria polii* encapsulating body. *J. Zool.* **224**, 419-429 (1991).

31 Caulier, G., Hamel, J.-F. & Mercier, A. From coelomocytes to colored aggregates: cellular components and processes involved in the immune response of the holothuroid *Cucumaria frondosa*. *Biol. Bull.* **239**, 95-114 (2020).

32 Branco, P. C., Borges, J. C. S., Santos, M. F., Junior, B. E. J. & da Silva, J. R. M. C. The impact of rising sea temperature on innate immune parameters in the tropical subtidal sea urchin *Lytechinus variegatus* and the intertidal sea urchin *Echinometra lucunter*. *Mar. Environ. Res.* **92**, 95-101 (2013).

33 Wendelaar Bonga, S. E. The stress response in fish. *Physiol. Rev.* **77**, 591-625 (1997).

34 Xu, R. A. Annual changes in the steroid levels in the testis and the pyloric caeca of *Sclerasterias mollis* (Hutton) (Echinodermata: Asteroidea) during the reproductive cycle. *Invertebr. Reprod. Dev.* **20**, 147-152 (1991).

35 Binder, A. R. D., Pfaffl, M. W., Hiltwein, F., Geist, J. & Beggel, S. Does environmental stress affect cortisol biodistribution in freshwater mussels? *Conserv. Physiol.* **7**, coz101 (2019).

36 Pei, S., Dong, S., Wang, F., Tian, X. & Gao, Q. Effects of density on variation in individual growth and differentiation in endocrine response of Japanese sea cucumber (*Apostichopus japonicus* Selenka). *Aquaculture* **356**, 398-403 (2012).

37 Xu, R. A. & Barker, M. F. Annual changes in the steroid levels in the ovaries and the pyloric caeca of *Sclerasterias mollis* (Echinodermata: Asteroidea) during the reproductive cycle. *Comp. Biochem. Phys. A* **95**, 127-133 (1990).

38 Satoh, N., Rokhsar, D. & Nishikawa, T. Chordate evolution and the three-phylum system. *Proc. R. Soc. B* **281**, 20141729 (2014).

39 Hamel, J.-F. *et al.* Active buoyancy adjustment increases dispersal potential in benthic marine animals. *J. Anim. Ecol.* **88**, 820-832 (2019).

40 Thompson, R. F. & Spencer, W. A. Habituation: a model phenomenon for the study of neuronal substrates of behavior. *Psychol. Rev.* **73**, 16 (1966).

41 Denson, T. F., Spanovic, M. & Miller, N. Cognitive appraisals and emotions predict cortisol and immune responses: a meta-analysis of acute laboratory social stressors and emotion inductions. *Psychol. Bull.* **135**, 823 (2009).

42 Pagán, O. R. The brain: a concept in flux. *Philos. Trans. R. Soc. Lond. B* **374**, 20180383 (2019).

43 Durrieu, M., Wystrach, A., Arrufat, P., Giurfa, M. & Isabel, G. Fruit flies can learn non-elemental olfactory discriminations. *Proc. R. Soc. B* **287**, 20201234 (2020).

44 Díaz-Balzac, C. A. & García-Arrarás, J. E. *Echinoderm Nervous System*. (Oxford Research Encyclopedia of Neuroscience https://doi.org/10.1093/acrefore/9780190264086.013.205, 2018).

45 Landenberger, D. E. Learning in the Pacific starfish *Pisaster giganteus*. *Anim. Behav.* **14**, 414-418 (1966).

46 McClintock, J. B. & Lawrence, J. M. Photoresponse and associative learning in *Luidia clathrata* Say (Echinodermata: Asteroidea). *Mar. Freshw. Behav. Phy.* **9**, 13-21 (1982).

47 Ginsburg, S. & Jablonka, E. The evolution of associative learning: A factor in the Cambrian explosion. *J. Theor. Biol.* **266**, 11-20 (2010).

48 Boisseau, R. P., Vogel, D. & Dussutour, A. Habituation in non-neural organisms: evidence from slime moulds. *Proc. R. Soc. B* **283**, 20160446 (2016).

49 Verheggen, F. J., Haubruge, E. & Mescher, M. C. Alarm pheromones—chemical signaling in response to danger. in *Vitamins & Hormones: Pheromones* Vol. 83 (ed Gerald Litwack) 215-239 (Elsevier, 2010).

50 Byrne, M. The ultrastructure of the morula cells of *Eupentacta quinquesemita* (Echinodermata: Holothuroidea) and their role in the maintenance of the extracellular matrix. *Journal of Morphology* **188**, 179-189 (1986).

51 Melillo, D., Marino, R., Italiani, P. & Boraschi, D. Innate immune memory in invertebrate metazoans: a critical appraisal. *Front Immunol* **9**, 1915 (2018).

52 Garcia-Arraras, J. E. *et al.* Cellular mechanisms of intestine regeneration in the sea cucumber, *Holothuria glaberrima* Selenka (Holothuroidea: Echinodermata). *Journal of Experimental Zoology* **281**, 288-304 (1998).

53 Sun, J. & Bai, Y. Predator-induced stress influences fall armyworm immune response to inoculating bacteria. *J. Invertebr. Pathol.* **172**, 107352, doi:https://doi.org/10.1016/j.jip.2020.107352 (2020).

54 Otti, O., Gantenbein-Ritter, I., Jacot, A. & Brinkhof, M. W. G. Immune response increases predation risk. *Evolution* **66**, 732-739, doi:10.1111/j.1558-5646.2011.01506.x (2012).

55 Powell, D. J. & Schlotz, W. Daily life stress and the cortisol awakening response: testing the anticipation hypothesis. *PLoS ONE* **7**, e52067 (2012).

56 Blackburn-Munro, G. & Blackburn-Munro, R. Pain in the brain: are hormones to blame? *Trends. Endorcin. Met.* **14**, 20-27 (2003).

57 Dedovic, K., Duchesne, A., Andrews, J., Engert, V. & Pruessner, J. C. The brain and the stress axis: the neural correlates of cortisol regulation in response to stress. *Neuroimage* **47**, 864-871 (2009).

58 Canero, E. M. & Hermitte, G. New evidence on an old question: Is the “fight or flight” stage present in the cardiac and respiratory regulation of decapod crustaceans? *J. Physiol. - Paris* **108**, 174-186 (2014).

59 Harding, E. J., Paul, E. S. & Mendl, M. Cognitive bias and affective state. *Nature* **427**, 312-312 (2004).

60 Gianasi, B. L., Hamel, J.-F., Montgomery, E. M., Sun, J. & Mercier, A. Current knowledge on the biology, ecology, and commercial exploitation of the sea cucumber *Cucumaria frondosa*. *Rev. Fish. Sci. Aquac.* **in press**, https://doi.org/10.1080/23308249.23302020.21839015 (2020).

61 Montgomery, E. M. *et al.* Functional significance and characterization of sexual dimorphism in holothuroids. *Invertebr. Reprod. Dev.* **62**, 191-201 (2018).

62 So, J. J., Hamel, J.-F. & Mercier, A. Habitat utilisation, growth and predation of *Cucumaria frondosa*: implications for an emerging sea cucumber fishery. *Fish. Manage. Ecol.* **17**, 473–484 (2010).

63 Legault, C. & Himmelman, J. H. Relation between escape behaviour of benthic marine invertebrates and the risk of predation. *J. Exp. Mar. Biol. Ecol.* **170**, 55-74 (1993).

64 Gianasi, B. L., Verkaik, K., Hamel, J.-F. & Mercier, A. Novel use of PIT tags in sea cucumbers: promising results with the commercial species *Cucumaria frondosa*. *PLoS ONE* **10**, e0127884 (2015).

65 Wasserstein, R. L., Schirm, A. L. & Lazar, N. A. Moving to a world beyond "p< 0.05". *Am. Stat.* **73**, 1-19 (2019).

66 Dushoff, J., Kain, M. P. & Bolker, B. M. I can see clearly now: reinterpreting statistical significance. *Methods Ecol. Evol.* **10**, 756-759 (2019).

Acknowledgements

This research was partly supported by grants to AM from the Canada Foundation for Innovation (CFI), the Natural Sciences and Engineering Research Council of Canada (NSERC) and the Ocean Frontier Institute (OFI), through an award from the Canada First Research Excellence Fund. The authors thank the Field Services of the Department of Ocean Sciences for assistance with the collection of holothuroids, F. Zanuzzo for collaboration on the ELISA protocol, K. Gamperl for allowing use of equipment during the cortisol analysis, and J.M. Lawrence (Emeritus Professor, University of South Florida) for emulating exchanges on drafts of this manuscript.

Authors contributions

J-FH and AM designed the study. J-FH, SJ and GC collected the data. J-FH and AM analysed the data and wrote the manuscript. All authors reviewed the manuscript.

Competing interests

The authors declare no competing interests.

Figures

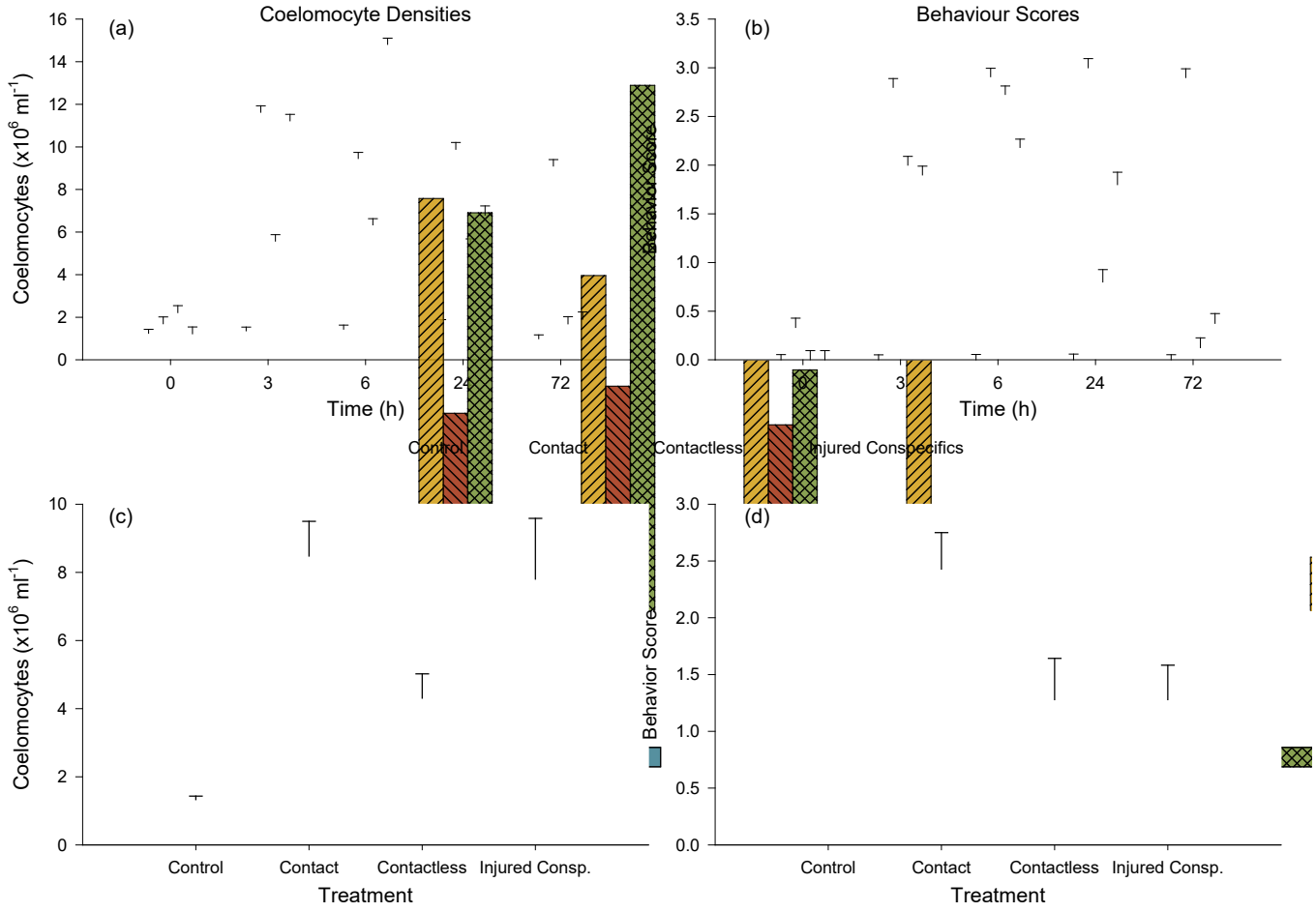

Figure 1. Immune and behavioural responses of *Cucumaria frondosa* to various treatments, including no stimulus (control), direct contact with the predator (contact), chemical signature of the predator (contactless), and chemical signature of injured conspecific (injured consp.). (a) Density of coelomocytes in the Polian vesicle and (b) corresponding behavioural score over 72-h exposure. Panels (c) and (d) illustrate the same metrics integrated over the duration of the experiment (72 h) for each treatment. Values in (a) and (b) are presented as mean ± S.E. (n = 3-9) and values in (c) and (d) are presented as mean ± 95% C.I. (n = 15-45).

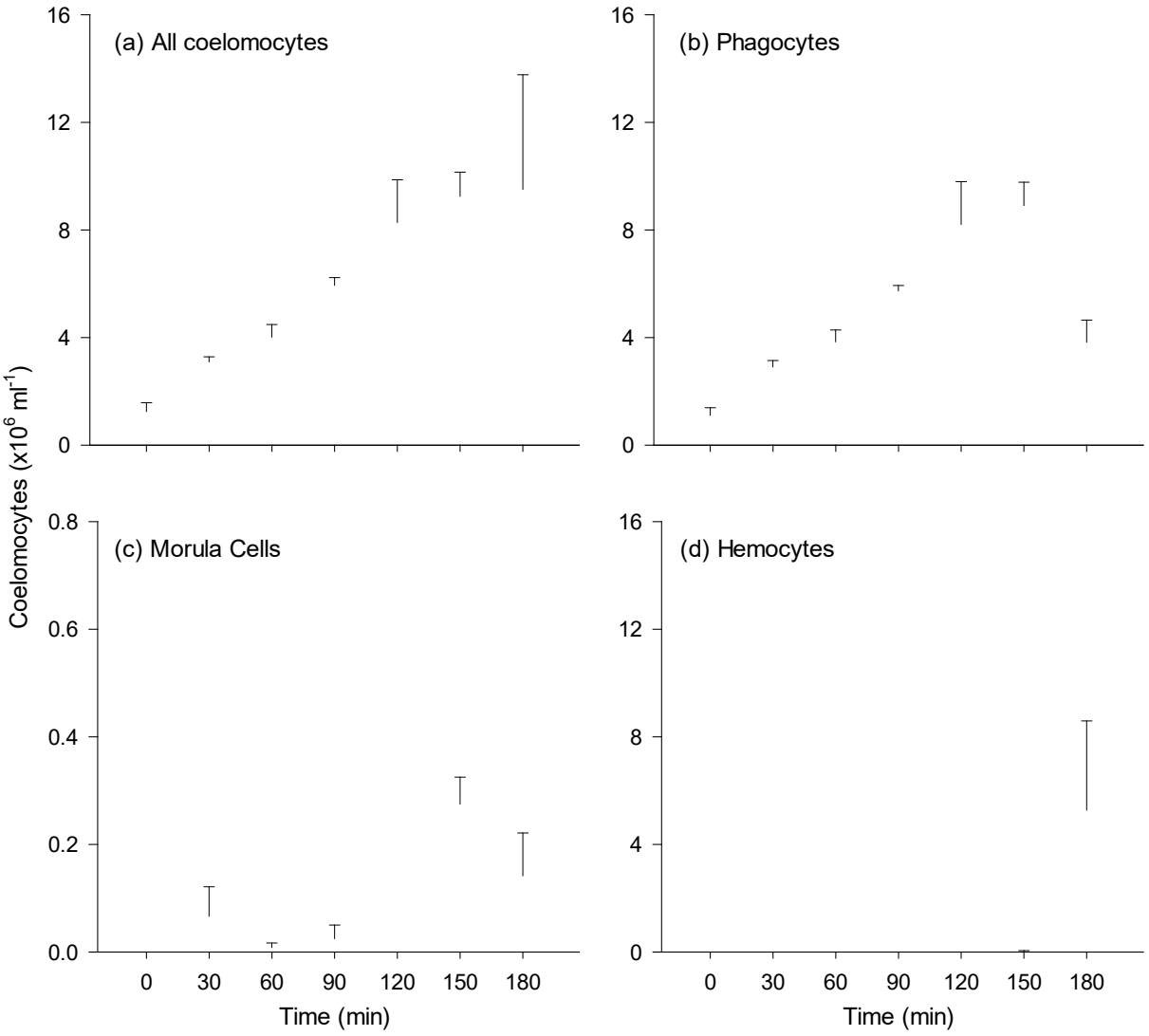

Figure 2. Immune response of *Cucumaria frondosa* to contactless exposure to the chemical signature of a predator over 180 min (3 h). Coelomocyte density was measured in the hydrovascular fluid of the Polian vesicle. (a) Global density of free coelomocytes (all types pooled). (b) Density of phagocytes. (c) Density of morula cells. (d) Density of hemocytes. Data presented as mean ± S.E. (n = 3). Note the different y-axis scale in (c).

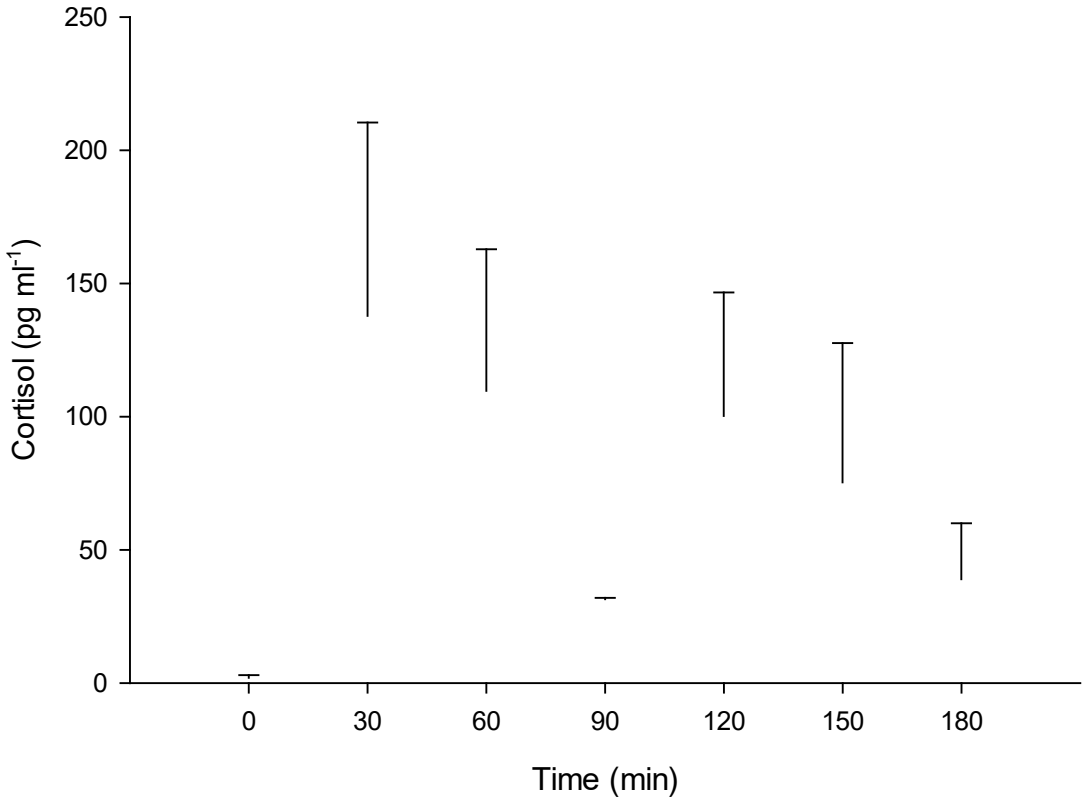

Figure 3. Hormonal response of *Cucumaria frondosa* to contactless exposure to the chemical signature of a predator over 180 min (3 h). Cortisol concentration in pg ml^{-1} (mean ± SE; n = 2-6) was measured in the hydrovascular fluid of the Polian vesicle.

Tables

Table 1. Behavioural scores used in the study of *Cucumaria frondosa*.

Score	**Definition**
0	Normal relaxed posture (not bloated), podia extended, firmly attached to substrate, tentacles extended or retracted, no displacement
1	Tensed posture (slightly bloated), podia extended, partly detached from substrate, tentacles extended or retracted, slow movement (crawling)
2	Tensed posture (slightly bloated), podia retracted, detached from substrate, tentacles retracted or limp, fast movement (rolling or crawling)
3	Fully developed active buoyancy adjustment reaction (as per Hamel et al. 2019); body nearly round (bloated), podia retracted, detached from substrate, tentacles retracted, severe contractions (peristaltic motion), fast movement (rolling, bouncing)